CHAPTER 1

INTRODUCTION

1.1 WEAR

Wear is a major cause of material wastage, so any reduction of wear can affect considerable savings. The friction will cause the displacement and removal of surface material, so wear can cause the failure of the element, which is in 70 to 80 percent of the total failure. Wear is the progressive damage, which occurs on the surface of a component as a result of its motion, relative to the adjacent working parts. It is defined as removal of material from the surface of component. Wear is one of the main cause that leads to replace the important components of any running system. It depends on many variables such as

i. Hardness
ii. Impact strength
iii. Toughness
iv. Modulus of elasticity
v. Corrosion resistance
vi. Fatigue resistance
vii. Surface finish
viii. Lubrication
ix. Load
x. Speed
xi. Temperature
xii. Properties of opposing surface etc.

1.1.1 THE HARM CAUSED BY WEAR

Influence the performance quality of machine ; e.g. The wear of the gear tooth surface will destroy the involute surface, and then cause the impact and vibration. The wear of the machinery mainshaft bearing will influence the machining precision of element.

1. Impaired the efficiency of machine; e.g.: The wear of cylinder sleeve of the diesel engines will cause inadequate functioning of power.
2. Reduced the reliability of machine: e.g. ：snaggletooth , wheel track

1.1.2 THE WEAR PROCESS

Three Phases of Machine Wear:

A. Running-in

Time: the initial stages of wearCharacteristic: high rate of wear (the contact area is small, so the contact stress is large.) the function of running-in: the material of high spots will be deformed, so the contact area becomes sufficiently large to support the load. It is a process that gradually to load, gradually to speed.

Attention to running-in ：

a.Load from light load to heavy load should be slow.

b.The lubricant should prevent from pollution; should replace after running-in.

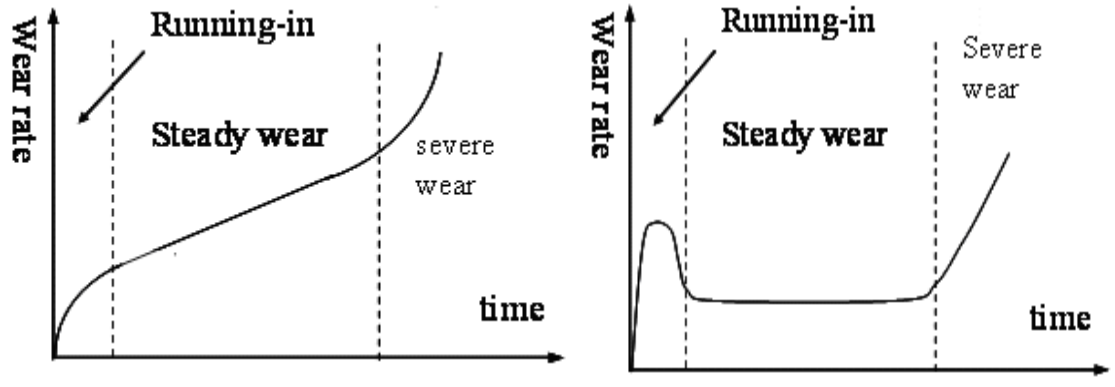

B. Steady Wear Phase:

Time : late stage of running-in, long-lasting; in the working stage of machine (stand for the useful time)

Characteristic: the speed of wear of slow-motion and reposeful

e.g. : the cylinder sleeve of locomotive and diesel engine replace every period

C. Severe Wear Phase:

Time : late stage of normal wear (late stage of life) characteristic : rate of wear will speed up, so the failure of surface element will occur or the clearance of kinematic pair will augment.

1.1.3 CLASSIFICATION OF WEAR

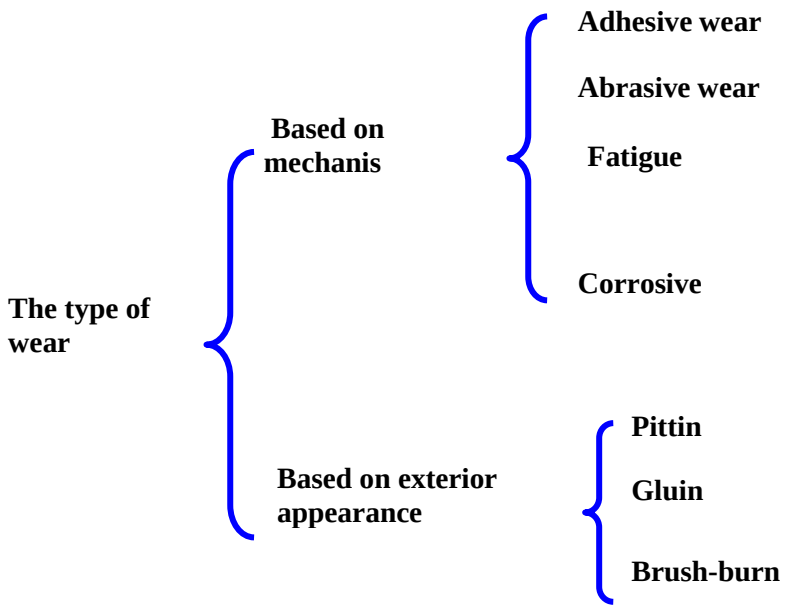

Figure 1: Classification of Wear

A)Adhesive Wear

The asperity of friction surface after cold welding the material will transfer to another surface when there is relative sliding, that is called adhesive wear. Adhesive Wear

occurs when two metal surfaces come in contact allowing particles to break away from the components. Insufficient lubrication or lubricant contamination normally causes this. Ensuring the proper viscosity grade lubricant is used can reduce adhesive wear. Reducing contamination in the oil will also help eliminate adhesive wear. Adhesive wear is produced by the formation and subsequent shearing of welded junction between two sliding surfaces. For adhesive wear it is necessary for the surfaces to be in intimate contact with each other. Surfaces, which are held apart by lubricating films, oxide films etc. reduce the tendency for adhesion to occur.

Archard's equation for adhesive wear is; **V/L= K W/H**

Where V = Wear volume

L = Sliding length

W = Normal load

H = Hardness

K = Wear coefficient.

B) Abrasive wear:

The wear is because of the dissociated rigid particles or the peak of asperity. Abrasive Wear is the results of hard particles coming in contact with internal components. Such particles include dirt and a variety of wear metals. Introducing a filtration process can reduce abrasive wear. It is also important to ensure vents, breathers, and seals are working properly. The harder asperities trapped at the interface, when moving relative to the surface, cause abrasion of the surface and the resulting damage is called abrasive wear. The abrasive wear mechanism is basically same as machining, grinding, polishing or lapping that are used for shaping materials. The body abrasive wear occurs when one surface (usually harder than the second) although this mechanism very often changes to three body abrasion as wear debris then acts as an abrasive between two surfaces.

Abrasive can act as in grinding where the abrasive is fixed relative to one surface of as in lapping where the abrasive tumble producing a series of indentations as opposed to scratch.

Archard has proposed an equation; **$V/L=K_{ab}\ W/H$**

In this equation K_{ab} represents the non-dimensional abrasive wear coefficient. The coefficient depends on the nature of the abrasive and extent of cutting action.

One important parameter is the relative hardness of the abrasive to that of the metal. When this ratio exceeds 1.4 strong abrasive action is expected. In general the adhesive wear coefficients tend to be higher for metallic material in comparison to adhesive wear. It is hence important to have efficient filtration system to remove abrasive contaminants.

Influenced factor：

(1)The harder the material is, the higher the staying quality is.

(2)The wearing capacity is increasing along with the augment of the particles' size.

(3)The wearing capacity is increasing along with the augment of the hardness of the particles.

C)Fatigue wear(pitting)

It occurs when there is a slight vibratory movement among loaded surfaces in contact and which manifests itself by the pitting of the surfaces and accumulation of oxidized debris. The debris occupies a greater volume than that of the metal destroyed and in a limited space. Fatigue Wear results when cracks develop in the component surface allowing the generation and removal of particles. Fatigue wear can occur in non-conforming machine elements such as rolling element bearing and gas in the form of rolling contact fatigue and pitting. It occurs when the contact stresses approaches the elastic limit. The number of stress cycles necessary to cause failure decreases with increasing stress. Leading causes of fatigue wear include insufficient lubrication, lubricant contamination, and component fatigue.

Influenced factors：

(1)The harder of the element surface is, the safer of the fatalness of the endurance crack is;

(2)When the value of the roughness concentration is comparatively large, the probability of element fatigue is increased.

D)Corrosive Wear

The acid and fuel from the air combusting little inorganic acid (like sulphuric acid), and electrochemical action of water together cause the lessening of the surface of material. Corrosive Wear is caused by a chemical reaction that actually removes material from a component surface. Corrosion can be a direct result of acidic oxidation. A random electrical current can also cause corrosion. Electrical current corrosion results in welding and pitting of the wear surface. The presence of water or combustion products can promote corrosive wear.

E) Cutting Wear

Cutting Wear can be caused when an abrasive particle has imbedded itself in a soft surface. Equipment imbalance or misalignment can contribute to cutting wear. Proper filtration and equipment maintenance is imperative to reducing cutting wear.

F) Fretting wear

Fretting wear is a small amplitude oscillatory motion, usually between two solid surfaces in contact. Fretting wear occurs when repeated loading and unloading causes cyclic stresses, which induces surface or subsurface break-up and loss of material. Vibration is a common cause of fretting wear.

G) Sliding Wear

Sliding Wear is caused by equipment stress. Subjecting equipment to excessive speeds or loads can result in sliding wear. The excess heat in an overload situation weakens the lubricant and can result in metal-to-metal contact. When a moving part comes in contact with a stationary part sliding wear becomes an issue.

H) Erosive wear

Erosive wear is caused by a gas or liquid, which may or may not carry entrained solid particles, impinging on a surface. When the angle of impingement is small, the wear produced is closely analogous to abrasive. When the angle of impingement is normal to the surface, material is displaced by plastic flow or is dislodged by brittle failure.

1.2 FRICTION

1.2.1 INTRODUCTION

Friction is the force resisting the relative lateral (tangential) motion of solid surfaces, fluid layers, or material elements in contact. It is usually subdivided into several varieties: Dry friction resists relative lateral motion of two solid surfaces in contact. Dry friction is also subdivided into static friction between non-moving surfaces, and kinetic friction (sometimes called sliding friction or dynamic friction) between moving surfaces. Lubricated friction or fluid friction resists relative lateral motion of two solid surfaces separated by a layer of gas or liquid. Fluid friction is also used to describe the friction between layers within a fluid that are moving relative to each other. Skin friction is a component of drag, the force resisting the motion of a solid body through a fluid. Internal friction is the force resisting motion between the elements making up a solid material while it undergoes deformation**.** Several famous scientists and engineers contributed to our understanding of friction. They include Leonardo da Vinci, Guillaume Amontons, John Theophilus Desaguliers, Leonard Euler, and Charles-Augustin de Coulomb. Their findings are codified into these laws:

1. The force of friction is directly proportional to the applied load.
2. The force of friction is independent of the apparent area of contact.(Amontons' 2nd Law) (Amontons' 2nd Law does not work for elastic, deformable materials. For example, wider tires on cars provide more traction than narrow tires for a given vehicle mass because of surface deformation of the tire)
3. Kinetic friction is independent of the sliding velocity. (Coulomb's Law of Friction)friction is not a fundamental force, as it is derived from electromagnetic force between charged particles, including electrons, protons, atoms, and molecules, and so cannot be calculated from first principles, but instead must be found empirically. When contacting surfaces move relative to each other, the friction between the two surfaces converts kinetic energy into thermal energy, or heat. Contrary to earlier explanations, kinetic friction is now understood not to be caused by surface roughness but by chemical bonding between the surfaces.

Surface roughness and contact area, however, do affect kinetic friction for micro- and nano-scale objects where surface area forces dominate inertial forces.

4. Coulomb friction
5. Coulomb friction, named after Charles-Augustin de Coulomb, is a model used to calculate the force of dry friction. It is governed by the equation:
6. $F_{\mathrm{f}} \leq \mu F_{\mathrm{n}}$,Where is the force exerted by friction (in the case of equality, the maximum possible magnitude of this force. $\mu$is the coefficient of friction, which is an empirical property of the contacting materials, $F_{\mathrm{n}}$is the normal force exerted between the surfaces.

For surfaces at rest relative to each other $\mu = \mu_{\mathrm{s}}$, where $\mu_{\mathrm{s}}$is the coefficient of static friction. This is usually larger than its kinetic counterpart. The Coulomb friction F_{f}may take any value from zero up to μF_{n}, and the direction of the frictional force against a surface is opposite to the motion that surface would experience in the absence of friction. Thus, in the static case, the frictional force is exactly what it must be in order to prevent motion between the surfaces; it balances the net force tending to cause such motion. In this case, rather than providing an estimate of the actual frictional force, the Coulomb approximation provides a threshold value for this force, above which motion would commence.

For surfaces in relative motion $\mu = \mu_{\mathrm{k}}$, where $\mu_{\mathrm{k}}$is the coefficient of kinetic friction. The Coulomb friction is equal to F_{f}, and the frictional force on each surface is exerted in the direction opposite to its motion relative to the other surface. This approximation mathematically follows from the assumptions that surfaces are in atomically close contact only over a small fraction of their overall area, that this contact area is proportional to the normal force (until saturation, which takes place when all area is in atomic contact), and that frictional force is proportional to the applied normal force, independently of the contact area (you can see the experiments on friction from Leonardo Da Vinci). Such reasoning aside, however, the approximation is fundamentally an empirical construction. It is a rule of thumb describing the approximate outcome of an extremely complicated physical interaction. The strength of

the approximation is its simplicity and versatility – though in general the relationship between normal force and frictional force is not exactly linear (and so the frictional force is not entirely independent of the contact area of the surfaces), the Coulomb approximation is an adequate representation of friction for the analysis of many physical systems.

1.2.2 Coefficient of Friction

The coefficient of friction (COF), also known as a frictional coefficient or friction coefficient and symbolized by the Greek letter μ, is a dimensionless scalar value which describes the ratio of the force of friction between two bodies and the force pressing them together. The coefficient of friction depends on the materials used; for example, ice on steel has a low coefficient of friction, while rubber on pavement has a high coefficient of friction. Coefficients of friction range from near zero to greater than one – under good conditions.

When the surfaces are conjoined, Coulomb friction becomes a very poor approximation (for example, adhesive tape resists sliding even when there is no normal force, or a negative normal force). In this case, the frictional force may depend strongly on the area of contact. Some drag racing tires are adhesive in this way. However, despite the complexity of the fundamental physics behind friction, the relationships are accurate enough to be useful in many applications.

The force of friction is always exerted in a direction that opposes movement (for kinetic friction) or potential movement (for static friction) between the two surfaces. For example, a curling stone sliding along the ice experiences a kinetic force slowing it down. For an example of potential movement, the drive wheels of an accelerating car experience a frictional force pointing forward; if they did not, the wheels would spin, and the rubber would slide backwards along the pavement. Note that it is not the direction of movement of the vehicle they oppose, it is the direction of (potential) sliding between tire and road.

The coefficient of friction is an empirical measurement – it has to be measured experimentally, and cannot be found through calculations. Rougher surfaces tend to have higher effective values. Most dry materials in combination have friction coefficient

values between 0.3 and 0.6. Values outside this range are rarer, but teflon, for example, can have a coefficient as low as 0.04. A value of zero would mean no friction at all, an elusive property – even magnetic levitation vehicles have drag. Rubber in contact with other surfaces can yield friction coefficients from 1 to 2. Occasionally it is maintained that μ is always < 1, but this is not true. While in most relevant applications μ < 1, a value above 1 merely implies that the force required to slide an object along the surface is greater than the normal force of the surface on the object. For ex, silicone rubber or acrylic rubber-coated surfaces have a coefficient of friction that can be substantially larger than 1.

Both static and kinetic coefficients of friction depend on the pair of surfaces in contact; their values are usually approximately determined experimentally. For a given pair of surfaces, the coefficient of static friction is usually larger than that of kinetic friction; in some sets the two coefficients are equal, such as Teflon-on-teflon.

In the case of kinetic friction, the direction of the friction force may or may not match the direction of motion: a block sliding atop a table with rectilinear motion is subject to friction directed along the line of motion; an automobile making a turn is subject to friction acting perpendicular to the line of motion (in which case it is said to be 'normal' to it). The direction of the static friction force can be visualized as directly opposed to the force that would otherwise cause motion, were it not for the static friction preventing motion. In this case, the friction force exactly cancels the applied force, so the net force given by the vector sum, equals zero. It is important to note that in all cases, Newton's first law of motion holds.

While it is often stated that the COF is a "material property," it is better categorized as a "system property." Unlike true material properties (such as conductivity, dielectric constant, yield strength), the COF for any two materials depends on system variables like temperature, velocity, atmosphere and also what are now popularly described as aging and deaging times; as well as on geometric properties of the interface between the materials. For example, a copper pin sliding against a thick copper plate can have a COF that varies from 0.6 at low speeds (metal sliding against metal) to below 0.2 at high speeds when the copper surface begins to melt due to frictional heating. The latter speed, of course, does not determine the COF uniquely; if the pin diameter is

increased so that the frictional heating is removed rapidly, the temperature drops, the pin remains solid and the COF rises to that of a 'low speed' test.

1.2.3 The Normal Force

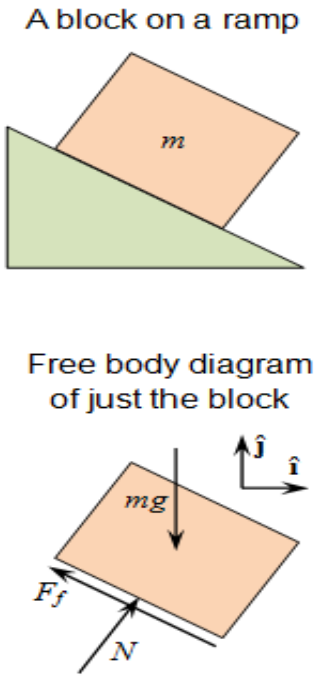

Figure 2: Friction force block diagram

Block on a ramp (top) and corresponding free body diagram of just the block (bottom).

The normal force is defined as the net force compressing two parallel surfaces together; and its direction is perpendicular to the surfaces. In the simple case of a mass resting on a horizontal surface, the only component of the normal force is the force due to gravity, where $N = mg$. In this case, the magnitude of the friction force is the product of the mass of the object, the acceleration due to gravity, and the coefficient of friction. However, the coefficient of friction is not a function of mass or volume; it depends only on the material. For instance, a large aluminum block has the same coefficient of friction as a small aluminum block. However, the magnitude of the friction force itself depends on the normal force, and hence the mass of the block. If an object is on a level surface and the force tending to cause it to slide is horizontal, the normal force N between the object and the surface is just its weight, which is equal to its mass multiplied by the acceleration due to earth's gravity, g. If the object is on a tilted surface such as an

inclined plane, the normal force is less, because less of the force of gravity is perpendicular to the face of the plane. Therefore, the normal force, and ultimately the frictional force, is determined using vector analysis, usually via a free body diagram. Depending on the situation, the calculation of the normal force may include forces other than gravity.

Static friction is friction between two solid objects that are not moving relative to each other. For example, static friction can prevent an object from sliding down a sloped surface. The coefficient of static friction, typically denoted as μ_s, is usually higher than the coefficient of kinetic friction.

The static friction force must be overcome by an applied force before an object can move. The maximum possible friction force between two surfaces before sliding begins is the product of the coefficient of static friction and the normal force: $f = \mu_s F_n$. When there is no sliding occurring, the friction force can have any value from zero up to F_{max}. Any force smaller than F_{max}attempting to slide one surface over the other is opposed by a frictional force of equal magnitude and opposite direction. Any force larger than F_{max}overcomes the force of static friction and causes sliding to occur. The instant sliding occurs, static friction is no longer applicable and kinetic friction becomes applicable.

An example of static friction is the force that prevents a car wheel from slipping as it rolls on the ground. Even though the wheel is in motion, the patch of the tire in contact with the ground is stationary relative to the ground, so it is static rather than kinetic friction.

The maximum value of static friction, when motion is impending, is sometimes referred to as limiting friction, although this term is not used universally.

1.2.4 Kinetic friction

Kinetic (or dynamic) friction occurs when two objects are moving relative to each other and rub together (like a sled on the ground). The coefficient of kinetic friction is typically denoted as μ_k, and is usually less than the coefficient of static friction for the same materials. In fact, Richard Feynman reports that "with dry metals it is very hard to show

any difference." Finally, new models are beginning to show how kinetic friction can be greater than static friction.

Examples of kinetic friction:

- Kinetic friction is when two objects are rubbing against each other. The resistance felt when pushing a book across a desk is an example of kinetic friction.
- Fluid friction is the interaction between a solid object and a fluid (liquid or gas), as the object moves through the fluid. The skin friction of air on an airplane and of water on a swimmer are two examples of fluid friction.This kind of friction is not only due to rubbing, which generates a force tangent to the surface of the object (such as sliding friction). It is also due to forces that are orthogonal to the surface of the object. These orthogonal forces significantly (and mainly, if relative velocity is high enough) contribute to fluid friction.. Since rubbing is not its only cause, in modern fluid dynamics the same force is typically referred to as drag or fluid resistance, while the force component due to rubbing is called skin friction. Notice that a fluid can in some cases exert, together with drag, a force orthogonal to the direction of the relative motion of the object (lift).

1.2.5 Angle of friction

For certain applications it is more useful to define static friction in terms of the maximum angle before which one of the items will begin sliding. This is called the angle of friction or friction angle. It is defined as:

$$\tan\theta = \mu$$

where $\theta$is the angle from horizontal and $\mu$is the static coefficient of friction between the objects. This formula can also be used to calculate $\mu$from empirical measurements of the friction angle.

1.2.6 Rolling resistance

Rolling resistance is the force that resists the rolling of a wheel or other circular object along a surface caused by deformations in the object and/or surface. Generally the force of rolling resistance is less than that associated with kinetic friction. Typical values

for the coefficient of rolling resistance are 0.001. One of the most common examples of rolling resistance is the movement of motor vehicle tires on a road, a process which generates heat and sound as by-products.

1.2.7 Energy of friction

According to the law of conservation of energy, no energy is destroyed due to friction, though it may be lost to the system of concern. Energy is transformed from other forms into heat. A sliding hockey puck comes to rest because friction converts its kinetic energy into heat. Since heat quickly dissipates, many early philosophers, including Aristotle, wrongly concluded that moving objects lose energy without a driving force.

When an object is pushed along a surface, the energy converted to heat is given by:

$$E_{th} = \mu_{\mathrm{k}} \int F_{\mathrm{n}}(x)dx$$

This is proved by mass balancing on a differential control volume and a flow chart is developed for solving Reynold's equation and also to find film thickness and other properties for given boundary conditions.

1.2.8 Work of friction

In the reference frame of the interface between two surfaces, static friction does no work, because there is never displacement between the surfaces. In the same reference frame, kinetic friction is always in the direction opposite the motion, and does negative work. However, friction can do positive work in certain frames of reference. One can see this by placing a heavy box on a rug, then pulling on the rug quickly. In this case, the box slides backwards relative to the rug, but moves forward relative to the frame of reference in which the floor is stationary. Thus, the kinetic friction between the box and rug accelerates the box in the same direction that the box moves, doing positive work.

The work done by friction can translate into deformation, wear, and heat that can affect the contact surface properties (even the coefficient of friction between the surfaces). This can be beneficial as in polishing. The work of friction is used to mix and join materials such as in the process of friction welding. Excessive erosion or wear of mating

surfaces occur when work due frictional forces rise to unacceptable levels. Harder corrosion particles caught between mating surfaces (fretting) exacerbates wear of frictional forces. Bearing seizure or failure may result from excessive wear due to work of friction. As surfaces are worn by work due to friction, fit and surface finish of an object may degrade until it no longer functions properly.

Materials		Static friction, μ_s	
		Dry & clean	Lubricated
Aluminum	Steel	0.61	
Copper	Steel	0.53	
Brass	Steel	0.51	
Cast iron	Copper	1.05	
Cast iron	Zinc	0.85	
Concrete (wet)	Rubber	0.30	
Concrete (dry)	Rubber	1.0	
Concrete	Wood	0.62	
Copper	Glass	0.68	
Glass	Glass	0.94	
Metal	Wood	0.2-0.6	0.2 (wet)
Polythene	Steel	0.2	0.2
Steel	Steel	0.80	0.16
Steel	Teflon	0.04	0.04
Teflon	Teflon	0.04	0.04
Wood	Wood	0.25-0.5	0.2 (wet)

Table1:Approximate coefficients of friction

1.2.9 Surface roughness

Surface roughness, more commonly shortened to roughness, is a measure of the finely spaced surface irregularities. In engineering, this is what is usually meant by "surface finish".

1.2.10 Waviness

It is the measure of surface irregularities with a spacing greater than that of surface roughness. These usually occur due to warping, vibrations, or defection during machining.

1.2.11 Lay

Lay is a measure of the direction of the predominant machining pattern. A lay pattern is a repetitive impression created on the surface of a part. It is often representative of a specific manufacturing operation.

1.2.12 Measurement of surface Finish

Surface finish may be measured in two ways: contact and non-contact methods. Contact methods involve dragging a measurement stylus across the surface; these instruments are called profilometers. Non-contact methods include: interferometry, confocal microscopy, focus variation, structured light, electrical capacitance, electron microscopy, and photogrametry.

The most common method is to use a diamond stylus profilometer. The stylus is run perpendicular to the lay of the surface. The probe usually traces along a straight line on a flat surface or in a circular arc around a cylindrical surface. The length of the path that it traces is called the measurement length. The wavelength of the lowest frequency filter that will be used to analyze the data is usually defined as the sampling length. Most standards recommend that the measurement length should be at least seven times longer than the sampling length, and. The assesmental length or evaluation length is the length of data that will be used for analysis. Commonly one sampling length is discarded from each end of the measurement length. 3D measurements can be made with a profilometer by scanning over a 2D area on the surface.

The disadvantage of a profilometer is that it is not accurate when the size of the features of the surface are close to the same size as the stylus. Another disadvantage is that profilometers have difficulty detecting flaws of the same general size as the roughness of the surface. There are also limitations for non-contact instruments. For example, instruments that rely on optical interference cannot resolve features that are less than some fraction of the frequency of their operating wavelength. This limitation can make it difficult to accurately measure roughness even on common objects, since

the interesting features may be well below the wavelength of light. The wavelength of red light is about 650 nm,[3] while the R_a of a ground shaft might be 2000 nm.

The first step of analysis is to filter the raw data to remove very high frequency data since it can often be attributed to vibrations or debris on the surface. Next, the data is separated into roughness, waviness and form. This can be accomplished using reference lines, envelope methods, digital filters, fractals or other techniques. Finally, the data is summarized using one or more roughness parameters, or a graph. In the past, surface finish was usually analyzed by hand. The roughness trace would be plotted on graph paper, and an experienced machinist decided what data to ignore and where to place the mean line. Today, the measured data is stored on a computer,

Many factors contribute to the surface finish in manufacturing. In forming processes, such as molding or metal forming, surface finish of the die determines the surface finish of the workpiece. In machining the interaction of the cutting edges and the microstructure of the material being cut both contribute to the final surface finish. In general, the cost of manufacturing a surface increases as the surface finish improves.

Just as different manufacturing processes produce parts at various tolerances, they are also capable of different roughness. Generally these two characteristics are linked: manufacturing processes that are dimensionally precise create surfaces with low roughness. In other words, if a process can manufacture parts to a narrow dimensional tolerance, the parts will not be very rough.

Due to the abstractness of surface finish parameters, engineers usually use a tool that has a variety of surface roughness created using different manufacturing methods.

1.2.13 The surface texturisation

The surface texturisation refers to making a very precise shapes cut on a surface. The size of the cut is in Microns and that is why it is called as Texture. In our setup we have made a surface texture on our discs with chemical etching process.

The standard process for texturizsation includes wet chemical etching, which creates specific surface morphologies, depending on the type of silicon and etching solutions

used. Laser surface texturisation, which avoids chemicals and is insensitive to local crystal orientation etc, is considered as a promising

1.3 LUBRICATION

1.3.1 Lubricants

Lubrication is the most effective means of reducing friction and controlling wear. The lubrication system in an engine serves four major purposes: to prevent seizure in the components, to remove the heat generated by friction, reduce the friction between components, and to reduce the wear of the internal components. These four byproducts of the lubrication system are achieved by effectively separating the internal components to varying degrees with a layer of oil lubricant. A common way to reduce friction is by using a lubricant, such as oil, water, or grease , which is placed between the two surfaces, often dramatically lessening the coefficient of friction. The science of friction and lubrication is called tribology. Lubricant technology is when lubricants are mixed with the application of science , especially to industrial or commercial objectives.

The essential properties which a good cylinder lubricant must have are as follows:

1) It must reduce sliding friction between the rings and the liner to a minimum, thereby minimizing metal to metal contact and frictional wear.
2) It must possess adequate viscosity at high working temperatures and still be sufficiently fluid to spread over the entire working surfaces to form a good adsorbed oil film.
3) It must form an effective seal in conjunction with the piston rings, preventing gas blow by and burning away of the oil film and lack of compression.
4) It must burn cleanly, leaving as little and as soft a deposit as possible. This is especially true of high additive content oils as unsuitable types can form objectionable ash deposits.
5) It must effectively prevent the buildup of deposits in the ring zone and in ports of port exhausted two stroke engines.

6) It must effectively neutralize the corrosive effects of mineral acids formed during combustion of the fuel.

The odds against cylinder lubricating oil:

in first glance it would appear that no lubricant, neither mineral nor synthetic, could withstand all above difficulties to fulfill the above requirements, but significant developments in the lubricating oil field have made it possible.

1. Friction and Wear The surfaces of machinery components appear well-finished to the naked eye. When magnified, however, surface imperfections become readily apparent. These microscopic hills and valleys are called asperities. When dry surfaces move relative to one another, asperities may rub, lock together, and break apart. The resistance generated when these adjacent surfaces come in contact is called friction. The welding together and breaking apart of asperities is a form of adhesive wear. Another form of wear may occur when a hard contaminant particle becomes trapped between two opposing surfaces. When this occurs, the contaminant acts as a miniature lathe, cutting into the softer machinery surface. This process is termed abrasive wear. Another consequence of friction is that the energy created by resistance is converted into heat. The primary functions of a lubricant, then, are the formation of a protective film between adjacent surfaces to reduce wear, and the dissipation of heat generated at these wear surfaces.

2. Corrosion Protection A second role provided by a lubricant is the prevention of system corrosion. In environments where contamination of the system with water is likely, protection of machinery components from corrosion is of the utmost importance. Salt water is considerably more corrosive than fresh water; thus naval machinery must be well protected from this contaminant. Water molecules may also diffuse through the lubricant and enter surface micro cracks, causing hydrogen embrittlement and subsequent surface failure. It is thus imperative that water contamination of machinery systems be minimized. To achieve corrosion protection, lubricants must form a protective barrier on machinery surfaces. Modern-day lubricants often contain corrosion inhibitors which chemically bond to the metallic surfaces of equipment components.

Corrosion inhibitors are an example of a class of compounds called additives.

1.3.2 KINDS OF LUBRICATION

Lubrication can be further be broken down into three major types:
(1) no lubrication,
(2) boundary layer lubrication
(3) full lubrication.
When there is no lubrication, the surfaces of the interacting components physically interact with each other, most commonly in sliding friction when there is dynamic movement. Under these circumstances, friction is the greatest under static loads, and lowers during dynamic movement. It is also important to notice that as the speed of interaction between the two surfaces increases, the generated heat also increases because of the energy released from the surface reactions. Boundary layer lubrication occurs when there is provided a layer of lubricant to partially separate the interaction components. Under these conditions, the lubricant can significantly reduce the sliding friction between the components, as well as have the added benefit of cooling the components by absorbing the heat generated from the partial interaction as well as the shear force in the lubricant. Components such as cams operate under this type of lubrication. Full lubrication occurs when there is no interaction between the machine elements because of a think layer of lubrication. The advantage of this type of lubrication is that it effectively stops wear between the machine elements because there is only an interaction between the lubricant and the element, but unfortunately, wear still occurs. This type of lubrication takes place in mechanisms such as the valves in the cylinder heads. In applications such as the valves and cylinders, it is also important to take into consideration the prominent effect of viscosity, because as the lubricant's temperature increases, the viscosity of the lubrication decreases. So it must be taken into consideration that the lubricant is viscous enough under operating conditions, but also not be too viscous that the engine cannot turn over in the ignition sequence.

1.3.3 COMMON LUBRICANTS

The most common types of oils used in the engine lubrication system are either vegetable oil or mineral oil. Vegetable oil was used in the past for racing applications because of its high film strength, and excellent protection against wear from its high lubricity. But it was not widely used in other applications because of its rapid rate of deterioration, which produces gums and lacquers on the machine elements. So mineral oils are more commonly used because they are much more cost effective, readily responsive to additives, can be produced in a wide range of viscosities, as well as deteriorate much less rapidly than vegetable oils. Today, lubricants such as synthetic oils replace natural oils as lubrication for the engine. Besides the higher cost, synthetic oils are much more effective lubricants than mineral oils because they can be chemically developed to have whatever the particular engines specifications require for proper operation.

1.3.4 THE FUNCTION OF LUBRICANT

1. Reduced the friction and wear
2. Rust prevention
3. Cooling effect and thermolysis
4. The oil film is buffering and shock-absorbing
5. Clean the friction surface, gland and dustproof

1.3.5 BASIC TYPES OF LUBRICANT

Introduction

The three major types of lubricants are lubricating oils, greases, gases and solid lubricants. The selection of a lubricant type is dependent on the type of machinery to be lubricated, the complexity of the lubricating system allowed by machinery design, and the frequency of lubrication required.

Lubricating Oil

Lubricating oils are used for the majority of applications. They may be classified according to their viscosities and any special properties imparted to them by additives. Oils whose base stocks are derived primarily from crude oil refining are called mineral or petroleum oils. Petroleum oils may be further classified as being paraffinic or naphthenic based on the types of hydrocarbons comprising the base stock. Oils that have been manufactured by chemical synthesis such as polymerization are called synthetic oils. Additives may be blended into the base stock to impart special properties to the finished product.

Reciprocating Internal Combustion Engine (R.I.C.E.) Oil

Reciprocating Internal Combustion Engine (R.I.C.E.) lube oils are formulated with detergent or dispersant additives to keep soot and other combustion by-products from depositing on engine parts. In addition, alkaline additive packages act to neutralize the acidic products of combustion. A third type of additive reduces the wear of internal parts such as cylinder liners, rings, pistons, and bearings. This oil is a single grade SAE 40 oil to be used in all shipboard internal combustion engines operating in ambient temperatures of 0°C (32°F) or higher.

Solid Lubricants Solid lubricants are typically used in situations where unusual temperature or environmental conditions preclude the use of conventional fluid lubricants, or when the application of a fluid lubricant is difficult. Solid lubricants form an essentially dry lubricating film between adjacent surfaces. The lubricant may be applied directly in powdered form, or as a colloidal suspension in a vehicle such as isopropanol. Evaporation of the vehicle leaves a thin film of the lubricant on machinery surfaces. The two most commonly used solid lubricants are powdered graphite and molybdenum disulfide (MoS2). Other materials such as powdered zinc dust and red lead suspended in petrolatum or mineral oil may also be used. Specific solid lubricant applications are as follows:

Dry graphite may be used for the lubrication of such equipment as security locks. Powdered molybdenum disulfide is used primarily as a thread antiseize compound. For the lubrication of threaded steel nuts and bolts, including superheated steam

components up to 565°C (1050°F); high temperature antiseize compound is typically used. This lubricant consists of a mixture of graphite and molybdenum disulfide suspended in mineral oil. For threaded aluminium parts engaged with similar or dissimilar metals, zinc dust-petrolatum antiseize compound shall be used. Additional lubricants for use on threaded fasteners include colloidal graphite in isopropanol and molybdenum disulfide in isopropanol [9].

Specialty Lubricants The operating parameters encountered in high pressure (>1500 psi) air, oxygen, and oil-free nitrogen systems require a lubricant that will resist autogenous ignition. For lubrication of these systems, halocarbon oils shall be used.

1.3.6 CLASSIFICATION OF LUBRICANT

1. Natural Oil: animal oil, seed fat (performed well)
2. Synthetic Oil: deploy based on the requirement, high cost
3. Mineral Oil：efficient supplies, stable property, low cost, extensive be applicable.

1.3.7 THE CLASSIFICATION OF LUBRICATION

For unlubricated metallic surfaces, the friction coefficient normally lies above 0.5. Such high u-values are generally unacceptable for applications, since they would lead to enormous energy losses. In order to reduce the frictional forces, lubricants are normally employed. Lubricants form a layer of lower shear strength than the sliding surfaces. In many situations, the lubricatnt totally separates the sliding surfaces, such that they no longer have any interaction with each other. In other situations the lubricant reduces the interaction, reducing the extent of junction growth.

Lubrication can be subdivided into five categories:

Hydrodynamic lubrication,-in which the sliding surfaces are separated by a thick lubricant film (thickness > height of the asperities).

Hydrostatic lubrication- in which the oil is pumped under pressure between the sliding surfaces.

Elastohydrodynamic lubrication (EHL)-In which the local pressures are so high that significant elastic deformation of the sliding surfaces occurs.

Boundary lubrication, in which the surfaces are separated by monomolecular (or nearly monomolecular) films.

Solid lubrication, which is based on a solid interfacial layer of low shear strength.

1. Hydrodynamic Lubrication-

In this kind of lubrication, the asperities on the sliding partners never come into contact with each other. These surfaces are kept apart by hydrodynamic pressure. The sliding surfaces have to be conformal; in other words, they need to be geometrically similar and held apart by a small lubricant-filled gap.

2. Hydrostatic Lubrication-

In this type of lubrication obtians the load-carrying pressure from an external pump. The biggest advantage over hydrodynamic lubrication is that the lubricant film continues to exist, and the load continues to be carried, even at zero relative velocity of the sliding surfaces.

3. Elastohydrodynamic Lubrication-

When the sliding surfaces are not conformal, but have point or line contact (e.g. in the case of gears, ball-bearing races, or in cam-followers), much higher local pressures are present.under these conditions, the pressure dependence of the lubricant as well as the elastic deformation of the sliding surfaces play important roles. This kind of lubrication is known as elasto hydrodynamic lubrication (EHL).

4.Boundary Lubricants

At very high loads or low speeds, hydrodynamic forces can no longer maintain a lubricant film between the sliding surfaces and direct contact between the asperities starts to become important. A boundary lubricant is essential under these conditions, in order to avoid excessive friction and wear. Boundary lubricants form adsorbed

molecular films on the surfaces. The repulsive forces between the films carry a significant part of the load and shield the asperities from unprotected contact.

5.Solid Lubrication

In various circumstances it is not practicable to use liquid lubricants, e.g. in the food industry or in high-temperature or vacuum environments. In such situations, solid lubricants are frequently employed, e.g. graphite, molybdenum disulfide and PTFE (Teflon).

1.3.8 Regimes of Lubrication

As lubrication is an important component of Tribology, here is a convenient point to introduce the reader to its structure, in a very simple and approximate way. We will assume that two rubbing (or rolling) solid surfaces are like steel on steel. They are also rough, because a perfectly smooth surface cannot exist. The act of lubrication is to have between the surfaces a layer of a different material that reduces the friction force between them, either by being softer than the surfaces, or by being a coherent liquid lubricant or gas, entrained between the two surfaces by their relative movement. Now most engineering structures are in normal atmosphere, so the primary friction-reducing layer is a low shear strength oxide film, formed naturally by the interaction of the steel surfaces with the atmosphere. In a clean environment or a vacuum, the surfaces have no oxide film, resulting in a high friction force.

Stribeck originally devised a convenient way of relating roughness and film thickness by a parameter λ_s = film thickness /roughness height , the roughness height being some representative value of the undistorted roughness features, and the film thickness being measured from i.He devised the Stribeck curve, shown in Fig. 1.3, where the coefficient of friction is plotted against λ_s.

The frictional contact of clean surfaces is represented by point A at the beginning of the boundary lubrication regime in Fig. 1.3. The subsequent formation of an oxide film, or additionally by the controlled deposition of a softer material, insertion of special

boundary lubricants such as tallow, castor oil or additives to a mineral oil, will reduce the friction force. Regime AB represents this behaviour.

At point B, where the surface roughness equals the film thickness, we enter the partial or mixed lubrication regime BC. In this case, the load is partly supported by a coherent flowing oil film and partly by a regime AB type contact, or alternatively, by thin micro-scale films formed between the distorted surface features themselves. Regime BC is one of the most common in practice. In some ways, it represents a design failure, because a coherent lubricant film is not present everywhere. As in regime AB, in regime BC the surfaces wear, perhaps producing debris.

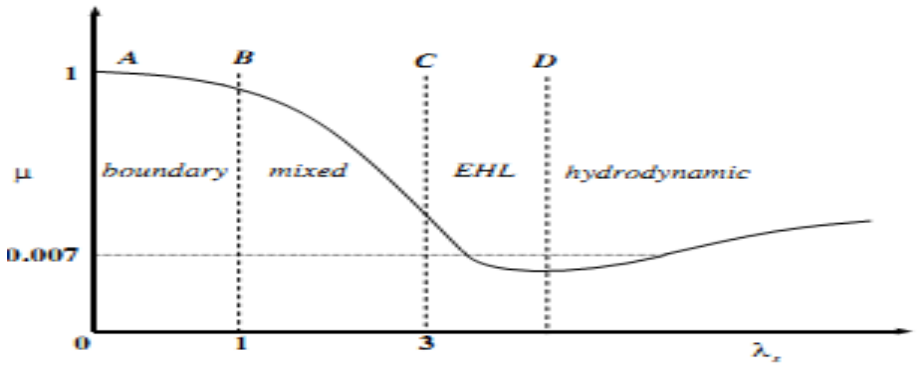

Figure 3:. Stribeck curve

A progressive reduction in the value of /x carries further into the regime CD, where a coherent elasto hydrodynamic lubricant (EHL) film is produced. Here, the values of A_s are large enough for the surface features not to influence much the lubricant film thickness. The high pressures encountered in this zone cause the surfaces to distort elastically and the lubricant viscosity to increase. Rolling element bearings and gears fall into this category. The word elasto hydrodynamic clearly defines the lubrication mechanism. It is characterized by a film thickness of a couple of micrometers or less, requiring quite smooth surfaces. Modern manufacturing methods and design improvements have increased this zone at the expense of zone BC. Remarkably, Dowson [3] points out that it has also been nature's choice for the EHL regime of lubrication to occur in the synovial joints of creatures ranging from elephants to shrews!

1) The next regime, beyond D, covers the hydrodynamic and externally pressurized types of bearing. An example is a pair of hydrodynamic journal bearings used to support a steam turbine, where the film thickness is about 15-30 micrometers. In certain cases, increasing speeds and reducing loads in zone CD can cause a reduction in elastic distortion of surfaces that were previously in EHL contact, making them also candidates for the zone beyond D. This situation sometimes occurs in ball bearings, where some of the rolling elements have become unloaded during their orbital path.

1.3.9 CHARACTERISTICS OF LUBRICATING OILS

A) Viscosity - The capability of liquid to resistance to deformation, which is expressed by friction drag of liquid. Technically, the viscosity of an oil is a measure of the oil's resistance to shear. Viscosity is more commonly known as resistance to flow. If lubricating oil is considered as a series of fluid layers superimposed on each other, the viscosity of the oil is a measure of the resistance to flow between the individual layers. A high viscosity implies a high resistance to flow while a low viscosity indicates a low resistance to flow. Viscosity varies inversely with temperature. Viscosity is also affected by pressure; higher pressure causes the viscosity to increase, and subsequently the load-carrying capacity of the oil also increases. This property enables use of thin oils to lubricate heavy machinery. The load carrying capacity also increases as operating speed of the lubricated machinery is increased. Two methods for measuring viscosity are commonly employed: shear and time .

i)Shear. When viscosity is determined by directly measuring shear stress and shear rate, it is expressed in centipoise (cP) and is referred to as the absolute or dynamic viscosity. In the oil industry, it is more common to use kinematic viscosity, which is the absolute viscosity divided by the density of the oil being tested. Kinematic viscosity is expressed in centistokes (cSt). Viscosity in centistokes is conventionally given at two standard temperatures: 40 EC and 100 EC (104 EF and 212 EF).

ii)Time. Another method used to determine oil viscosity measures the time required for an oil sample to flow through a standard orifice at a standard temperature. Viscosity is then expressed in SUS (Saybolt Universal Seconds). SUS viscosities are also conventionally given at two standard temperatures: 37 EC and 98 EC (100 EF and 210 EF). As previously noted, the units of viscosity can be expressed as centipoises (cP), centistokes (cST), or Saybolt Universal Seconds (SUS), depending on the actual test method used to measure the viscosity.

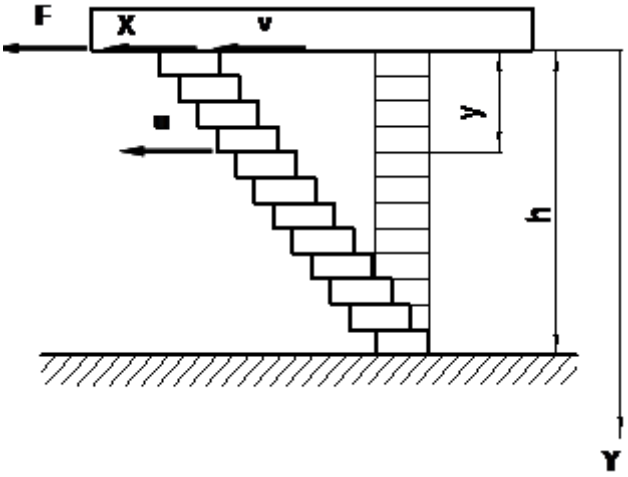

Flow of Fluid

laminar flow of oil between parallel plates

Speed of oil layer in the $u = v$ vicinity of active plate

Speed of oil layer in the $u = 0$ vicinity of active plate

Every oil layer moves u in different speed

τ and velocity gradient $\frac{du}{dy}$ is directly proportional.

$\tau = -\eta \frac{du}{dy}$ (Newton's law of viscous)

proportionality constant, namely kinetic viscosity η (use in the calculation of hydrokinetics)

Assuming the liquid of $1 \times 1 \times 1 m^3$, if there is relative sliding of the speed of 1m/s between the two plate, when the force is1N in that way the viscosity of liquid is one International System of Units' kinematic viscosity Pa.s

kinematic coefficient of viscosity γ (the viscosity of lubricant)

The ratio between kinetic viscosity η and the fluid density ρ at the same temperature.

A.)Viscosity index The viscosity index, commonly designated VI, is an arbitrary numbering scale that indicates the changes in oil viscosity with changes in temperature. Viscosity index can be classified as follows: low VI - below 35; medium VI - 35 to 80; high VI - 80 to 110; very high VI - above 110. A high viscosity index indicates small oil viscosity changes with temperature. A low viscosity index indicates high viscosity changes with temperature. Therefore, a fluid that has a high viscosity index can be expected to undergo very little change in viscosity with temperature extremes and is considered to have a stable viscosity. A fluid with a low viscosity index can be expected to undergo a significant change in viscosity as the temperature fluctuates. For a given temperature range, say -18 to 370EC (0 - 100 EF), the viscosity of one oil may change considerably more than another. An oil with a VI of 95 to 100 would change less than one with a VI of 80. Knowing the viscosity index of an oil is crucial when selecting a lubricant for an application, and is especially critical in extremely hot or cold climates. Failure to use an oil with the proper viscosity index when temperature extremes are expected may result in poor lubrication and equipment failure. Typically, paraffinic oils are rated at 38 EC (100 EF) and naphthenic oils are rated at -18 EC (0 EF). Proper selection of petroleum stocks and additives can produce oils with a very good VI.

A. **Pour point** The pour point is the lowest temperature at which an oil will flow. This property is crucial for oils that must flow at low temperatures. A commonly used rule of thumb when selecting oils is to ensure that the pour point is at least 10 EC (20 EF) lower than the lowest anticipated ambient temperature.

B. **Cloud point** The cloud point is the temperature at which dissolved solids in the oil, such as paraffin wax, begin to form and separate from the oil. As the temperature drops, wax crystallizes and becomes visible. Certain oils must be maintained at temperatures above the cloud point to prevent clogging of filters.

C. **Flash point and fire point** The flash point is the lowest temperature, to which a lubricant must be heated before its vapour, when mixed with air, will ignite but not continue to burn. The fire point is the temperature at which lubricant combustion will be sustained. The flash and fire points are useful in determining a lubricant's volatility and fire resistance. The flash point can be used to determine the transportation and storage temperature requirements for lubricants. Lubricant producers can also use the flash point to detect potential product contamination. A lubricant exhibiting a flash point significantly lower than normal will be suspected of contamination with a volatile product. Products with a flash point less than 38 EC (100 EF) will usually require special precautions for safe handling. The fire point for a lubricant is usually 8 to 10 percent above the flash point. The flash point and fire point should not be confused with the auto-ignition temperature of a lubricant, which is the temperature at which a lubricant will ignite spontaneously without an external ignition source.

D. **Neutralization Number** The acid or neutralization number is a measure of the amount of potassium hydroxide required to neutralize the acid contained in a lubricant. Acids are formed as oils oxidize with age and service. The acid number for an oil sample is indicative of the age of the oil and can be used to determine when the oil must be changed. As lubricants degrade from oxidation they form a number of acids. These acids are corrosive to Babbitt, yellow metals, carbon steel, cast iron, and if left uncorrected for a period of time will begin a corrosion process and possibly eventual bearing failure. While small increases in the Total Acid Number (TAN) usually indicate oxidation and lubricant degradation, contaminants with acidic constituents can also be a factor. Monitoring the oil's Total Acid Number should be an important part of lubricant maintenance program. Generally when a lubricant's acid number reaches a condemning limit, replacement or sweetening is best option.

E. **Total Acid Number (TAN**) is the standard neutralization number test for industrial lubricating oils. It is performed by titrating a solution of oil and diluents with an alcohol/potassium hydroxide (KOH) solution, a base, until all the acids present are neutralized. The results are reported as milligrams of potassium-hydroxide per gram of sample, or mg/Gm

F. **Strong Acid Number (SAN**) is similar to TAN, except the 'strong' acids are first extracted from the lubricant. That extract is then titrated with KOH and the SAN reported as mg/gm.

G. **Total Base Number (TBN**) is a standard test for engine lubricants. It is a measurement of the amount of protection in the lubricant remaining to neutralize acids formed as a result of combustion. A solution of oil and diluents is titrated with an alcohol/Hydrochloric Acid (HCl) solution until all the alkaline or base constituents in the oil are neutralized. Results are reported as milligrams of HCl per gram of sample, or mg/gm.

Most lubricating oils have a baseline Acid Number as a result of additives. R&O (rust and oxidation) industrial oils generally have a baseline in the 0.03 to 0.06 mg/gm range. AW (anti-wear) and EP (extreme pressure) industrial oils will have much higher baselines because of the additional additives that give them their AW or EP qualities. Baselines for these lubricants can be over 1.0 mg/gm.

1.3.10 EFFECT OF WATER IN THE OIL

Precautions shall be taken to keep water from entering the lubrication system; any water detected shall be removed as soon as possible. Water in the oil increases frictional resistance causes the oil to break down prematurely, corrodes journals and any parts not continuously covered with oil, and may cause corrosion in the entire system. Rusting generally originates on exposed surfaces such as gear casings and upper portions of sump tanks where condensation occurs and, unless remedied, progresses throughout the system. Rusting due to condensation is most likely to occur

in cold climates and in installations where portions of the lube oil sump tanks are integral with the skin of the ship. Precautions to be taken include the following:

a. Any drain fitted in the lowest part of a bearing pedestal should be opened and the bearings drained of any water a few hours after securing the lube oil system.

b. Lube oil from bilges, oily waste drain tanks, or miscellaneous tanks shall not be reclaimed nor added to the lubrication system.

c. Because warm, moisture-laden vapour condenses on any cool, exposed surface, any factor tending to cool casings or sump surfaces shall be eliminated. All forced draft ventilation ducts shall be permanently arranged so that no air can blow directly or indirectly on a gear casing.

d. When securing the main propulsion machinery, circulate oil through the turbines and reduction gear lubrication system by means of the ship's oil pumps for at least 1 hour (or until the machinery reaches ambient temperature), to allow machinery component temperatures to equalize. The motor-driven shaft turning gear (if provided) shall be operated during the oil circulation period. If hand jacking only is provided, the propeller shaft shall be jacked intermittently until machinery reaches ambient temperature. The circulation period will vary, depending upon the air and injection temperatures. For ships operating under low air and injection temperature conditions, the period will be somewhat longer.

e. If electrostatic precipitators are installed on turbine and reduction gear and sump vent pipes, the vented air is cleaned of oil and water mist particles only. Moisture, in the form of vapour, will flow through the precipitator unrestricted. A haze of moist air visible at the electrostatic precipitator vent discharge indicates that excessive moisture is entering the lubrication system elsewhere. Test the purifier operating efficiency and check every possible point at which water might enter the system.

f. If the propulsion reduction gear has a dehumidifier installed, the moisture in the air within the gear case and oil sump shall be maintained at 30-35 percent relative humidity, when the propulsion plant has cooled down and been secured. Prior to starting and warm up of the lubricating oil system, the dehumidifier shall be secured, isolation valves in the dehumidification ducts shall be locked shut, and the electrostatic precipitator activated and its positive closure assembly opened. To secure the

machinery, allow the oil temperature during oil circulation to cool down to approximately 10° F above ambient. Then, secure the electrostatic precipitator, close the positive closure assembly, stop the lubricating oil system pumps, unlock and open the dehumidification duct isolation valves and activate the dehumidifier. Verify once per watch that the humidity in the gear case is being maintained within the specified limits. Refer to applicable dehumidifier operational/maintenance manual if the specified gear-case humidity requirements cannot be maintained.

LITERATURE REVIEW

The study of the frictional characteristics in response to changes of the dynamic parameter of a pin-on-disk apparatus were experimentally investigated for dry sliding. The apparatus has been designed and built to allow control of sliding speed, load, stiffness.Dynamic friction and normal force measured for various conditions of the system parameters e.g. different stiffness in the normal direction, loading mechanisms and test materials Stiffness in the loading direction was also varied using a spring with different stiffness. Steel, rosin and poly tetra fluoro ethylene when tested because they have different types of frictional behaviour. Test results showed that frictional characteristics at various loading mechanisms when different even though the operating parameters were the same. They are alto strongly dependent on both the sliding velocity and the run-out of the disk surface. Effects of the surface run-out on the friction behaviour were further evaluated using a tapered steel disk. When the surface run was high, the coefficient of friction was computed differently with the data processing. A theoretical analysis for a simple model of a pin-on-disk apparatus showed that surface angularities, such as surface roughness, waviness and run-out, result in dynamic normal forces which depend on both the dynamic parameters of the system and the sliding velocity. [1]

The aseptic loosening of orthopaedic implants is a biomechanical phenomenon initiated mechanically and propelled by biological responses to the presence of wear debris released from the biomaterial. A triphasic composite, fabricated by the heterogeneous sintering of titanium and graphite powders was developed to address the fracture and wear performance of titanium. The composite is designed to smear graphite on both articulating surfaces and hence reduced wear and maintained a low friction tribosystem with fracture properties better than conventional bio ceramics. The composite is made up of ductile titanium and a colony of hard, wear resistant titanium carbide produced by

the controlled sintering of titanium and graphite particles. Free graphite is present in varying quantities depending upon compaction pressure and initial graphite composition. Initial graphite content composites of 4% and 8% were made with different compaction pressure to give a range of porosities from 10% to 45%. The coefficient of frictional was measured on a pin-on-disc (hardened steel) configuration. Under dry state, the coefficient of friction was observed to reduce with increasing porosity. Graphite smearing and the entrapment of debris by the pores contributed to the reduction of the wear components which in tum reduced the coefficient of friction. Under lubricated conditions, the sintered titanium and its composites were observed to be independent of porosity and pore size. The frictional behaviour of the titanium-8% graphite composites showed first, a titanium carbide dominated-wear stage and the second, a free graphite smearing stage. The results proved the concept that the coefficient of friction of titanium-graphite composites approaches that between graphite-graphite surfaces after the running-in period. This proof of concept is the first realisation of a biomaterial that could reduce the coefficient of friction on both articulating surfaces, a step closer to the development of fracture and wear resistant biomaterials that also protects the other counter surface.[2]

The wear of ultrahigh molecular weight polyethylene _UHMWPE. bearing surfaces and cytotoxic effects associated with wear particles are believed to play a significant role in the mechanical failure of artificial joint prostheses. The objective of this study was to determine the effects of surface patterning on GUR 415 grade UHMWPE friction and wear characteristics under in vitro dynamic loading conditions. A pin-on-disk wear and friction apparatus was used for the dynamic tests which were conducted at 67–708F and 60% relative humidity in bovine serum. An undulating surface geometry, consisting of 2732 0.16-mm diameter, 0.32-mm deep holes, was machined onto the surface of six of the 12 disk specimens tested. Disk specimens were tested at 112 rpm _0.11 msy1. using a Co–Cr–Mo pin contact load of 56.5 N, which corresponded to an initial mean Hertzian contact stress of 30 MPa. Friction forces were recorded throughout the 3-h test period. Following testing, the wear track width, plow height, and wear depth were measured using a profilometer. The undulating pattern of surface cavities produced a

significant reduction _42%. in the friction coefficient in comparison to the non-patterned UHMWPE surfaces. Such findings are hypothesized to reflect the fact that patterned surfaces act as a reservoir for the lubricating fluid and also trap wear particles, minimizing third body-type wear. Under the relatively high load condition examined in this study, however, patterning of the UHMWPE surface was not effective in reducing wear presumably because the polyethylene surface was plastically deformed by the high contact stresses.[3]

The friction and wear behavior of four hard coatings (Metco, Diamalloy, Stellite, and Zn–SiC) was determined using a pin-on-disk machine. The coatings were thermal sprayed on cast iron disks. The coating compositions were Ni–17Cr–2.5Fe–2.5Si–2.5B–0.15C (Metco), Fe–30Mo–2C (Diamalloy), Co–30Cr–12W–2.4C (Stellite), and Zn–50SiC (Zn–SiC). Sliding was performed between cylindrical pins machined from non-asbestos organic (NAO) brake lining and the coated and uncoated disks. The lining, consisting of resin, aramid pulp, zirconia, graphite, calcium fluoride, rubber and barium sulfate, was developed as a material for automotive brake pads. The coatings were characterized by measuring their hardness, porosity, and corrosion resistance. The Metco and Stellite coatings had a uniform morphology in all directions. The Diamalloy coating had a lamellar microstructure whereas the Zn–SiC coating was very porous. The corrosion resistance of the coatings was tested with exposure to 5% NaCl for 168 h. The Stellite coating had the best corrosion resistance. The friction and wear tests were conducted at contact pressures of 1.72, 3.45 and 6.89MPa and sliding speeds of 1 and 3m/s. The wear of the lining material was lowest when it slid against the Stellite coated disks and the highest coefficient of friction was observed for the Metco coated disks.
The gray cast iron used in this study had a composition of Fe–3.45C–2.15Si–0.5Mn–0.25Cr–0.2Cu. This material was specifically developed for brake rotors. Optical microscopy showed that a maximum of 10% free ferrite appeared at the surface and the graphite was randomly distributed. The lining material used for the friction pins consisted of a thermoset resin, aramid pulp, zirconia, graphite, calcium fluoride, rubber and barium sulfate. This material was developed as a potential candidate for automotive brake pads as a replacement for the conventional metallic and semi-metallic brake

pads. Iron-, nickel-, cobalt-, and SiC-based coatings are hard coatings commonly applied by thermal spray processing. Typical compositions of these coatings include Ni–Cr–Si–B–C, Co–Cr–W–C and Fe–Mo–C. Although the Ni- and Co-based coatings have good corrosion resistance, Fe-based coatings are often used in place of the Ni- and Co-based coatings because the Fe-based coatings are less expensive. Therefore, Fe–30Mo–2C (Diamalloy), Ni–17Cr–2.5Fe–2.5Si–2.5B–0.15C (Metco) and Co–30Cr–12W–2.4C (Stellite) coatings were selected here because of their superior wear and corrosion properties and that they can be easily deposited on cast iron substrates. Since zinc has been applied to ferrous substrates to provide corrosion resistance by cathodic protection for nearly 100 years, the Zn–SiC coating was selected to provide a combination of wear resistance and corrosion protection.[4]

The cotton spinning machines fibres which are twisted to a yarn by the high-speed revolution of a traveller on a ring. Wear of the ring–traveller system is thought to be attenuated by the lubricating properties of cotton fibre, but few experimental studies of the phenomenon have been reported. A new methodology has been developed to study both the formation of a cotton transfer film on a steel disc and the effect of such films on the tribological behaviour of a steel-on-steel contact. A ball-on-disc tribometer placed in a controlled humidity chamber was used. Cotton transfer films were produced reproducibly by rubbing a cotton pad on a steel disc. The chemical composition of the films analysed by IR was similar to that of films formed on the ring during operation of an industrial spinning machine. In addition to the cotton peaks the IR spectra contained a peak attributed to cotton wax. The film coated steel discs were subjected to rubbing against a steel ball at different relative humidity. In all cases, the measured friction coefficient in presence of the cotton film was lower than in absence of a film. The transfer films produced at a relative humidity of 30% were thicker than those produced at 50 or 75% relative humidity and presented no case of failure during the tribological tests. The wear volume of the steel ball was found to be negligible in the presence of the transfer film compared to the wear obtained during the rubbing after the destruction of this transfer film.

A cotton pad was fixed on a specially designed pin holder. The 6.0mm diameter 100Cr6 steel ball was used to support the cotton. The cotton pad was loaded against a rotating disc of 25mm diameter and 3mm height. The discs made of 100Cr6 steel (nominal composition: 1% C, 0.3% Si, 0.3% Mn, 1.5% Cr) were heat treated and annealed yielding a microhardness of 220 Vickers as measured using a load of 0.2 kg. They were ground and the resulting average surface roughness Ra characterised by non-contact laser scanning probe profilometry (UBM Instrument®) was in the range 0.03–0.1 _m, both in the track direction and perpendicular to it. The discs and the ball were cleaned ultrasonically in acetone for 5 min, in ethanol for 5 min, then dried using an air jet. The cotton used for forming the transfer film was supplied by Rieter Textile Systems (Winterthur, Switzerland). It was taken from a production lot just before being subjected to spinning. Its density was 600 tex (g km−1). [5]

The duplex coating with an external nano-smooth fine-grained diamond (SFGD) layer, a thin titanium carbide interlayer and a carbon diffusion layer have been deposited by PACVD on titanium alloy at 600 ◦C. These coatings have already shown low wear against various counterfaces in ambient air. They might have potential applications in the field of prostheses because of their high resistance to corrosion and wear. Rotating pin-on-disc friction tests have been carried out here at room temperature in ambient air, Ringer's solution and synthetic serum to approach the in vivo wear conditions, with a sliding velocity of 0.1ms−1 and a normal load varying in the 0.5–13N range. Diamond-coated Ti–6Al–4V samples were used as the discs. The counterface materials were hemispherical pins fabricated from diamond-coated Ti–6Al–4V, Ti–6Al–4V and Co–28Cr–6Mo alloys, 316L steel and UHMWPE. During the sliding tests, the total wear heights were measured and recorded on-line. After the tests, the final mean wear rates of the pins were determined from the diameter of their wear scars. The friction coefficients and wear rates of the different materials allow one to compare their performance and to demonstrate the potential of the nano-smooth diamond coatings for biomechanical applications.[6]

The carbon fabric composites filled with the particulates of polyfluo-150 wax (PFW), nano-particles of ZnO (nano-ZnO), and nanoparticles of SiC (nano-SiC), respectively, were prepared by dip-coating of the carbon fabric in a phenolic resin containing the particulates to be incorporated and the successive curing. The friction and wear behaviors of the carbon fabric composites sliding against AISI-1045 steel in a pin-on-disk configuration are evaluated on a Xuanwu-III high-temperature friction and wear tester. The morphologies of the worn surfaces of the filled carbon fabric composites and the counterpart steel pins are analyzed by means of scanning electron microscopy. The effect of the fillers on the adhesion strength of the adhesive is evaluated using a DY35 universal materials tester. It is found that the fillers PFW, nano-ZnO, and nano-SiC contribute to significantly increasing anti-wear abilities of the carbon fabric composites, however, nano-SiC increase the friction coefficient of the carbon fabric composites. The wear rates of the composites at elevated temperature above 180 ◦C are much larger than that below 180 ◦C, which attribute to the degradation and decomposition of the adhesive resin at an excessively elevated temperature. That the interface bonding strength among the carbon fabric, the adhesive, and the particles is significantly increased after solidification and with the transferred film of the varied features largely account for the increased wear-resistance of the filled carbon fabric composites as compared with the unfilled one.[7]

The surface texture of a harder mating surface has a great influence on frictional behaviour during sliding against softer materials. In the present investigation, experiments were conducted using a Pin-on-Plate inclined sliding tester to study the effect of the surface texture of hard surfaces on the coefficient of friction and transfer layer formation. 080 M40 (EN8) steel plates were ground to attain surfaces of different texture with different roughness. Pure magnesium pins were then slid at a sliding speed of 2 mm/s against the prepared steel plates. Scanning electron micrographs of the contact surfaces of pins and plates were used to reveal the morphology of transfer layer. It was observed that the coefficient of friction, formation of
transfer layer, and the presence of stick–slip motion depend primarily on the surface texture of hard surfaces, but independent of surface roughness of hard surfaces. The

effect of surface texture on coefficient of friction was attributed to the variation of ploughing component of friction for different surfaces. [8]

Micro- and nano-sized hot-pressed silicon carbide pins have been characterized by room-temperature unlubricated disk-on-pin tribological tests on hot-pressed silicon carbide and silicon nitride discs. The mean grain size was shown not to influence the steady state friction coefficient. The mean grain size clearly affected the disc wear rate: the finer was the grain size the lower was the disc wear rate. No impact of the grain size was observed on the pin wear rate. The basic wear mechanisms were grain fracture and fine abrasion. By depth-sensing indentation, it was shown that a possible explanation of the different wear behaviour between micro- and nano-sized silicon carbide are the values of mechanical properties, especially hardness, when they are measured on volumes scaling with the material microstructure. [9]

The friction and wear properties of an epoxy resin (EP) reinforced by either a glass fiber weave (G/EP) or a carbon/aramid hybrid weave (CA/EP) are reported. The tribological data is collected using a custom-made Pin-On-Disk apparatus which measures wear rates ($\dot{w}$), coefficients of friction (μ) and disk temperatures. The composites are worn by dry-sliding against smooth steel counter faces under ambient conditions. Tests are performed at nine different combinations of contact pressure (p) and sliding velocity (v) also referred to as pv conditions. The purpose is to systematically compare the performance of the differently reinforced materials while going from mild to rougher sliding conditions. It is found that μ on average is reduced by 35% by substituting the glass fiber weave with the carbon/aramid weave. The coefficient of friction furthermore seems to be roughly independent of p and v. CA/EP shows superior wear behaviour at the six mildest pv conditions with the wear rate an average factor of 22 lower than the G/EP rates. At the three roughest pv conditions CA/EP shows complete failure, while G/EP shows a relatively steady tribological behaviour despite decomposition and development of larger-scale cracks. [10]

The dry friction and wear characteristics of several kinds of cast irons under the conditions of high sliding speed and high contact pressure was intended here. The friction tests with a cast iron pin sliding on a mild steel disk were carried out by using the originally designed pin-on-disk type test rig. Five kinds of cast irons which had difference in the structure, the component, the hardness and the thermal conductivity were tested here. The variations of the friction force, the wear rate and the temperature rise were experimentally measured, and the relations among them were clarified from the points of aforementioned properties of cast irons. From the experimental results, the following things became clear. The wear rate of each cast iron under severe sliding conditions was strongly influenced by the hardness change with the friction-induced temperature rise. The coefficient of friction of each cast iron converged to some constant value with the increment of sliding distance, and this converged value was independent of the contact pressure and decreased with the increment of sliding speed. Finally, some empirical formulae were derived for the friction and wear characteristics of each cast iron. [11]

AA2219 aluminium alloy which has gathered wide acceptance in the fabrication of light weight structures requiring a high strength to weight ratio. Compared to the fusion welding processes that are routinely used for joining structural aluminium alloys, friction stir welding (FSW) process is an emerging solid state joining process in which the material that is being welded does not melt and recast. This process uses a non-consumable tool to generate frictional heat in the abutting surfaces. The welding parameters and tool pin profile play major roles in deciding the weld quality. In this investigation, an attempt has been made to understand the effect of welding speed and tool pin profile on FSP zone formation in AA2219 aluminium alloy. Five different tool pin profiles (straight cylindrical, tapered cylindrical, threaded cylindrical, triangular and square) have been used to fabricate the joints at three different welding speeds. The formation of FSP zone has been analysed macroscopically. Tensile properties of the joints have been evaluated and correlated with the FSP zone formation. From this investigation it is found that the square pin profiled tool produces mechanically sound and metallurgically defect free welds compared to other tool pin profiles. [12]

The influence of the counter materials on wear and friction performance of polytetrafluoroethylene (PTFE) reservoirs arranged in distinct patterns on coated surfaces. Al-bronze and Mo coatings were deposited on a mild steel substrate using an atmospheric plasma spray process. Three patterns of PTFE reservoirs were used. Pins, which served as counter surface, were made of three different materials. Wear tests were carried out in a pin-on-disc test rig at room temperature and under dry contact conditions. The tests were carried out at a constant pressure of 10 MPa. An average linear speed of the test disc was 0.036 m/s. The importance of appropriately matched hardness of two surfaces in sliding contact is emphasised. Due to inadequate hardness of the counter material, performance of Mo coating was adversely affected and expected beneficial action of PTFE reservoirs severely hindered. Al-bronze coating proved to be performing far better than Mo coating. Serious deterioration of Mo coating occurred faster than that for Al-bronze coating. [13]

The frictional behaviour of wet clutches in vehicle drive trains is critical for their overall behaviour. During the development of new wet clutch systems there is a need to know this friction behaviour. The transferred torque is normally investigated in test rigs where the friction in a sliding interface between a friction disc and separator disc is investigated. These test rigs can be designed differently, depending on the working conditions of the investigated clutch. However, it is possible today to simulate the clutch behavior and not limit ourselves to only using measurements from test rigs for the design of the wet clutch. The torque transferred by the clutch during engagement can be roughly divided into full film torque and boundary lubrication torque. The full film regime is possible to simulate quite well, whereas the friction in the boundary regime is much more difficult to simulate due to its strong additive dependency. To obtain a good prediction of the total engagement, friction measurements in the boundary lubrication regime are still needed. These measurements should be easy to perform and fast tests are preferable. Friction coefficients for the whole range of sliding speed, interface temperature and nominal surface pressure should be measured. To use these measurements in simulations and get a better understanding of the friction behaviour, it is also preferable to conduct these measurements on a small test sample, for which the

temperature and sliding speed can be regarded as constant. Here, the friction of a small sample of a wet clutch friction disc is investigated in a pin on disc test and the temperature is measured in the sample during the tests. Measurements are compared with measurements from a test rig for whole friction discs. A good correspondence between the frictional behaviours of the different measurement methods is achieved. [14]

The wear phenomena of implants is a challenge: friction–corrosion of biomaterials, which constitute orthopaedic implants, is a significant issue concerning the aseptic loosening. This work aims at studying AISI 316L/bone cement friction which is a tribological problem related to hip joint cemented prostheses. This study focuses on the ionic strength effect on the tribological behaviour of 316L/bone cement and 316L/PMMA contacts. PMMA poly (methylmethacrylate), can be considered as a model material for bone cement because of vicinity of mechanical properties and PMMA transparency. Pin on disk friction tests were investigated, in different media with the increase in NaCl concentration. Friction coefficient and free corrosion potential of 316L sample were monitored. Moreover, SEM-FEG and micro Raman spectroscopy analyses were investigated on samples surfaces. Friction coefficient evolution according to ionic strength, for 316L/bone cement and 316L/PMMA contacts, are opposite. Indeed, when the ionic strength increases, the friction coefficient decreases, for 316L/PMMA contact (for 316L/bone cement contact). The free corrosion potential decreases in both cases but more drastically for 316L/PMMA contact with increasing of ionic strength. One might suggest that ions adsorption on 316L and PMMA surfaces involves attraction between surfaces in contact. On the contrary, ions adsorption on bone cement has no effect in terms of surface attraction forces, the gap between surfaces is too big due to roughness of bone cement. If ions concentration increases, the tribofilm viscosity between 316L and bone cement could increase. Attraction forces between surfaces are the less significant phenomenon compared to lubricant effect of tribofilm, 316L/bone cement contact. SEM-FEG analysis highlighted principally deep grooves on 316L surface, corrosive wear after destruction of passive film by friction. Finally micro-Raman spectroscopy results, on metal surface, show principally Fe3O4 and Cr2O3 oxides

deposits. Further investigations are in progress for understanding surfaces interactions during friction. [15]

Sliding experiments were conducted using pure magnesium pins against steel plates using an inclined pin-on-plate sliding tester. The inclination angle of the plate was varied in the tests and for each inclination angle, the pins were slid both perpendicular and parallel to the unidirectional grinding marks direction under both dry and lubricated conditions. SEM was used to study morphology of the transfer layer formed on the plates. Surface roughness of plates was measured using an optical profilometer. Results showed that the friction, amplitude of stick-slip motion and transfer layer formation significantly depend on both inclination angle and grinding marks direction of the plates. These variations could be attributed to the changes in the level of plowing friction taking place at the asperity level during sliding. [16]

Surface texture of harder mating surfaces plays an important role during sliding against softer materials and hence the importance of characterizing the surfaces in terms of roughness parameters. In the present investigation, basic studies were conducted using inclined pin-on-plate sliding tester to understand the surface texture effect of hard surfaces on coefficient of friction and transfer layer formation. A tribological couple made of a super purity aluminium pin against steel plate was used in the tests. Two surface parameters of steel plates, namely roughness and texture, were varied in the tests. It was observed that the transfer layer formation and the coefficient of friction along with its two components, namely, the adhesion and plowing, are controlled by the surface texture and are independent of surface roughness (*R*a). Among the various surface roughness parameters, the average or the mean slope of the profile was found to explain the variations best. Under lubricated conditions, stick–slip phenomena was observed, the amplitude of which depends on the plowing component of friction. The presence of stick–slip motion under lubricated conditions could be attributed to the molecular deformation of the lubricant component confined between asperities.

In the present experimental study, pins and plates were made of 99.997wt.% purity aluminium and 080 M40 steel, respectively. The pins were 10mm long, 3mm in diameter with a tip radius of 1.5mm. The dimensions of the 080 M40 steel plates were 28mm×20mm×10mm(thickness). The pins were first machined, and then electro-polished to remove any work-hardened layer that might have formed during the machining. Hardness measurements of aluminium pin and steel plate were made at room temperature using a Vickers micro hardness tester with 100 g load and 10-sdwell time. Average hardness numbers, obtained from 5 indentations, was found to be 31 and 208 for the pin and plate, respectively. [17]

considered the advancing, frictional contact problem for a rigid pin indenting an infinite plate with a circular hole. The formulation is general, and considers remotely applied plate-stresses in addition to pin loads. Using the theory of generalized functions, it is found that the governing equation in full sliding is a singular integro-differential equation (SIDE). Partial-slip behaviour is governed by an implicit, coupled singular integral equation (SIE) pair. Numerical solutions are presented for both types of problems. It is found that the contact tractions in monotonic loading become independent of the coefficient of friction above a certain threshold value. Finally, problems involving typical 'fretting-type' pin loads with and without remote-stresses are also investigated, revealing remarkable effects of the degree of conformality and load path on the steady-state traction distributions. [18]

Frictional and wear properties of Al–25Zn–3Cu–3Si alloy were investigated over a range of pressure and sliding speed using a pin-on-disc test machine. The friction coefficient of the alloy increased with sliding speed, but decreased with increasing pressure up to 1.5MPa, above which the trend reversed. However, the temperature and wear volume of the alloy increased continuously with increasing pressure and sliding speed. A fine-grained layer and a region with flow lines were observed underneath the surface of the wear samples. The formation of these regions was related to smearing of wear particles and heavy deformation of surface material, respectively. [19]

The tribological test done with using a pin-on-disc geometry with textured SKD 11 pin on bearing steel disc, under sliding in paraffin oil .Micro-grooved cross-hatch pattern has been fabricated with various angles and widths.The effects of geometrica lparameters on friction were mainly examined in mixed and elasto hydrodynamic lubrication. The results show that friction control can be achieved by fabricating the micro-grooved cross hatch pattern on a contact surface .It is observed that each geometrica lparameter of texture influence on friction, especially decrease of groove aspect ratio and increases of groove sliding length show friction reduction performance. Crucial parameter GI was proposed for micro-grooved cross hatch texture. The friction mechanism is explained by micro fluid flow with limited theoretical approach. [20]

Friction coefficients and specific wear rates of an existed Ni3Al-based NAC-alloy with composition of Ni–18.8Al–10.7Fe–0.5Mn–0.5Ti–0.2B (at.%) and its composites reinforced by 6 vol.% Cr3C2- and 6 vol.% MnS-particles, respectively were investigated for the initial understanding of sliding wear behaviours of the materials under unlubricated condition. The testing materials were prepared by hot isostatic pressing (HIP) process. Pin-on-Disk (POD) measurements were carried out under room temperature condition. A commercial vermicular graphite cast iron was selected as a reference material. The disks used in this study were made of a grey cast iron as cylinder liner materials of ship engines. The contact pressure of 2.83MPa and 5.66MPa were applied in POD tests. The experimental results revealed that the monolithic NAC alloy has the almost same values of friction coefficient and specific wear rate under the testing condition as compared to a commercial vermicular cast iron. The wear mechanism is probably conducted to its intrinsic deformation mechanism of the Ni3Al-type of intermetallics. For the composite with 6 vol.% hard Cr3C2-particle, wear rate was reduced on both sides of pin and disk up to 50%, comparing to the single phase NAC-alloy at a high load of 5.66 MPa. By an addition of 6 vol.% soft MnS-particle, wear rate of the disk was dramatically decreased and friction coefficient also slightly reduced on the test. But, the wear rate of pin is maintaining as the same level as the monolithic NAC-alloy and the reference vermicular cast iron. The present investigation recognized that it will be potential to develop Ni3Al-matrix composites reinforced by hard Cr3C2-

and/or soft MnS-particles for a certain tribological applications, especially other excellent physical, chemical and mechanical properties of the Ni3Al-based intermetallic materials were considered. [21]

A pin-on-disk configuration was used to perform the unlubricated sliding wear tests. Low alloy and tool steels were employed as pin and disk materials, respectively. A normal load of 35 N and a sliding velocity of 0.1 m/s were selected. Interrupted tests were performed to study the evolution of worn surfaces in terms of appearance, surface roughness and microhardness. Measurements of temperature below the sliding surface of pins were conducted to evaluate the thermal effect on the operating wear regimes. The removal of wear particles was carried out to analyze the role of debris on the action of the oxidative wear mechanism. The characterization of worn surfaces was complemented with stereoscopy microscopy (SM) and scanning electron microscopy (SEM) methods. The theoretical and experimental analysis of surface temperature showed that the thermal effect was not considerable to promote the oxides formation and there was not a significant difference between those conditions exhibiting the mild and severe wear regimes. The friction and wear results of the sliding test with removal of wear debris showed that wear particles had a relevant contribution on the value of the friction coefficient (approximately 50%) and an insignificant role on the oxidative wear mechanism. Surface roughness and microhardness evolution of worn surfaces suggest that a transition from elastic to plastic contact seems to be crucial to promote the wear regime transition from mild to severe wear, respectively. [22]

The effect of the microstructure on the dry sliding wear of six aluminium alloy 6061 matrix composites reinforced with 15 vol.% of MoSi2 particles and two monolithic 6061 alloys processed by powder metallurgy with and without ball milling has been studied. Wear testing was undertaken using pin-onring configuration against an M2 steel counterface at 0.94 m/s and normal load of 42, 91 and 140 N. The wear resistance of the aluminium alloys was significantly improved by ball milling and the addition of reinforcing MoSi2 particles due to a more stable and more homogeneous microstructure, which avoids the detachment of the mechanically mixed layer. Wear rate

of materials in T6 decreases as solutionized hardness of the materials increases. This behaviour is rationalized by taking into account the precipitation
state of the matrix. In addition, wear rate follows a Hall–Petch type relationship, showing that
the reduction of matrix grain size plays an important role in the increase in the wear resistance of the composites. The results indicate that the present intermetallic reinforced composites can be considered potential substitutes for ceramic reinforced aluminium alloys in tribological applications. [23]

The irreversible thermodynamic theory is employed to study the rate of wear as a degradation process in a dry sliding system. It is shown that the wear rate is linearly related to the entropy flow rate. The linear correlation between rates of wear and entropy is verified experimentally for a pair of materials in dry sliding. Degradation coefficient is obtained and a simple approach is proposed for prediction of wear in dry sliding configuration. [24]

The developers of innovative automotive active systems have recently stimulated new interest toward the analysis of the frictional behaviour of brake and clutch facings. This paper presents the experimental results acquired with a laboratory setup on brake and clutch facing samples in sliding motion for different operating conditions. An artificial neural network has been used to obtain a comprehensive view of the influence of the main sliding parameters. The study has also taken into account the not weak influence of the sliding acceleration to improve the friction coefficient prediction during transient operations of these dry friction based devices. [25]

The model estimates the magnitude and direction of the frictional force, the pin torque, the probability of asperity contact and the real area of contact distinguishing between the part due to elastic and plastic asperity contacts respectively. Therefore, the proposed model is suitable for the prediction of adhesive wear. It can be applied to metal contacts for conductance characterisation through the plastically deformed asperities which is of great interest for electrical contact resistance studies. [26]

The effect of adding Cr3C2, VC or a mixture of both as a grain growth inhibitors to cemented carbides obtained from WC–12 wt.% Co nano-crystalline mixtures on the behaviour of friction and dry sliding wear have been studied. All the wear tests were performed on a tribometer with ball on disc configuration, using a WC–6 wt.% Co ball as a counterpart with normal contact loads of 40 and 60 N, sliding distance of 2000 m and a sliding speed of 0.1 m/s. A significant reduction in the wear rates was observed by the effect of the aforementioned additives, in particular for the VC, which showed an increase in the wear resistance of the order of 90%. The analysis of wear and surface damage were correlated to the observed behaviour. [27]

The wear of a W–25 wt%Cu composite against 52100 steel was used to demonstrate this approach with pin-on-disc tests conducted under three normal loads. An energy-dependent criterion, namely, specific wear volume (wear volume/dissipated energy (mm3/J)), was defined to evaluate the wear of the composite. The specific wear volume can be used as a substitute for the traditional wear rate due to the simultaneous expression of several wear parameters and because of its strong dependence on the wear mode. The specific wear volume appears to be constant in any particular “wear mode” regardless of the active “wear processes”. In the wear of this composite, processes such as particle pull-out, mechanically mixed layer (MML) formation, crack propagation and delamination were observed. But, combination of these processes in each test had identical specific wear volumes. Thus, all of these wear processes were considered to be consecutive stages of the same wear mode: fatigue wear. The amount of dissipated energy and the volumetric loss increased with increasing normal load. Also, changing the normal load changed the rate of energy dissipation per unit sliding distance. [28]

Compared to untextured gray cast iron surfaces, the texture patterns showed significant tribological improve- ments. Long durability tests also highlighted the long term usefulness of surface texturing. The dominant wear mode of the texture patterns was

found to be mechanical polishing and the tribological behaviour was found to be largely independent of the type of lubricant or refrigerant.

Scuffing is another tribological failure, which is of major concern for compressor manufactures as it occurs abruptly, leading to complete destruction of the sliding pair, thus rendering the device non-functional. Several factors affect scuffing such as contact pressure, sliding velocity, contact temperature, lubricant and lubrication regime, surface topography and materials. Thus there is a need to also investigate solutions other than the ‘‘traditional’’ approaches of protective coatings and explore innovative surface engineering solutions such as surface texturing.[29]

The literature review shows that laser surface texturing is widely used in tribological analysis. This technique is much costly and it rarely used in developing countries .By this technique micro dimples can be produced fastly and too much accurately but with the help of chemical etching this work can also be obtained cost-effectively. In developing countries where resources are not sufficient chemical etching can be effective technique to produce micro structures in surfaces where relative motion is occurring. It has been observed that in chemical etching the worker should be skilled and should have very good experience in transferring the photo film on disc and application of etchant. The researchers have not gone through chemical etching and then tribological analysis on it. It has been observed that work has been carried out to pin on disc so there is requirement that test may be taken on pin on disc with dry as well as wet condition according to ASTM norms.

CHAPTER 3

SYSTEM DEVELOPMENT AND EXPERIMENTAL PROCEDURE

3.1 DESIGN OF EXPERIMENT

The experiment is design to evaluate the coefficient of friction on textured plate and plain plate for two pins of Brass and Mild Steel on mating surface with Mild steel plate. This experiment is done with three parameters which are as following.

LOAD(N)	9.8	19.6	29.4	39.2	49
SPEED(RPM)	200	400	600	800	1000
TRACK DIAMETER (MM)	130	110	50		

All the three parameters are used for evaluating the coefficient of friction for the different regime of lubrication. And further there is comparision of coefficient of friction between plain plate and textured plate.

DIFFERENT REGIMES OF LUBRICATION-

1. Dry Lubrication
2. Elasto hydrodynamic Lubrication
3. Hydrodynamic Lubrication

3.2 PIN ON DISC SIMULATION

Fig 4: Pin on Disc type Tribometer Friction & Wear Machine set up

The Tribotech Tribometer uses a pin-on-disk system to measure wear. The unit consists of a gimballed arm to which the pin is attached, a fixture which accommodates disks up to 165 mm in diameter & 8 mm thick, an electronic force sensor for measuring the friction force, and a computer software (WINDUCOM) for displaying the parameters, printing, or storing data for analysis. The motor driven turntable produces up to 3000 rpm. Wear is quantified by measuring the wear groove with a profilometer (to be ordered separately) and measuring the amount of material removed. Users simply specify the turntable speed, the load, and any other desired test variables such as friction limit and number of rotations.

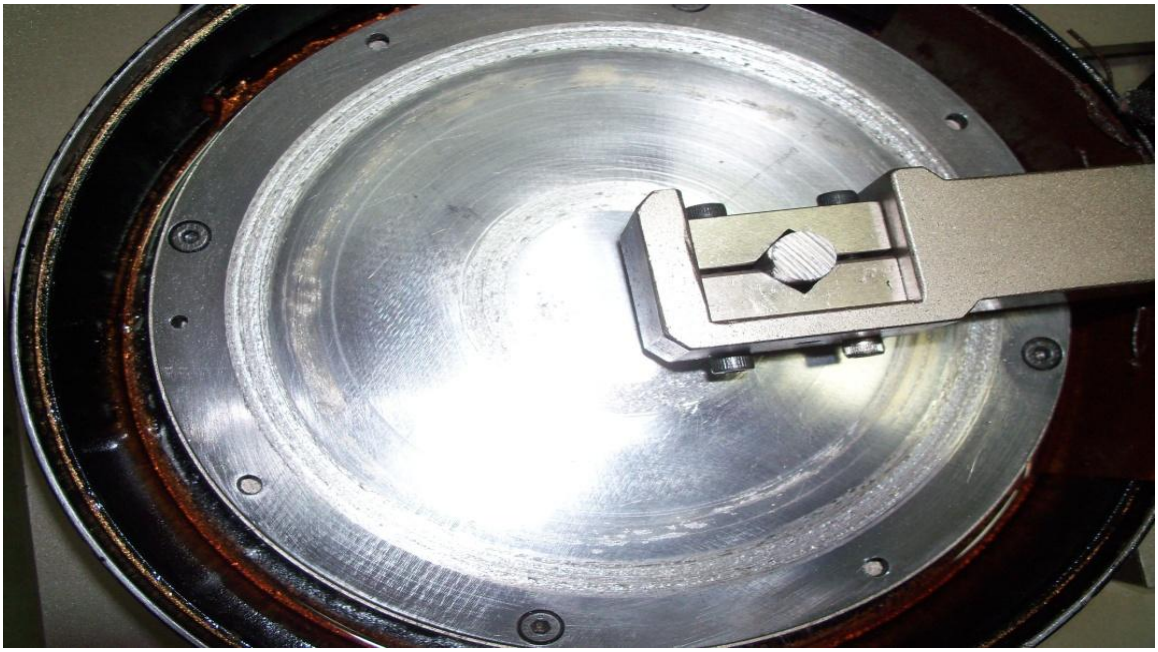

Fig 5: PIN CONTACT WITH DISC

Fig 6 : DISC WITH DIFFERENT TRACK DIAMETER

Designed for unattended use, a user need only place the test material into turntable fixture and specify the test variables. A pre-determined Hertzian pressure is automatically applied to the pin using a system of weights. while applying this force to the pin includes sliding wear as well as a friction force. Since pins can be fabricated from a wide range of materials virtually any combination of metal, glass, plastic, composite, or ceramic substrates can be tested.

Software included with this model provides for quick calculation of the Hertzian pressure between the pin and disk. The cup-like (housing) enclosed fixture permits the use of liquid lubricants during a wear test (optionally).

Specifications

Parameter	Unit	Min	Max
Pin Size	Mm	3	12
Ball Diameter	Mm	10	12.7
Disc Size	Mm	165 x 8 mm Thick	
Sliding Speed	M/s	0.05	10
Disc Rotation	RPM	200	2000
Normal Load	N	0	200
Frictional Force	N	0	200
Wear	Mm	0	2
Track Radius	Mm	to be set manually	

Table 2: Specification of pin on disc machine

Data Acquisition

The friction coefficient signal is displayed in real time on a PC Screen. Data can be viewed as it is logged for the entire specified test duration, which can be recalled later for detailed analysis. The software allows 9 different logged test files for on-line analysis

/ mapping The software displays the test time, turn count, linear velocity, and user-defined test parameters. This data can be stored and printed along with the friction traces.

Purpose

Records friction and wear in sliding contact in dry, lubricated, controlled environment and partial vacuum.

Application

Fundamental wear studies. Wear map ping and PV diagrams. Friction and wear testing of metals, ceramics, soft and hard coatings, plastics, polymers and composites, lubricants, cutting fluids, heat processed samples.

Features

- Displays and records friction, wear and pin temperature (optional).
- Dry, lubricated, controlled environment and vacuum tests (optional).
- Wide sliding speed range (continuously variable thru the variable drive)
- User can program RAMP tests to be specified by the user (available optionally)

Standards

ASTM G-99

Instrumentation and Data Acquistion System for the measurement of:

- RPM
- Wear
- Frictional force
- Temperature
- Electrical Contact resistance measurement (40 mV Signal)

PC acquires data online and displays it in several ways. Graphs of individual tests can be printed. Results of different tests can be superimposed for comparative viewing. Data can be exported to other software.

- Tests @ ambient temperature
- Dead weight loading
- Electrical contact resistance measurement
- Displays Load, Friction, temp, rpm / speed on the display panel
- Auto on/off (timer)

3.3 SPECTROSCOPY ANALYSIS

Spectrographic metals analysis is usually the 'heart' of most oil analysis programs. Using a Rotrode Emission 20 or more metals/substances can be simultaneously determined. The metals analyzed for include wear, additive, and contaminant metals and are reported in parts per million (ppm). The instrument is quick and easy to operate and is accurate within acceptable limits.

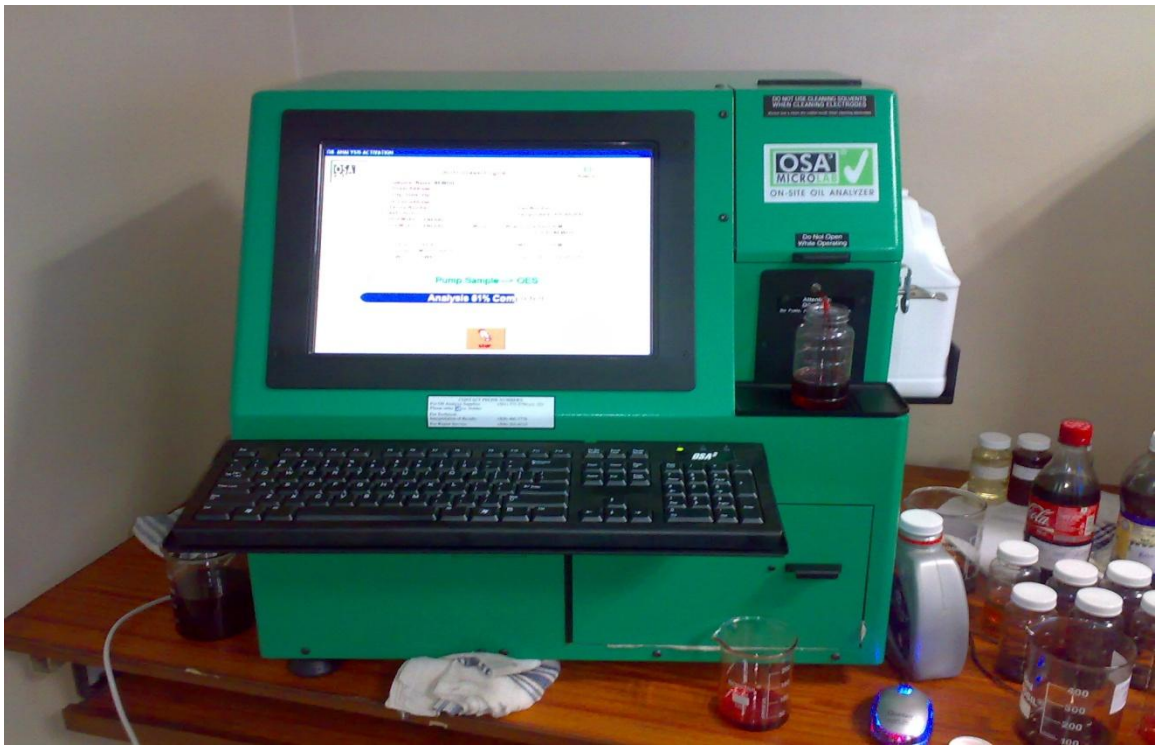

Figure 7 : Oil spectroscope

The Spectrometer has a particle size detection limitation of between 3µ and 10µ (depending on the particular metal in question and the amount of surface oxidation on the particle surface). Results of the Spectrometer are accurate to about 1 or 2 ppm. The advantage of the Spectrometer is that no dilution of the sample is required.
For routine lube oil analysis, accuracy below the 1 ppm level is not required. The results are very trendable from sample to sample if the sampling interval doesn't exceed every three months and proper sampling procedures are adhered.

3.4 DESIGN OF DISC

3.4.1 Experimental procedures for chemical Etching

Microscopic examination is usually limited to a maximum magnification of 1000X - the approxi- mate useful limit of the light microscope, unless oil immersion objectives are used. Many image analysis systems use relay lenses that yield higher screen magnifications that may make detection of fine structures easier. however, resolution is not improved beyond the limit of 0.2-0.3-µm for the light microscope. Microscopic examination of a properly prepared specimen will clearly re- veal structural characteristics such as grain size, segregation, and the shape, size, and distribution of the phases and inclusions that are present. examination of the microstructure will reveal prior mechanical and thermal treatments give the metal. Many of these microstructural features are measured either according to established im- age analysis procedures, e.g., ASTM standards, or internally developed methods.Etching is done by immersion or by swabbing (or electrolytically) with a suitable chemical solution that essentially produces selective corrosion. Swabbing is preferred for those metals and alloys that form a tenacious oxide surface layer with atmospheric exposure such as stainless steels, aluminum, nickel, niobium, and titanium and their alloys. It is best to use surgical grade cotton that will not scratch the polished surface. etch time var- ies with etch strength and can only be determined by experience. In general, for high magnification examination the etch depth should be shallow; while for low magnification examination a deeper etch yields better image contrast. Some etchants produce selective results in

that only one phase will be attacked or colored. A vast number of etchants have been developed.

etchants that reveal grain boundaries are very important for successful determination of the grain size. Grain boundary etchants are given in [1-3, 9]. Problems associated with grain boundary etching, particularly prior austenite grain boundary etching, are given in [2, 10 and 11]. Measurement of grain size in austenitic or face-centered cubic metals that exhibit annealing twins is a commonly encountered problem. etchants that will reveal grain boundaries, but not twin boundaries, are reviewed in.

3.4.2 Steps For Etching Steel

1-Choose the type of steel you want to etch. You can etch stainless steel, mild steel, or high-carbon steel. Which type of steel you etch will determine the best acid or chemical to use to etch it with.

2-Remove any burrs on the edges of the steel. File away any burrs on the side of the steel you plan to etch with acid. You can leave the burrs on the other side if you're etching a steel plate.

3- Scrub the steel. Use a chlorine cleanser on an abrasive sponge, a wire brush, fine steel wool, wet number 600 emery paper, or corundum paper, scrubbing in a circular motion. You want to leave the surface just gritty enough to grip the resist material, but not so scratched that you end up etching extra lines that aren't part of your design.

4- Rinse the steel with water. The water should sheet off the steel surface. Clean the steel a second time with isopropyl alcohol.

5-Choose the image you want to etch into the steel. You can either draw a freehand image or replicate an existing image onto the steel surface. Depending on which transfer method you use, you can have a fairly simple design or a complex one.

If you plan to replicate an existing design, choose something in high-contrast black and white.If you plan to make and sell prints of your etching, choose an image in the public domain or get the permission of the copyright holder, if there is one.

Transfer your design onto the steel surface. You can transfer the design in A of several ways, as described below. Be aware that however you transfer your design, it will print the reverse of the way you etch it into the steel. If you plan to use the etched steel plate solely as a decoration, not to print with, this won't matter to you.

The oldest method for transferring designs is to coat the steel surface with a liquid varnish or wax-like substance (like beeswax), or even enamel paint or nail polish. This coating is called a ground. You then scratch your design into the ground using needles or wider-bladed cutting tools. (This is similar to woodcutting.) The ground will serve as a resist to keep the etching acid off the steel it covers.

Another method is to cover the steel surface with permanent markers in those places where you want the acid not to etch the steel and leave the surface exposed where you want to etch the steel. You may need to experiment with several brands and colors of permanent marker to determine which make the best resists .

A third method is to create an iron-on stencil by either photocopying an image onto transfer paper or printing it onto glossy photo paper with an inkjet printer. Place the paper onto the steel surface, image-side down, and using a clothes iron set to "high," iron with smooth, circular strokes for 2 to 5 minutes. (Press gently if using transfer paper; press hard if using photo paper.) You can then remove the paper. (Transfer paper will peel away on its own, but photo paper requires soaking in a tray of hot water to soften it for removal.) The transferred ink becomes the resist for the etching acid. Cover the steel's edges. You can tape over the edges or paint them. Either method keeps the acid from etching the edges.Choose the acid you want to etch the steel with. Possible acids include muriatic (hydrochloric) acid (HCl), nitric acid (HNO_3), or sulfuric acid (H_2SO_4). Certain non-acids that form acid in water, such as ferric chloride ($FeCl_3$) or copper sulfate ($CuSO_4$), can also be used as etching chemicals. How strong the acid is generally determines how fast the steel will be etched, or "bitten." You can obtain etching acids and chemicals through chemical supply stores or electronics supply shops.

Ferric chloride is normally mixed with water in equal parts to form hydrochloric acid in solution. It's more commonly used to etch copper, but it also works well to etch stainless steel. It also works with a wider range of resist materials than pure acids do; however, it

can pit the surface if not attended to properly.Copper sulfate is better suited to etching mild steels than stainless steel. It is best mixed in a 1 to 1 ratio with sodium chloride (NaCl) to keep the copper sulfate from coating the steel with a deposit of copper that will stop the etching process. The blue solution gradually fades as the etching progresses and turns colorless when it'sfinished. Nitric acid is commonly mixed in a ratio of 1 part nitric acid to 3 parts water. It can also be mixed with acetic acid (vinegar), in a 1 to 1 ratio, or with hydrochloric acid.Sulfuric acid should be used only in concentrations from 10 to 25 percent. Generally, dilute solutions are more effective than concentrated ones. Acids generally take longer to etch steel than do chemicals that form acids in water, however.5Immerse the steel in a bath of the etching acid. Usually, you'll want to place the steel plate face-down in the solution so that the exposed metal flakes downward into the solution and away from the plate. This produces cleaner lines when etching the steel. If you put the plate in face up, you can sweep away the flakes as they form with a light brush or feather; this will also remove bubbles that form. (The bubbles impede the etching process, but they can also create interesting designs if left alone.) Leave the steel plate in the etching acid until the lines are cut to the depth you want.

Whether you put the steel plate in the etching acid face-up or face down, suspend it off the bottom of the container in some fashion. (This is particularly necessary when the plate is face down.)Tap the container holding the chemical bath periodically to keep the solution agitated.

6-Remove and clean the steel plate. Wash the plate with water to remove the acid. If you used a particularly strong acid, you may also need to use baking soda to neutralize it. You then need to remove the resist; depending on the resist material, use one of the following methods:

Use turpentine to remove paint or varnish grounds. (Use acetone if you used nail polish.)Use alcohol, methyl hydrate, or steel wool for wax-like grounds.Use running water for water-soluble inks and alcohol for inks insoluble in water.

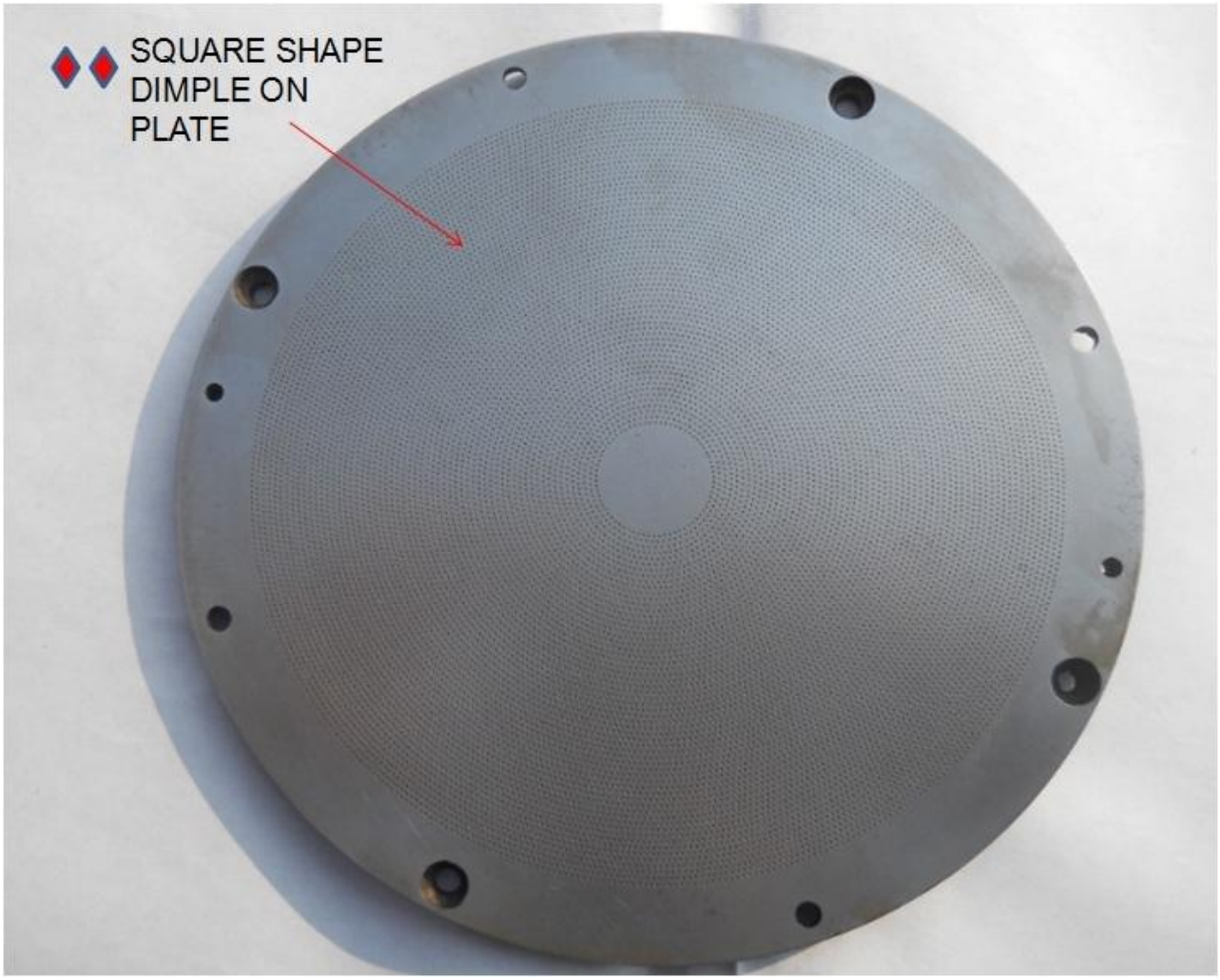

Fig 8: The original disc having the square dimples on the surface

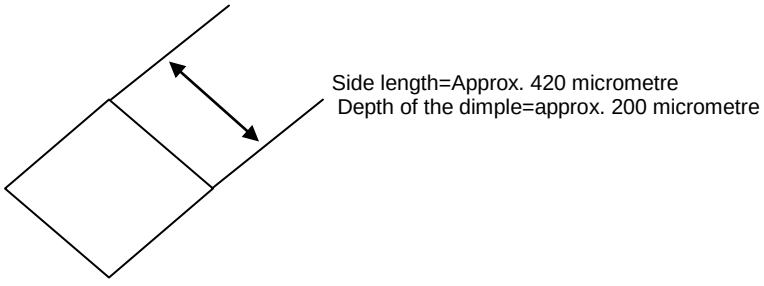

Fig 9: Size of square dimple on plate

Chapter 4

Results and Discussions

4.1 BRASS PIN ON MILD STEEL (M.S) PLATE -The graph between co-efficient of friction vs. speed at various loads for different region of lubrication are shown as following.

4.1.1.DRY LUBRICATION –

4.1.1(A):- Coefficient of Friction vs. Speed for Plain Plate at Track Dia 130 mm

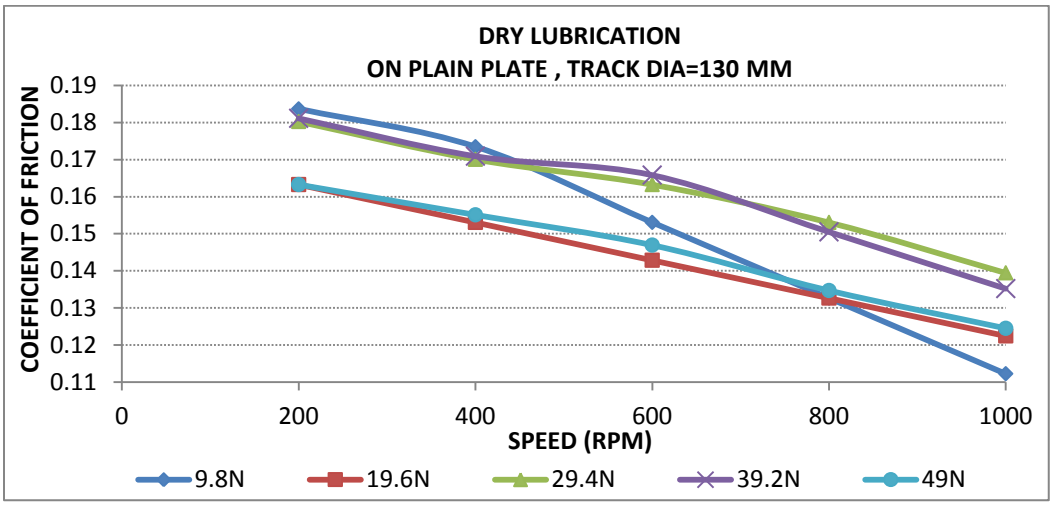

Figure 20

Figure 10 shows the graph between the co-efficient of friction vs. speed at various loading condition on plain plate for 130 mm track dia. The co-efficient of friction is decresing as incresing the load and also same for different sliding speed. At 9.8N load the maximum value of coefficient of friction is 0.18 for 200rpm. As incresing the speed upto 1000 rpm the coefficient of friction decreses and gives the value of 0.11 for same load 9.8N. Further incresing the load upto 49N and continuing the speed trend we get the graph trend same as the 9.8N load curve but the maximum and minimum values are decresing.For 49N the maximum value for coefficient of friction is 0.16 and minimum value is 0.12.

4.1.1(B):-Coefficient of Friction vs. Speed for Textured Plate at Track Dia 130 mm:-

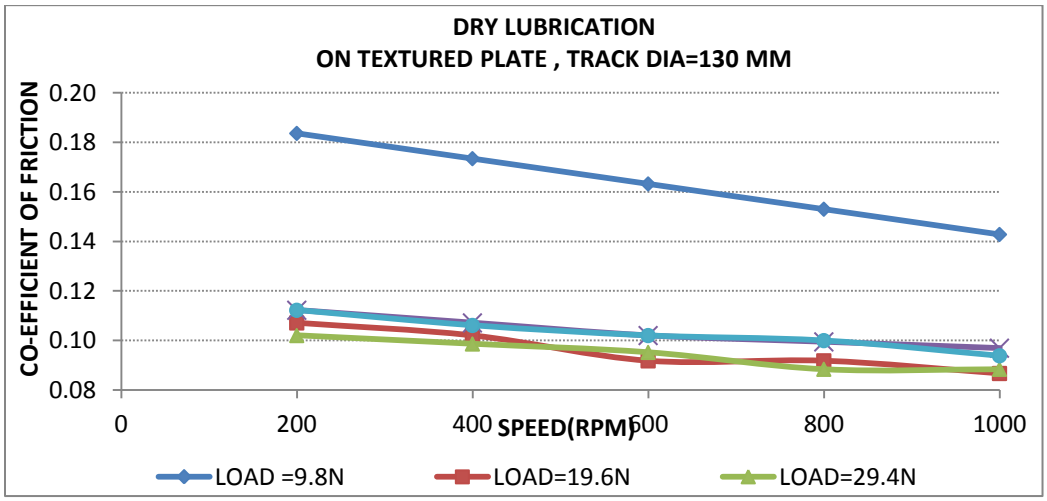

Figure 11

Figure 11 shows the graph the co-efficient of friction vs. speed at various loading condition on textured plate for track dia130mm. The trend is as same as the curve of plain plate. But the maximum and minimum value is less as compare to plain plate.At 9.8N loading the graph is as near to the graph of plain plate. Further incresing the load ,the co-efficient of friction is decresing and on comparing with co-efficient of friction for plain plate, the values are less .At 49N the maximum value of co-efficient of friction is 0.11 and minimum value is 0.95 on textured plate and on plain plate it was respectively 0.16 and 0.12 for same laod 49N.So the coefficient of friction is less on textured plate as compare to plain plate.

4.1.1(C):- Coefficient of Friction vs. Load for Plain Plate at Track Dia 130 mm

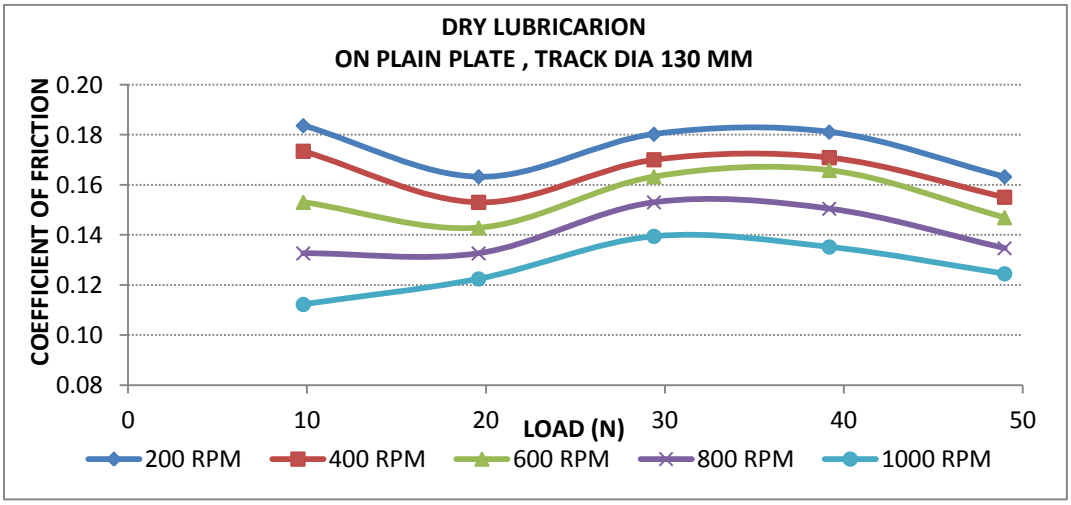

Figure 12

Figure 12 shows the graph between co-efficient of friction vs. load at various speed on plain plate at 130 mm track diameter for dry regime of lubrication. The co-efficient of friction is decresing as incresing the load for a same speed .Further increasing the speed the curve is again decresing in nature with incresing the load. At 200 rpm and the coefficient of friction is 0.18 for 9.8N load and 0.16 for 49 N load and at 1000 rpm, the coefficient of friction value is 0.11 and 0.12 for 9.8N load and 49N load respectively.

4.1.1(D):-Coefficient of Friction vs. Load for Textured Plate at Track Dia 130 mm:-

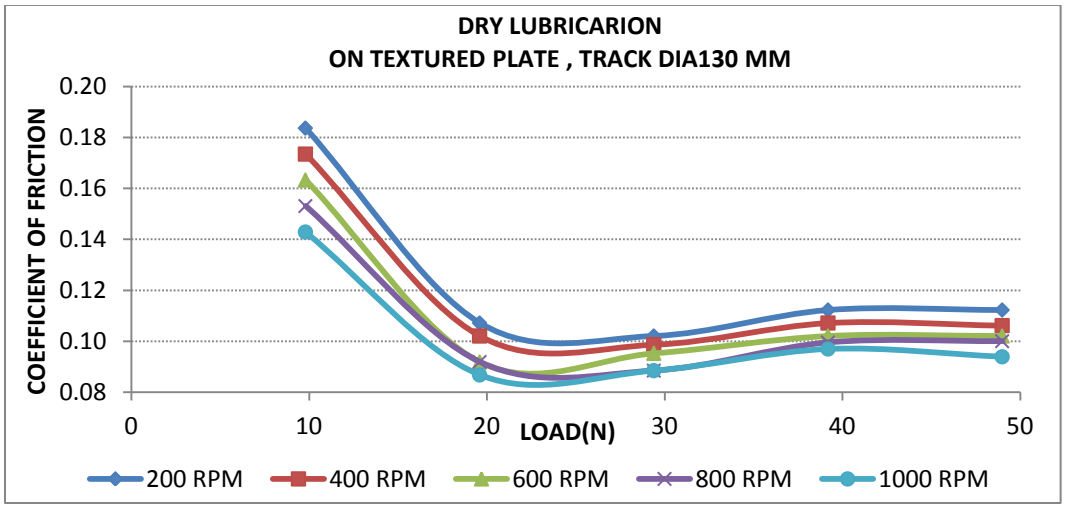

Figure 13

Figure 13 shows the graph between co-efficient of friction vs. load at various speed on textured plate at 130 mm track diameter. The co-efficient of friction is decresing as incresing the load for a same speed . further increasing the speed the curve is again decresing in nature with incresing the load. At 200 rpm, the coefficient of friction is 0.18 and 0.11for 9.8N and 49N load respectively and at 1000 rpm the coefficient of friction value is 0.14 and 0.09 for 9.8N and 49N load respectively. On comparing with palin palte the value of coefficient of friction is less significantly.

4.1.1(E):- Coefficient of Friction vs. Speed for Plain Plate at Track Dia 110 mm:-

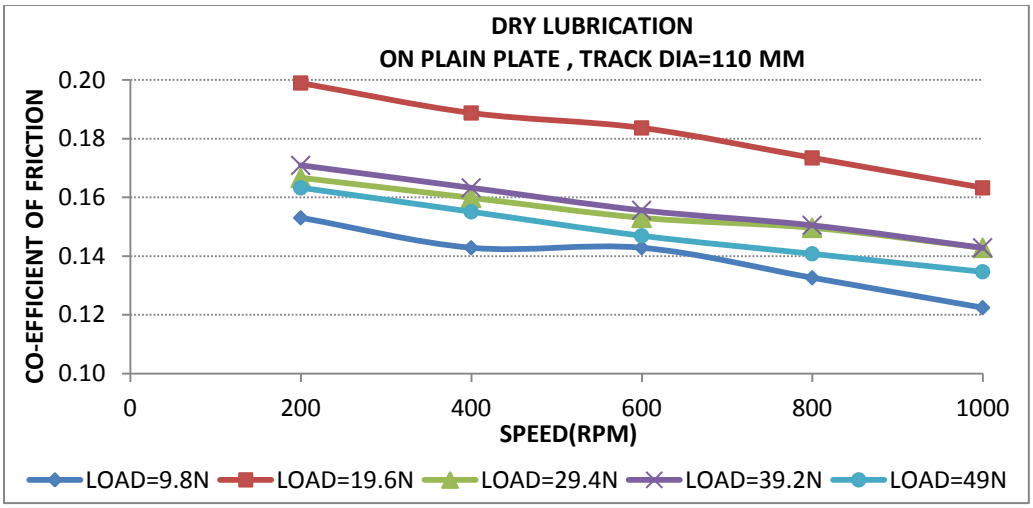

Figure :14

Figure 14 shows the graph between the co-efficient of friction vs. speed at various loading condition on plain plate for 110 mm track dia. On changing the track dia to 110 mm it follows the same pattern as for the 130 mm.At 9.8N load the maximum value of coefficient of friction is 0.17 and incresing the speed upto 1000 rpm it gives the minimum value of coefficient of friction 0.13 for 9.8N load. Further incresing the load upto 49N and continuing the speed trend we get the graph trend is similar as the previous loads graphs.The maximum value for coefficient of friction comes 0.20 for 9.8N.

4.1.1(F):-Coefficient of Friction vs. Speed for Textured Plate at Track Dia 110 mm:-

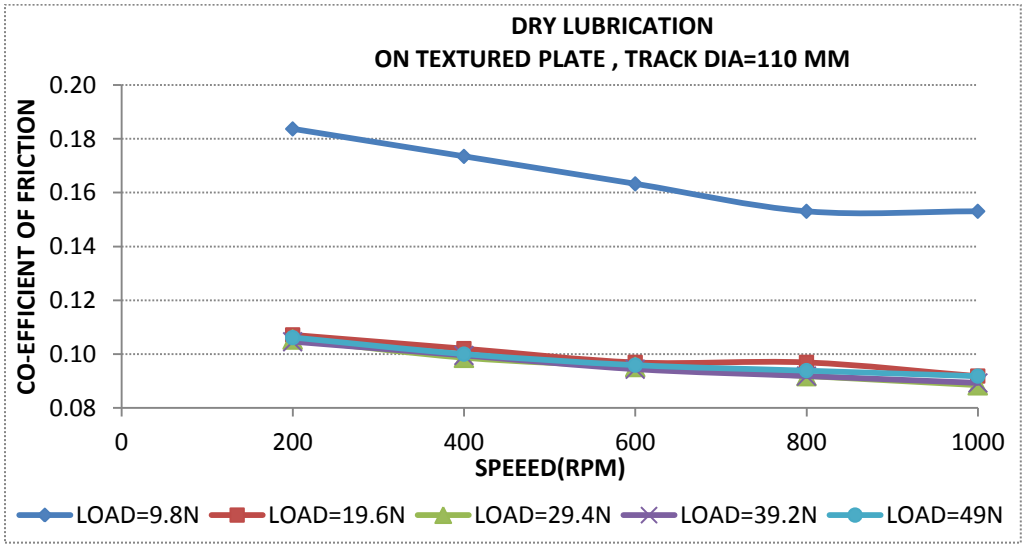

Figure :15

Figure15 shows the graph between the co-efficient of friction with respect to speed at various loading condition on textured plate for track dia110mm. The trend is as same as the curve of plain plate. But the maximum and minimum value is less as compare to plain plate. Further incresing the load, the co-efficient of friction is decresing and on comparing with co-efficient of friction for plain plate, the value are less.At 19.6N the maximum value of co-efficient of friction is 0.11 and minimum value is 0.94 on textured plate and on plain plate it was respectively 0.20 and 0.16 for same laod 19.6N.So the coefficient of friction is less on textured plate as compare to plain plate.

4.1.1(G):- Coefficient of Friction vs. Speed for Plain Plate at Track Dia 50 mm:-

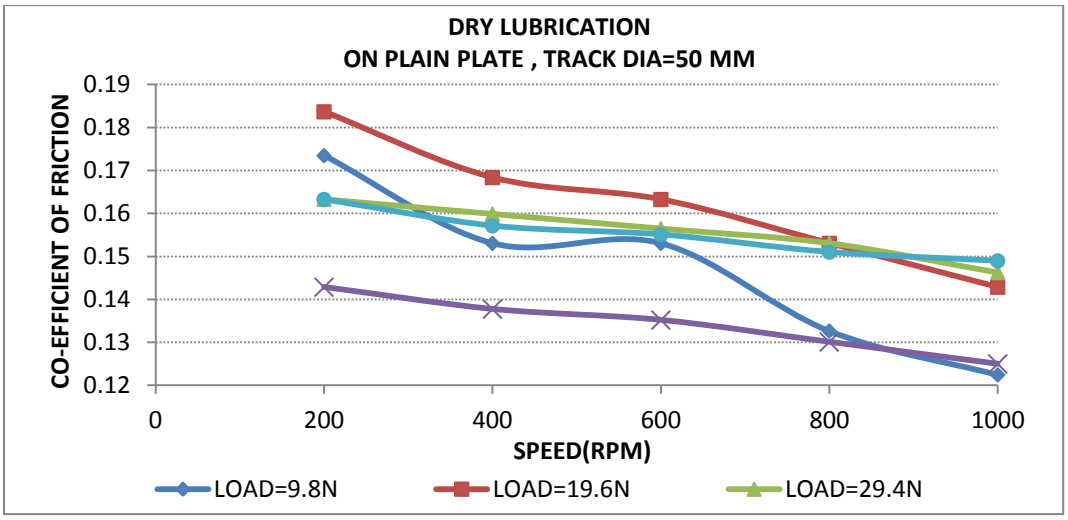

Figure 16

Figure 16 shows the graph between the co-efficient of friction vs. speed at various loading condition on plain plate for 50 mm track dia. The co-efficient of friction is decresing as incresing the load and also same for sliding speed. At 9.8N load the maximum value of coefficient of friction is 0.17 for 200rpm. As incresing the speed upto1000 rpm the coefficient of friction decreses and gives the value of 0.12 for same load 9.8N. Further incresing the load upto 49N , the minimum value for coefficient of friction is come for 39.2 N load and its value is 0.14 and the maximum value 0.18 comes for 19.6N load.

4.1.1(H):- Coefficient of Friction vs. Speed for Textured Plate at Track Dia 50 mm:-

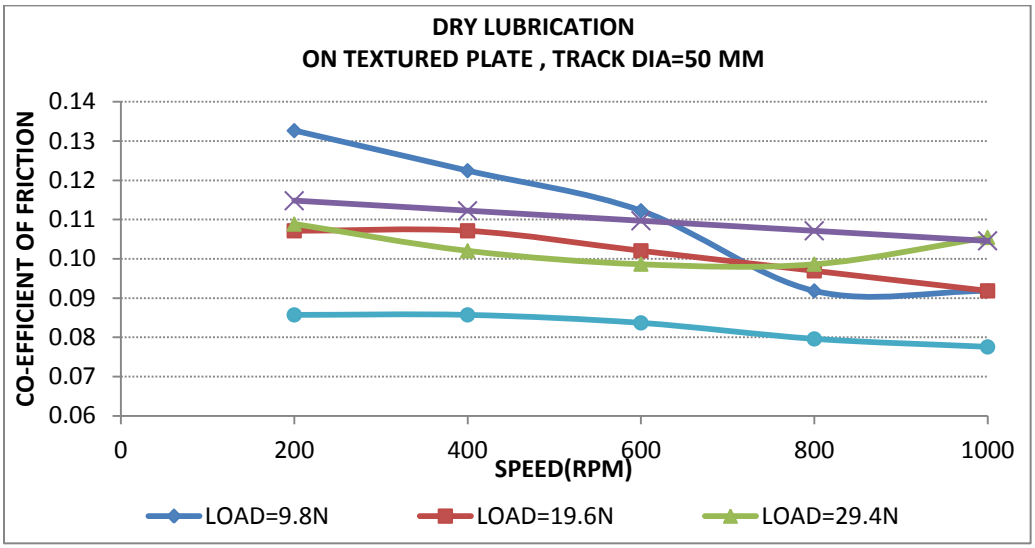

Figure 17

Figure 17 shows the graph between the co-efficient of friction with respect to speed at various loading condition on textured plate for track dia 50mm. The trend is as same as the curve of plain plate. But the maximum and minimum value is less as compare to plain plate.As Incresing the load the co-efficient of friction is decresing and on comparing with co-efficient of friction for plain plate, the value are less. At 49 N load the maximum value of co-efficient of friction is 0.13 at 200 rpm and minimum value is 0.08 at 1000 rpm. On comparing with plain plate at 49N load the coficient of friction is 0.08 at 200 rpm and 0.08 for 100 rpm on textured plate and on plain plate it was respectively 0.16 and 0.15 for 200rpm and 1000rpm at same laod 49N. So the coefficient of friction is less on textured plate as compare to plain plate.

4.1.2 ELASTO HYDRO DYNAMIC LUBRICATION:- The comparison of co-efficient of friction vs. speed at various loads for plain plate and textured plate for different track dia is as following.

4.1.2(A) Coefficient of Friction vs. Speed for Plain Plate at Track Dia 130 mm:-

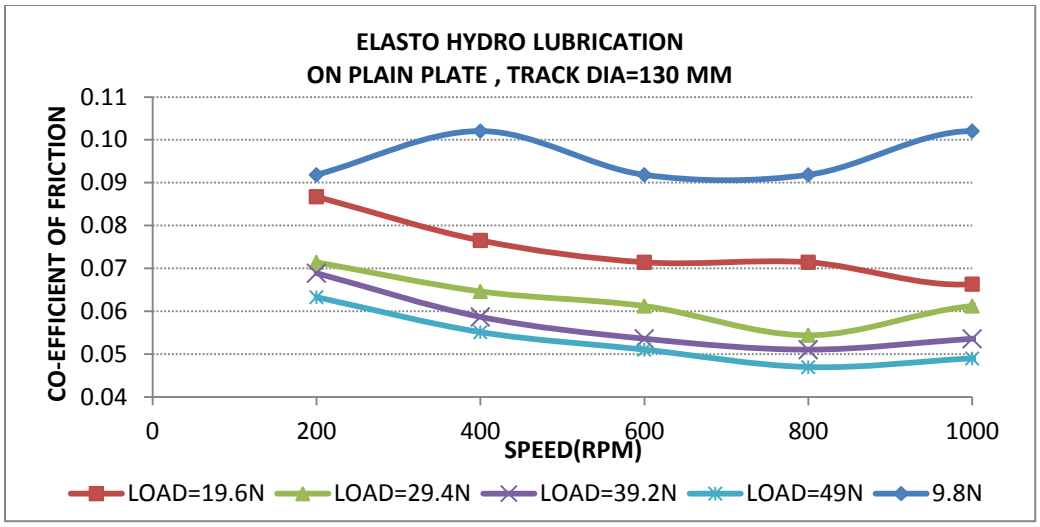

Figure 18

Figure 18 shows the graph between the variation of coefficient of friction vs. speed at different loading conditions for elastohydrodynamic lubrication at track dia 130 mm on plain plate. As the load is increasing the coefficient of friction is decreasing for varying speed. The maximum value for coefficient of friction is 0.10 at the load (9.8N), 400 rpm and the minimum value for coefficient of friction is 0.05 for 49 N, 800 rpm. The coefficient of friction is decreasing with increasing the load.

4.1.2(B) Coefficient of Friction vs. Speed for Textured Plate at Track Dia 130 mm:-

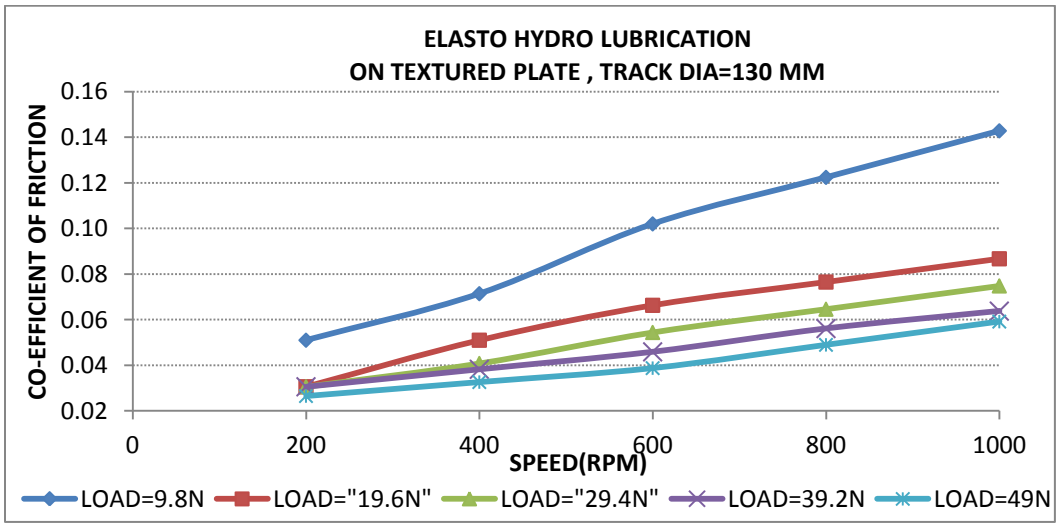

Figure 19

Figure 19 shows the graph between the coefficient of friction vs. speed at different loading conditions for elasto hydrodynamic lubrication at track dia 130 mm on textured plate. Comparing this graph with plain plate the coefficient of friction value is increasing with increases the load and keep on increasing with increasing the speed. Due to the debris this behaviour is coming. The maximum value for coefficient of friction is 0.14 at the load (9.8N), 1000 rpm and the minimum value for coefficient of friction is 0.02 for 49 N, 200 rpm. The coefficient of friction is decreasing with increasing the load and on comparing with plain plate the coefficient of friction is more on texture plate.

4.1.2(C) Coefficient of Friction vs. Load for Plain Plate at Track Dia 130 mm:-

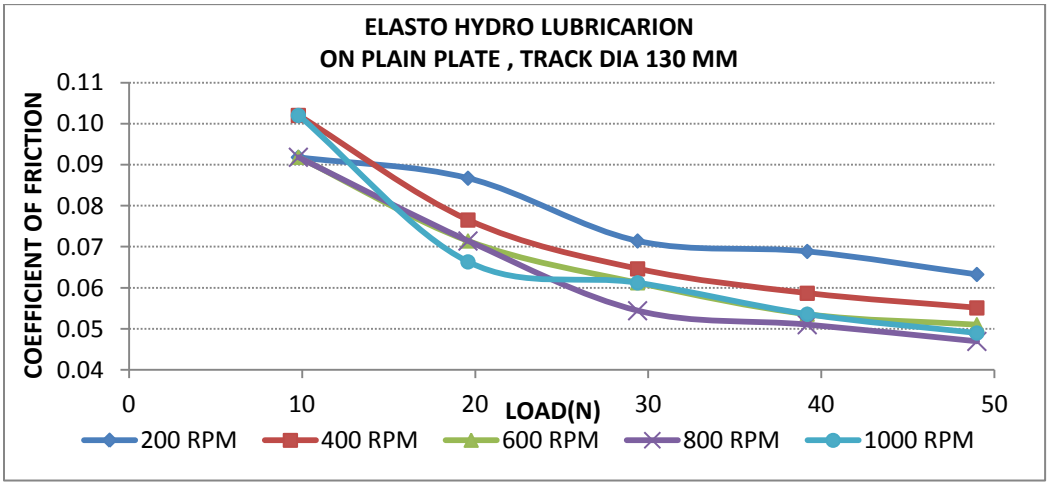

Figure 30

Figure 20 shows the graph between co-efficient of friction vs. load at various speed on plain plate at 130 mm track diameter for elasto hydrodynamic regime of lubrication. The co-efficient of friction is decresing as incresing the load for same speed. Further increasing the speed the curve is again decresing in nature with incresing the load. At 200 rpm and 9.8N load the coefficient of friction is 0.09 for and at 1000 rpm, the coefficient of friction value is 0.06.

4.1.2(D) Coefficient of Friction vs. Load for Textured Plate at Track Dia 130 mm:-

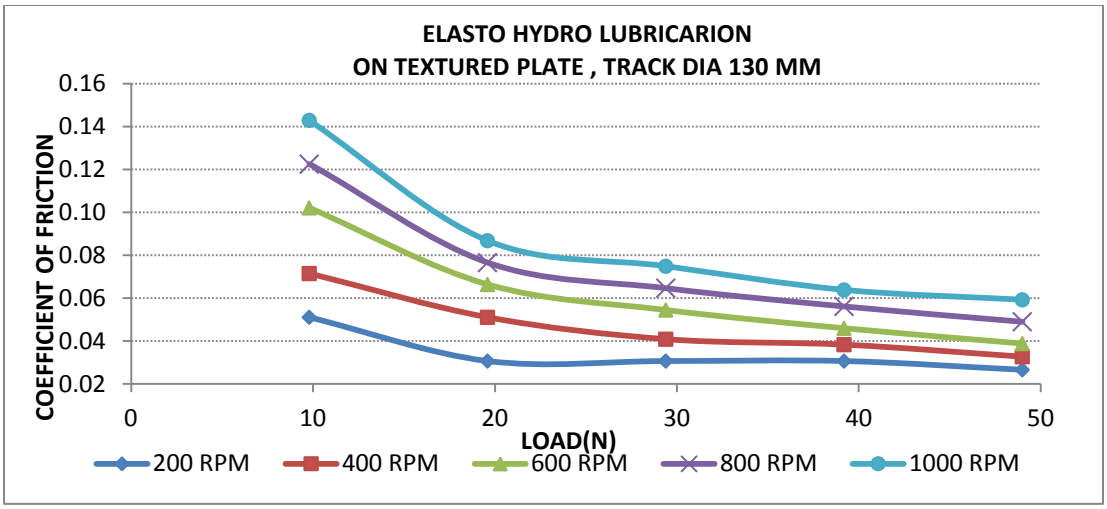

Figure 21

Figure 21 shows the graph between co-efficient of friction vs. load at various speed on textured plate at 130 mm track diameter for elato hydrodynamic regime of lubrication. The co-efficient of friction is decresing as incresing the load for a same speed . further increasing the speed the curve is again decresing in nature with incresing the load. At 200 rpm, the coefficient of friction is 0.05 and 0.02 for 9.8N and 49N load respectively and at 1000 rpm the coefficient of friction value is 0.14 and 0.06 for 9.8N and 49N load respectively. On comparing with palin palte the value of coefficient of friction is more on texture plate

4.1.2(E) Coefficient of Friction vs. Speed for Plain Plate at Track Dia 110 mm:-

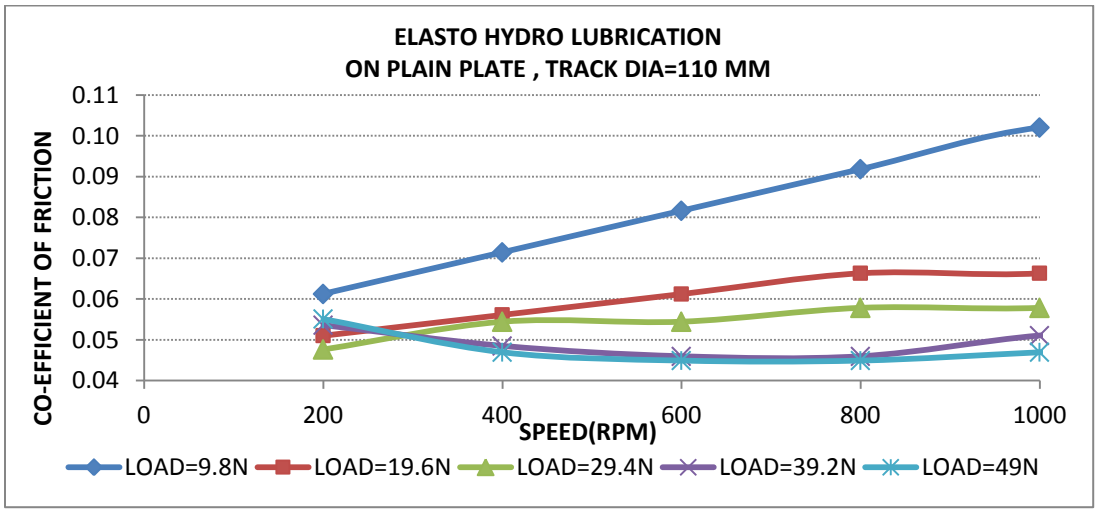

Figure 22

Figure 22 shows the variation of coefficient of friction vs. speed at different loading conditions for elastohydrodynamic lubrication at track dia 110 mm on plain plate. On changing the track dia the trend is as same as the 130 mm track dia for plain plate. As the load is increasing the coefficient of friction is decreasing for varying speed. The maximum value for coefficient of friction is 0.11 at the low load (9.8N), 1000 rpm and the minimum value for coefficient of friction is 0.04 for 49 N, 800 rpm. The coefficient of friction is decreasing with increasing the load.

4.1.2(F) Coefficient of Friction vs. Speed for Textured Plate at Track Dia 110 mm:-

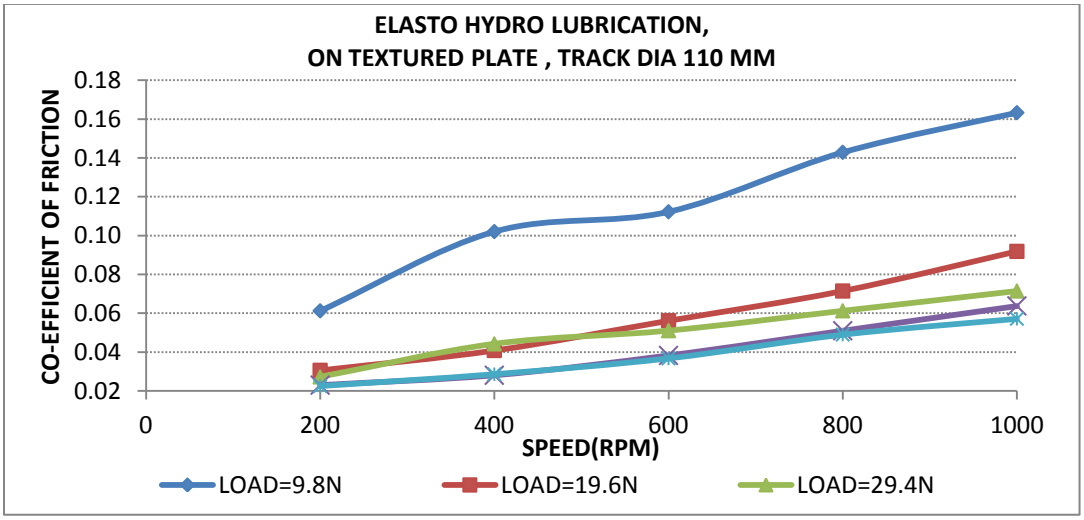

Figure 23

Figure 23 shows the variation of coefficient of friction vs. speed at different loading conditions for elasto hydrodynamic lubrication at track dia 110 mm on textured plate. Comparing this graph with plain plate the coefficient of friction value is increasing with increases the load and keep on increasing with increasing the speed. Due to the debris, this behavior is coming. The maximum value for coefficient of friction is 0.17 at the load (9.8N), 1000 rpm and the minimum value for coefficient of friction is 0.02 for 49 N, 200 rpm. The coefficient of friction is decreasing with increasing the load and on comparing with plain plate the value of coefficient of friction is more on texture plate

4.1.2(G) Coefficient of Friction vs. Speed for Plain Plate at Track Dia 50 mm:-

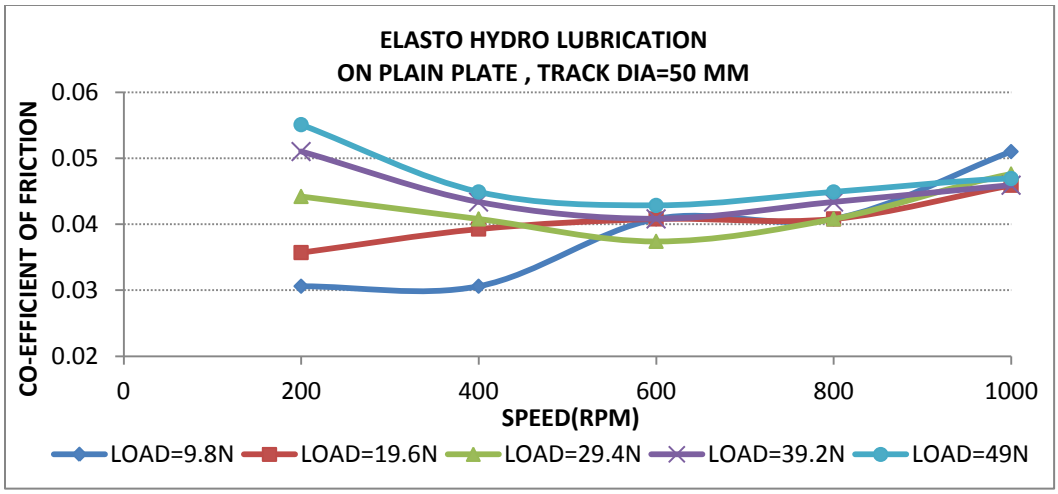

Figure 24

Figure 24 shows the variation of coefficient of friction vs. speed at different loading conditions for elastohydrodynamic lubrication at track dia 50 mm on plain plate. On changing the track dia the trend is as same as the 130 mm and 110 mm track dia for plain plate. As the load is increasing the coefficient of friction is decreasing for varying speed. The maximum value for coefficient of friction is 0.05 at the low load (49N), 200 rpm and the minimum value for coefficient of friction is 0.03 for 9.8 N, 200 rpm. The coefficient of friction is decreasing with increasing the load.

4.1.2(H) Coefficient of Friction vs. Speed for Textured Plate at Track Dia 50 mm:-

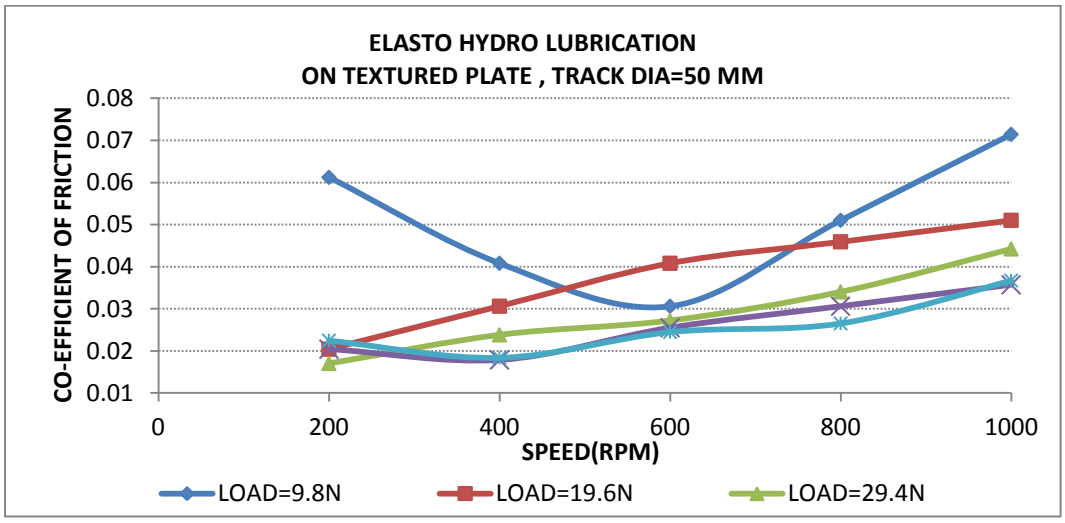

Figure 25

Figure 25 shows the variation of coefficient of friction vs. speed at different loading conditions for elasto hydrodynamic lubrication at track dia 50 mm on textured plate. Comparing this graph with plain plate the coefficient of friction value is increasing with increases the load and keep on increasing with increasing the speed. Due to the debris this behaviour is coming. The maximum value for coefficient of friction is 0.071at the load (9.8N), 1000 rpm and the minimum value for coefficient of friction is 0.01for 29.4 N, 200 rpm. As the coefficient of friction is decreasing with increasing the load and on comparing with plain plate the coefficient of friction is more on texture plate.

4.1.3 HYDRODYNAMIC LUBRICATION:- The comparison of co-efficient of friction vs. speed at various loads for plain plate and textured plate for different track dia is as following.

4.1.3(A) Coefficient of Friction vs. Speed for Plain Plate at Track Dia 130 mm:-

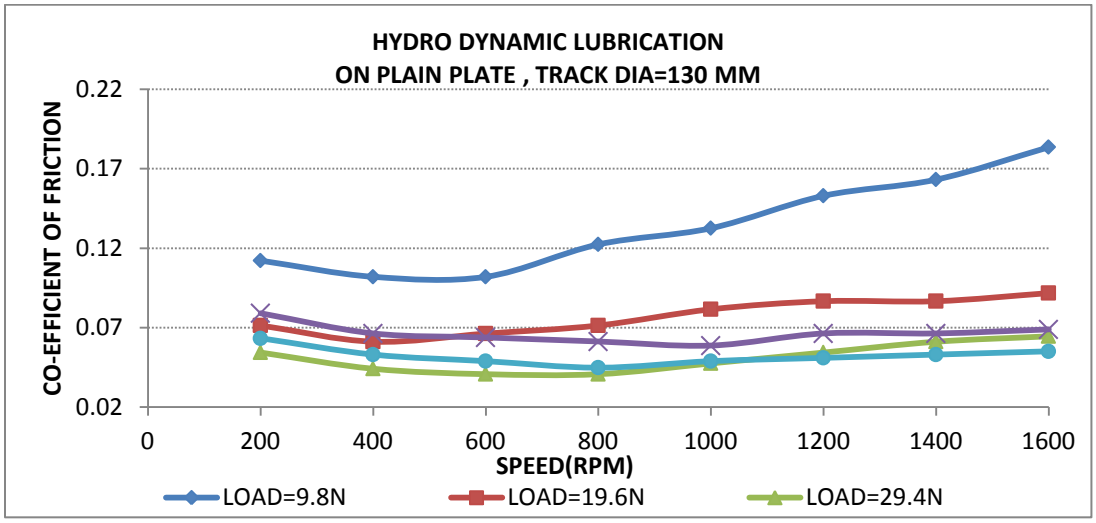

Figure 26

Figure 26 shows the variation of coefficient of friction vs. speed at different loading conditions for hydrodynamic lubrication at track dia 130 mm on plain plate. In this lubrication we have taken the speed upto 1600 rpm. As the load is increasing the coefficient of friction is decreasing and further varying speed the coefficient of friction is again increasing. The again increasing behaviour in curve is due to the less debris particles at the higher speed. The maximum value for coefficient of friction is 0.18 at the

low load (9.8N), 1600 rpm and the minimum value for coefficient of friction is 0.03 for 29.4 N, 600 rpm. The coefficient of friction is decreasing with increasing the load.

4.1.3(B) Coefficient of Friction vs. Speed for textured Plate at Track Dia 130 mm:-

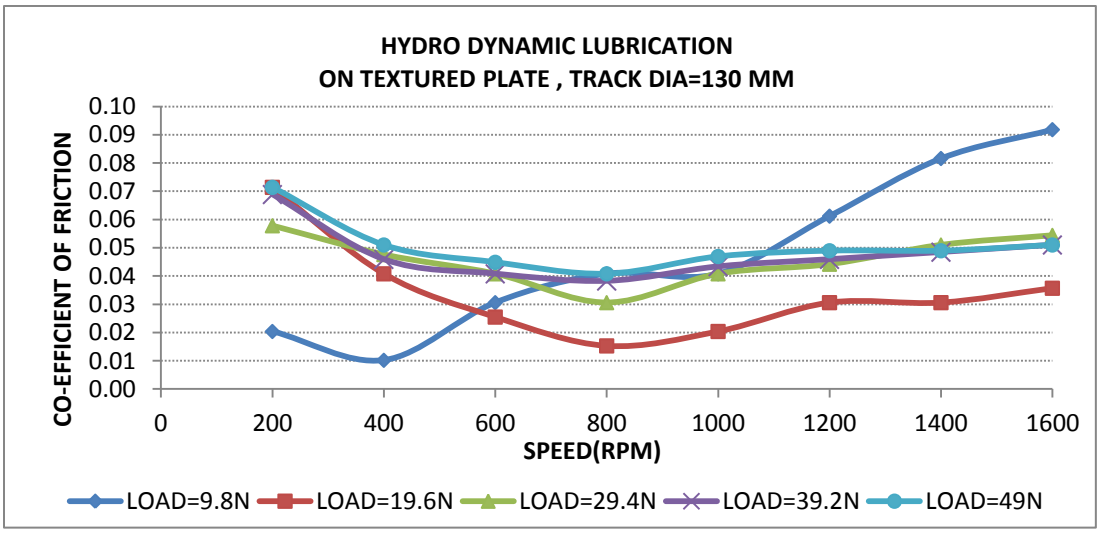

Figure 27

Figure 27 shows the graph between the co-efficient of friction vs. speed at various loading condition for hydrodynamic lubrication on textured plate for track dia 130mm. The trend is as same as the curve of plain plate. But the maximum and minimum value is less as compare to plain plate. As incresing the load the co-efficient of friction is decresing and on comparing with co-efficient of friction for plain plate, the value are less.At 49N the maximum value of co-efficient of friction is 0.07 and minimum value is 0.04 on textured plate and on plain plate it was respectively 0.06 and 0.03 for same laod 49N.So the coefficient of friction is less on textured plate as compare to plain plate.

4.1.3(C) Coefficient of Friction vs. Load for Plain Plate at Track Dia 130 mm:-

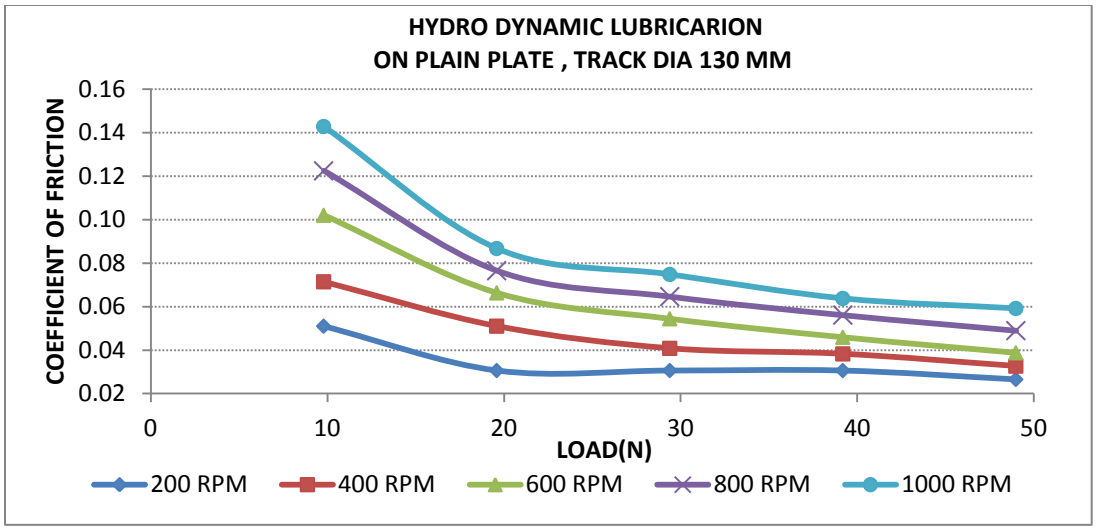

Figure 28

Figure 28 shows the graph between co-efficient of friction vs. load at various speed on plain plate at 130 mm track diameter for hydrodynamic regime of lubrication. The co-efficient of friction is decresing as incresing the load for a same speed .Further increasing the speed the curve is again decresing in nature with incresing the load. At 200 rpm and the coefficient of friction is 0.05 for 9.8N load and 0.03 for 49 N load and at 1000 rpm, the coefficient of friction value is 0.14 and 0.06 for 9.8N load and 49N load respectively.

4.1.3(D) Coefficient of Friction vs. Load for textured Plate at Track Dia 130 mm:-

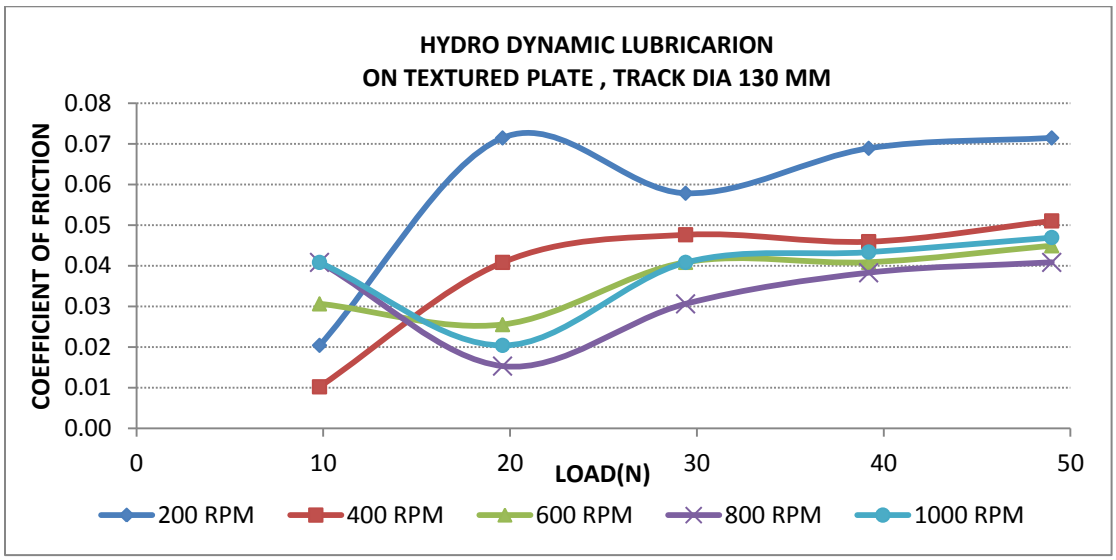

Figure 29

Figure 29 shows the graph between co-efficient of friction vs. load at various speed on textured plate at 130 mm track diameter. The co-efficient of friction is decresing as incresing the load for a same speed .Further increasing the speed the curve is again decresing in nature with incresing the load. At 200 rpm, the coefficient of friction is 0.02 and 0.07 for 9.8N and 49N load respectively and at 1000 rpm the coefficient of friction value is 0.04 and 0.05 for 9.8N and 49N load respectively. On comparing with palin palte the value of coefficient of friction is less significantly.

4.1.3(E) Coefficient of Friction vs. Speed for plain Plate at Track Dia 110 mm:-

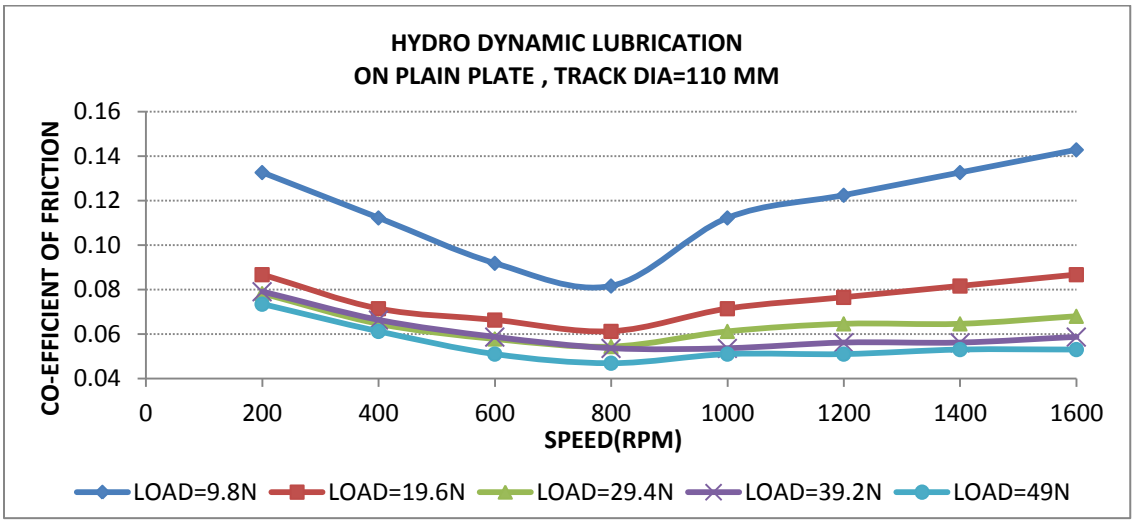

Figure 40

Figure 30 shows the graph between the coefficient of friction vs. speed at different loading conditions for hydrodynamic lubrication at track dia 110 mm on plain plate. In this lubrication we have taken the speed upto 1600 rpm. As the load is increasing the coefficient of friction is decreasing and further varying speed the coefficient of friction is again increasing. The again increasing behaviour in curve is due to the less debris particles at the higher speed The maximum value for coefficient of friction is 0.14 at the low load (9.8N), 1600 rpm and the minimum value for coefficient of friction is 0.04 for 49 N, 800 rpm.

4.1.3(F) Coefficient of Friction vs. Speed for Textured Plate at Track Dia 110 mm

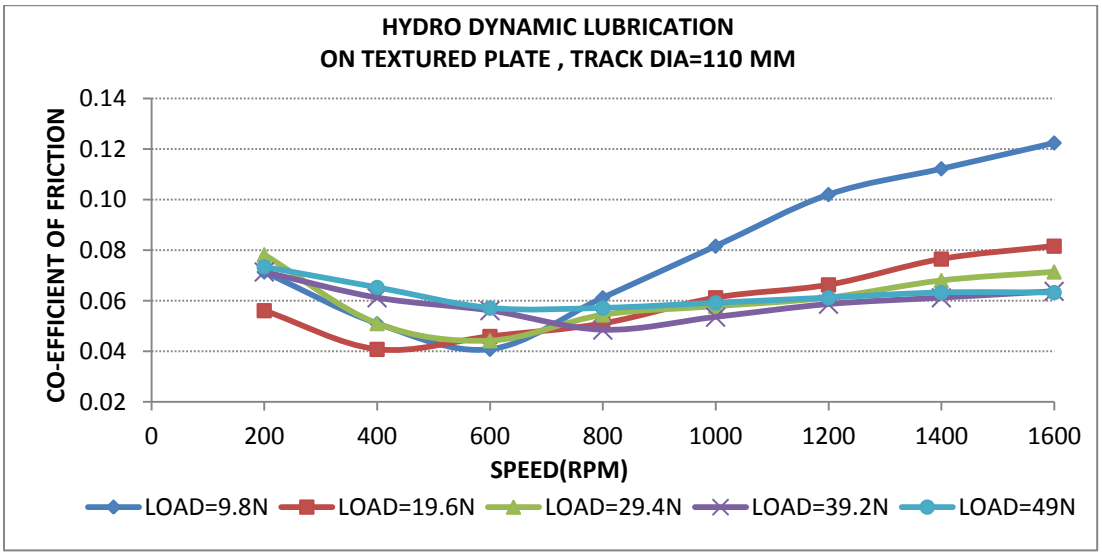

Figure 31

Figure 31 shows the co-efficient of friction with respect to speed at various increasing loading condition for hydrodynamic lubrication on textured plate for track dia 110mm. The trend is as same as the curve of plain plate. But the maximum and minimum value is less as compare to plain plate. As incresing the load the co-efficient of friction is decresing and on comparing with co-efficient of friction for plain plate, the value are less.At 49N the maximum value of co-efficient of friction is 0.07 and minimum value is 0.04 on textured plate and on plain plate it is 0.06 and 0.04 respectively for 49N laod.So the coefficient of friction is less on textured plate as compare to plain plate.

4.1.3(G) Coefficient of Friction vs. Speed for Plain Plate at Track Dia 50 mm:-

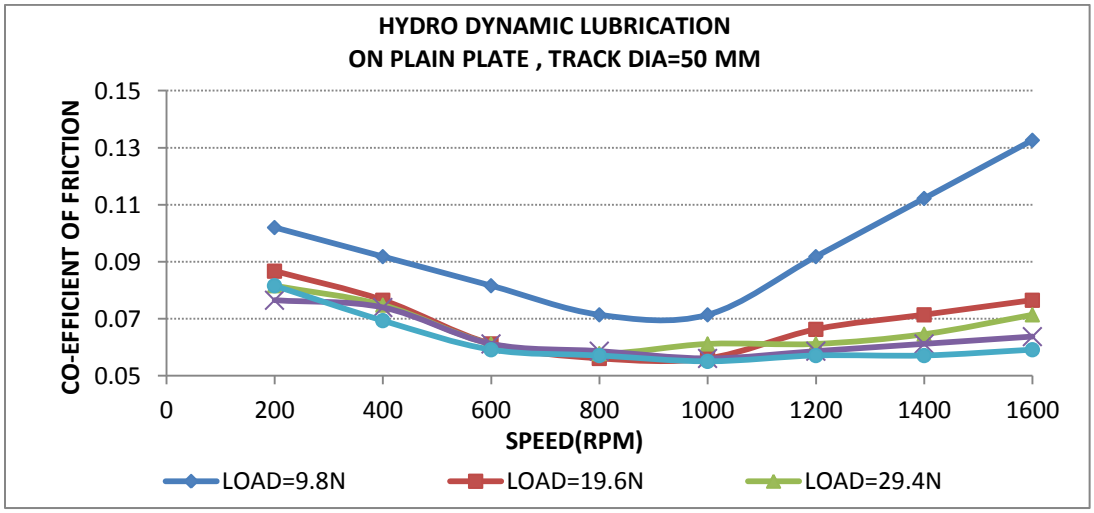

Figure 32

Figure 32 shows the variation of coefficient of friction vs. speed at different loading conditions for hydrodynamic lubrication at track dia 50 mm on plain plate. The trend of graph is same as the graph of previous track dia . As the load is increasing the coefficient of friction is decreasing and further varying speed the coefficient of friction is again increasing. The again increasing behaviour in curve is due to the less debris particles at the higher speed .The maximum value for coefficient of friction is 0.13 at the low load (9.8N), 1600 rpm and the minimum value for coefficient of friction is 0.05 for 49 N, 1000 rpm. The coefficient of friction is decreasing with increasing the load.

4.1.3(H) Coefficient of Friction vs. Speed for Textured Plate at Track Dia 50 mm:-

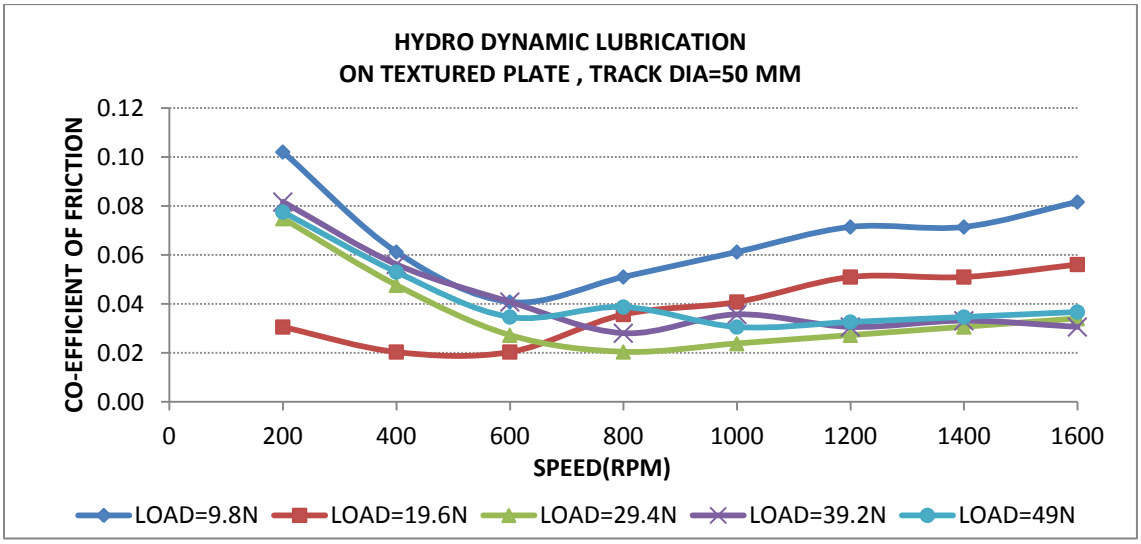

Figure 33

Figure 33 shows the graph between the co-efficient of friction vs. speed at various increasing loading condition for hydrodynamic lubrication on textured plate for track dia 50mm. The trend is as same as the curve of plain plate. But the maximum and minimum value is less as compare to plain plate. As incresing the load , the co-efficient of friction is decresing and on comparing with co-efficient of friction for plain plate, the value are less.At 19.5N the maximum value of co-efficient of friction is 0.06 and minimum value is 0.02 on textured plate and on plain plate it was respectively 0.08 and

0.56 for same laod 49N. So the coefficient of friction is less on textured plate as compare to plain plate.

4.2 M.S PIN ON MILD STEEL (M.S) PLATE:- The graph between co-efficient of friction vs. speed at various loads for different region of lubrication are shown as following

4.2.1 DRY LUBRICATION:- The comparison of co-efficient of friction vs. speed at various loads for plain plate and textured plate for different track dia is as following.

4.2.1(A) Coefficient of Friction vs. Speed for Plain Plate at Track Dia 130 mm:-

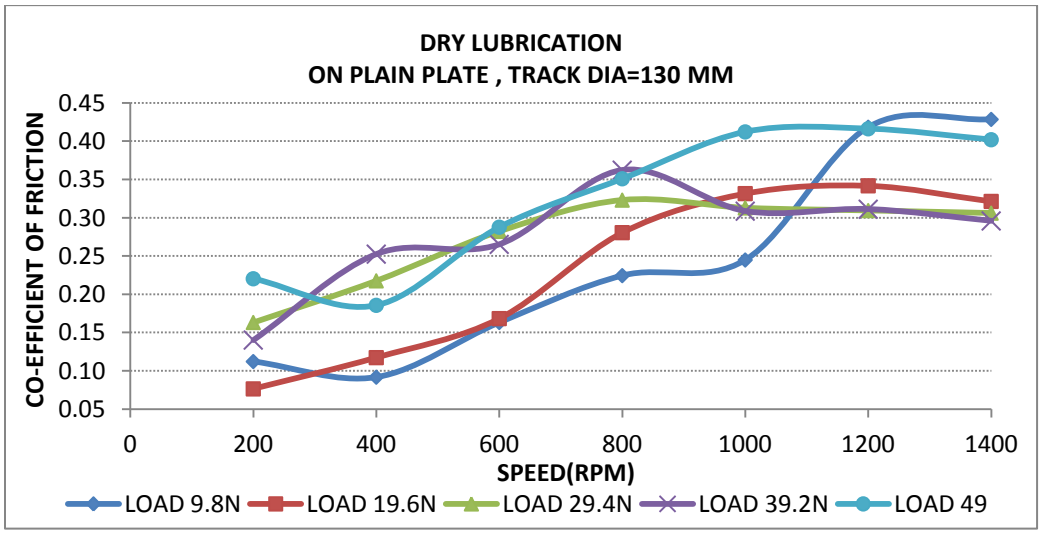

Figure 34

Figure 34 shows the graph between the co-efficient of friction vs.speed at various increasing loading condition for dry lubrication on plain plate for track dia 130mm. The graph comes waivey in nature because of metal to metal contact and debris sticking to the contact area.The maximum value for co-efficiect of friction is at low load and high speed condition, that is 0.43 for 1400 rpm at 9.8N and minmum value is 0.06 for 200 rpm at 19.6 N.

4.2.1(B) Coefficient of Friction vs. Speed for Textured Plate at Track Dia 130 mm:-

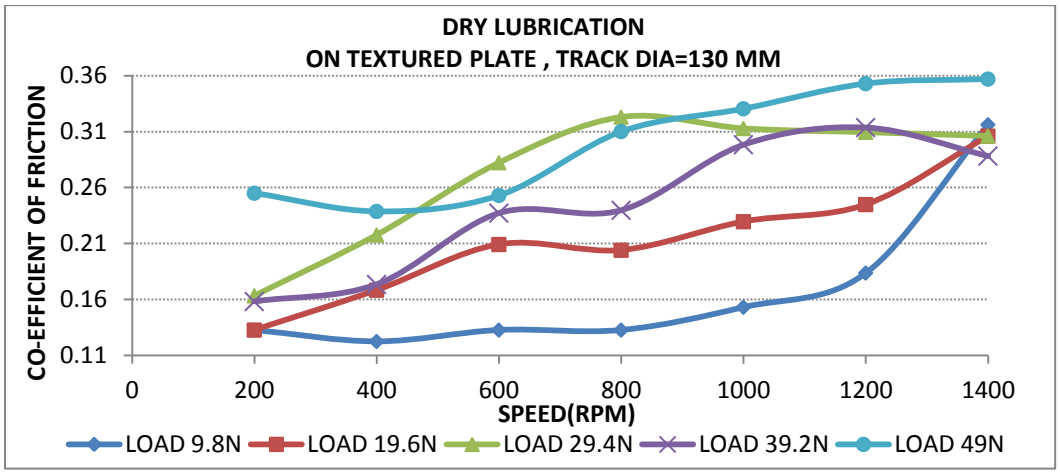

Figure 35

Figure 35 shows the graph between the co-efficient of friction vs. speed at various increasing loading condition for dry lubrication on textured plate for track dia 130mm. This graph also shows the same trend as the graph of plain plate.On comparision to the graph of plain plate, the coefficient of friction is less than the graph of plain plate with significant difference. The maximum value of co-efficiect of friction is 0.35 for 1400 rpm at 9.8N and minmum value is 0.12 for 400 rpm at 9.8 N.

4.2.1(C) Coefficient of Friction vs. Load for Plain Plate at Track Dia 130 mm:-

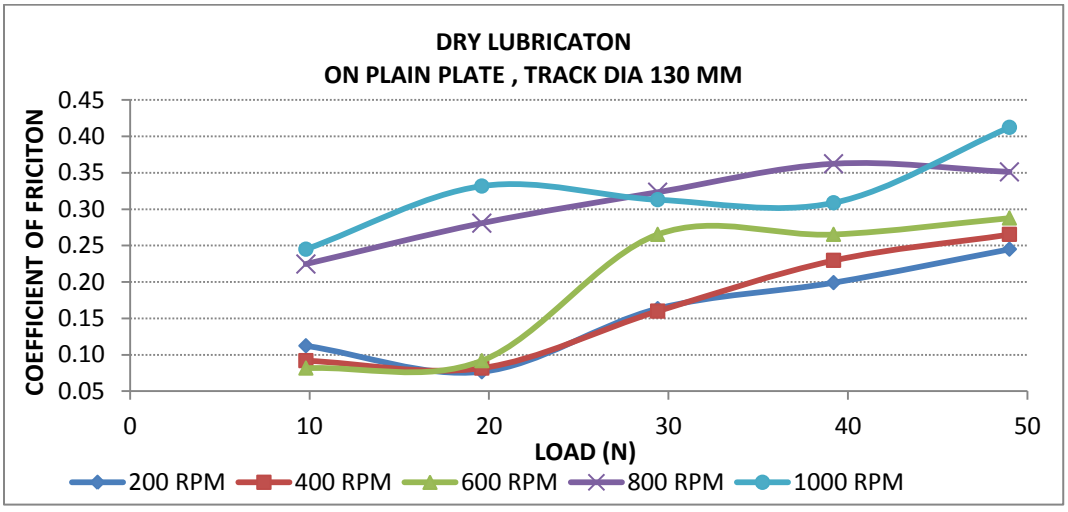

Figure 36

Figure 36 shows the graph between co-efficient of friction vs. load at various speed on plain plate at 130 mm track diameter for dry regime of lubrication. The co-efficient of friction is decresing as incresing the load for a same speed .Further increasing the speed the curve is again decresing in nature with incresing the load. At 200 rpm and the coefficient of friction is 0.11 for 9.8N load and 0.24 for 49 N load and at 1000 rpm, the coefficient of friction value is 0.24 and 0.41 for 9.8N load and 49N load respectively.

4.2.1(D) Coefficient of Friction vs. Load for Textured Plate at Track Dia 130 mm:-

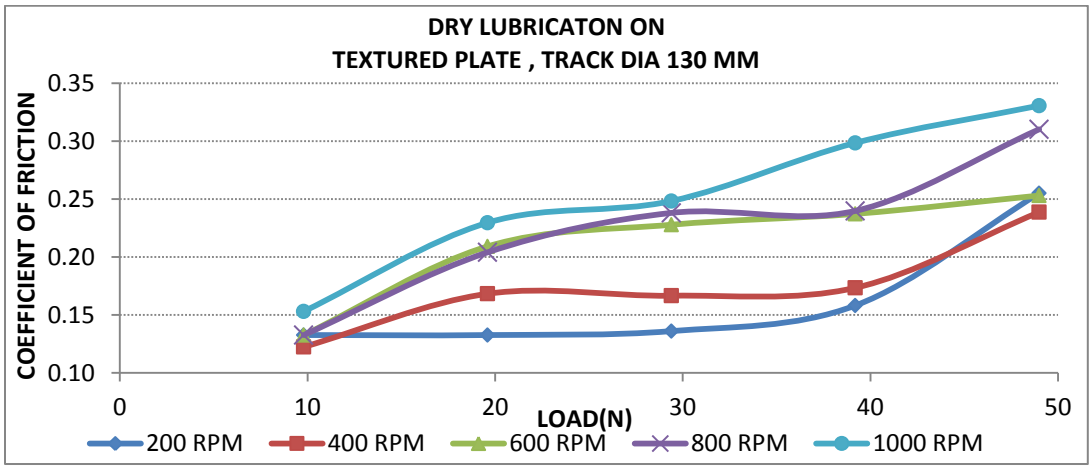

Figure 37

Figure 13 shows the graph between co-efficient of friction vs. load at various speed on textured plate at 130 mm track diameter.The co-efficient of friction is decresing as incresing the load for a same speed .Further increasing the speed the curve is again decresing in nature with incresing the load. At 200 rpm, the coefficient of friction is 0.13 and 0.26 for 9.8N and 49N load respectively and at 1000 rpm the coefficient of friction value is 0.15 and 0.33 for 9.8N and 49N load respectively. On comparing with palin palte the value of coefficient of friction is less significantly.

4.2.1(E) Coefficient of Friction vs. Speed for Plain Plate at Track Dia 50 mm:-

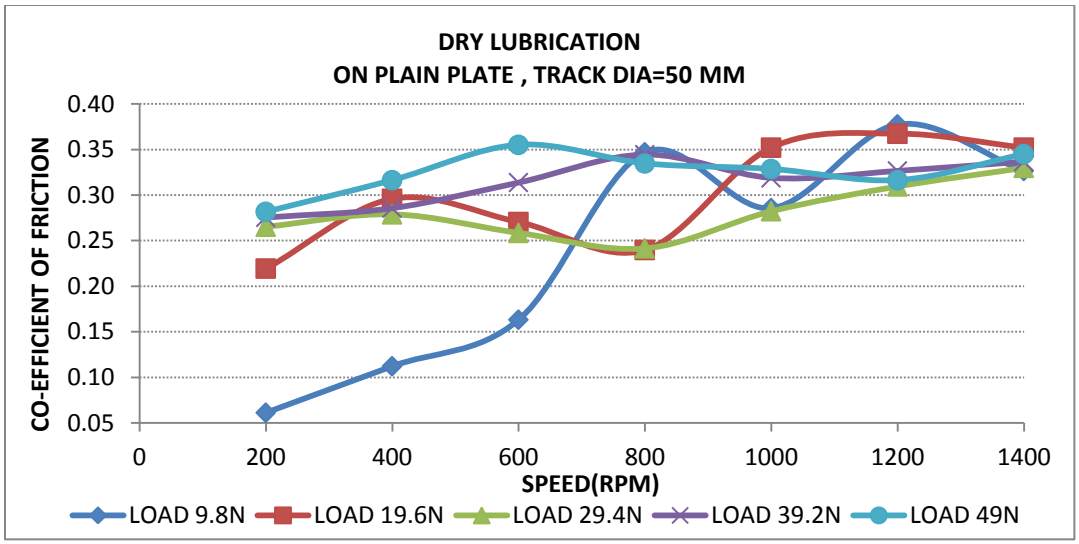

Figure 38

Figure 38 shows the co-efficient of friction with respect to speed at various increasing loading condition for dry lubrication on plain plate for track dia 50mm. On changing the track dia froom 110 mm to 50 mm the graph comes again waivey in nature because of metal to metal contact and debris sticking to the contact area.The maximum value for co-efficiect of friction is at low load and high speed condition, that is 0.35 for 800 rpm at 9.8N and minmum value is 0.06 for 200 rpm at 9.8 N.

4.2.1(F) Coefficient of Friction vs. Speed for Textured Plate at Track Dia 50 mm:-

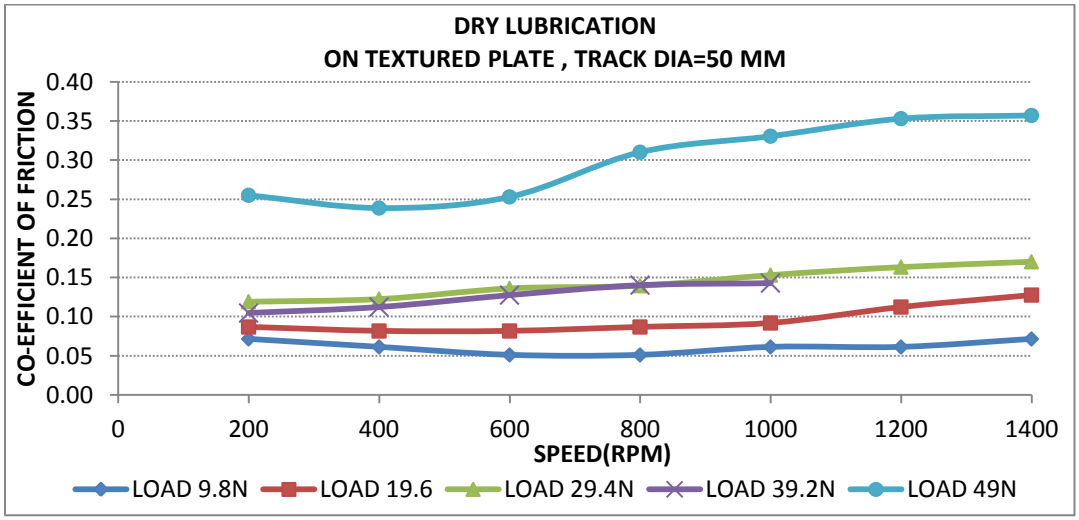

Figure 39

Figure 39 shows the co-efficient of friction with respect to speed at various increasing loading condition for dry lubrication on textured plate for track dia 50mm.On comparision to the graph of plain plate, the coefficient of friction is less than the graph of plain plate with significant difference. The maximum value of co-efficiect of friction is 0.35 for 1400 rpm at 9.8N and minmum value is 0.12 for 400 rpm at 9.8 N.

4.2.2 ELASTO HYDRODYNAMIC LUBRICATION:- The comparison of co-efficient of friction vs. speed at various loads for plain plate and textured plate for different track dia is as following.

4.2.2(A) Coefficient of Friction vs. Speed for Plain Plate at Track Dia 130 mm:-

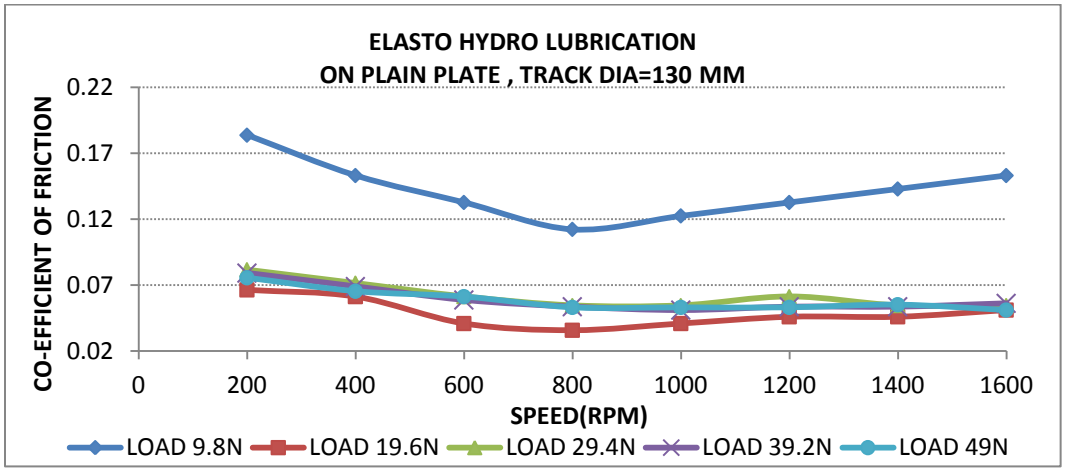

Figure 50

Figure 40 shows the variation of coefficient of friction vs. speed at different loading conditions for elastohydrodynamic lubrication at track dia 130 mm on plain plate. As the load is increasing the coefficient of friction is decreasing for varying speed. And after reaching a minimum point it started again increasing. The maximum value for coefficient of friction is 0.18 at the low load (9.8N), 200 rpm and the minimum value for coefficient of friction is 0.04 for 19.5 N, 800 rpm.

4.2.2(B) Coefficient of Friction vs. Speed for Textured Plate at Track Dia 130 mm:-

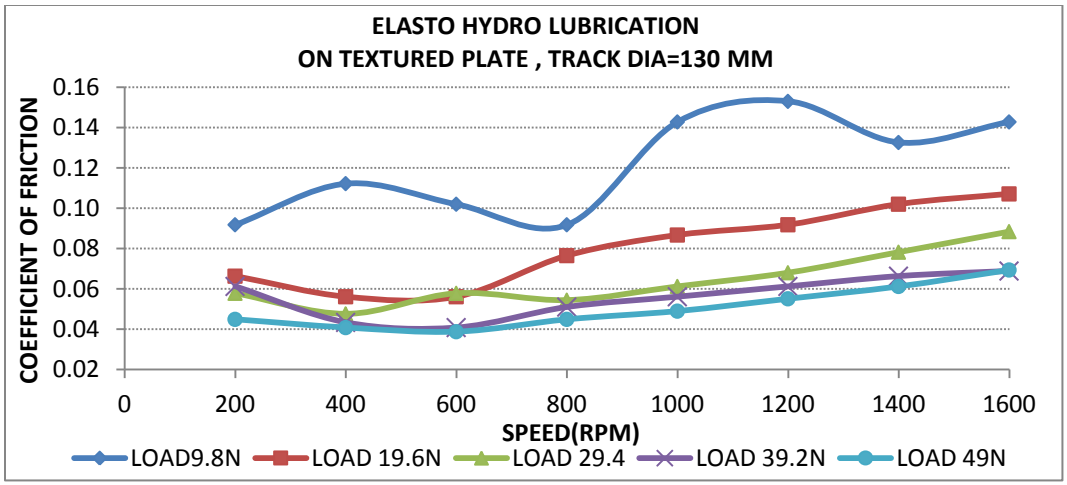

Figure 41

Figure 41 shows the variation of coefficient of friction vs. speed at different loading conditions for elasto hydrodynamic lubrication at track dia 130 mm on textured plate. On comparing this graph with plain plate the coefficient of friction value is increasing with increases the load as well as the speed. Due to the debris this behaviour is coming. The maximum value for coefficient of friction is 0.15 at the load (9.8N), 1200 rpm and the minimum value for coefficient of friction is 0.04 for 49 N, 600 rpm. The coefficient of friction is decreasing with increasing the load.

4.2.2(C) Coefficient of Friction vs. Load for Plain Plate at Track Dia 130 mm:-

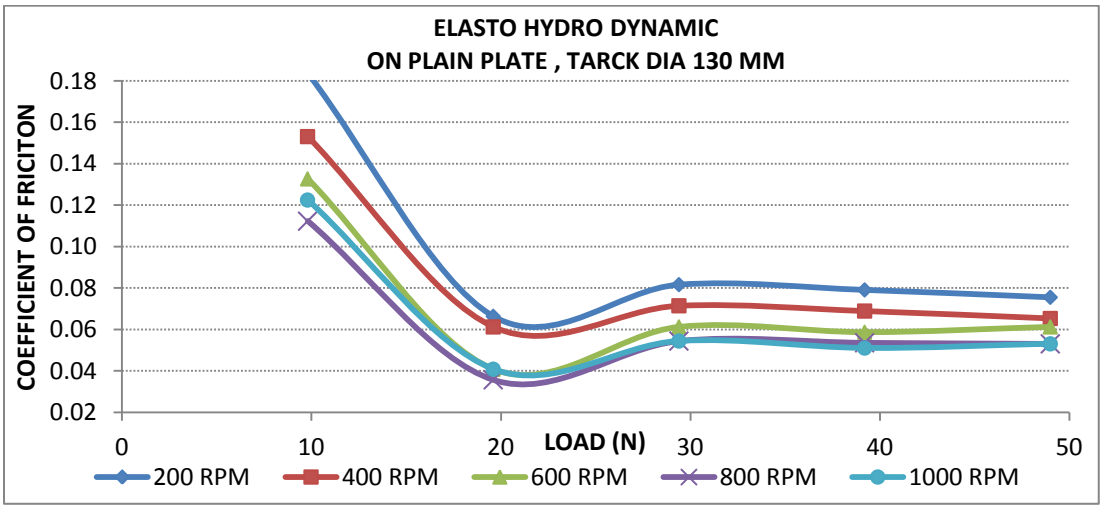

Figure 42

Figure 42 shows the graph between co-efficient of friction vs. load at various speed on plain plate at 130 mm track diameter for dry regime of lubrication. The co-efficient of friction is decresing as incresing the load for a same speed .Further increasing the speed the curve is again decresing in nature with incresing the load. At 200 rpm and the coefficient of friction is 0.18 for 9.8N load and 0.07 for 49 N load and at 1000 rpm, the coefficient of friction value is 0.12 and 0.05 for 9.8N load and 49N load respectively.

4.2.2(D) Coefficient of Friction vs. Load for Textured Plate at Track Dia 130 mm:-

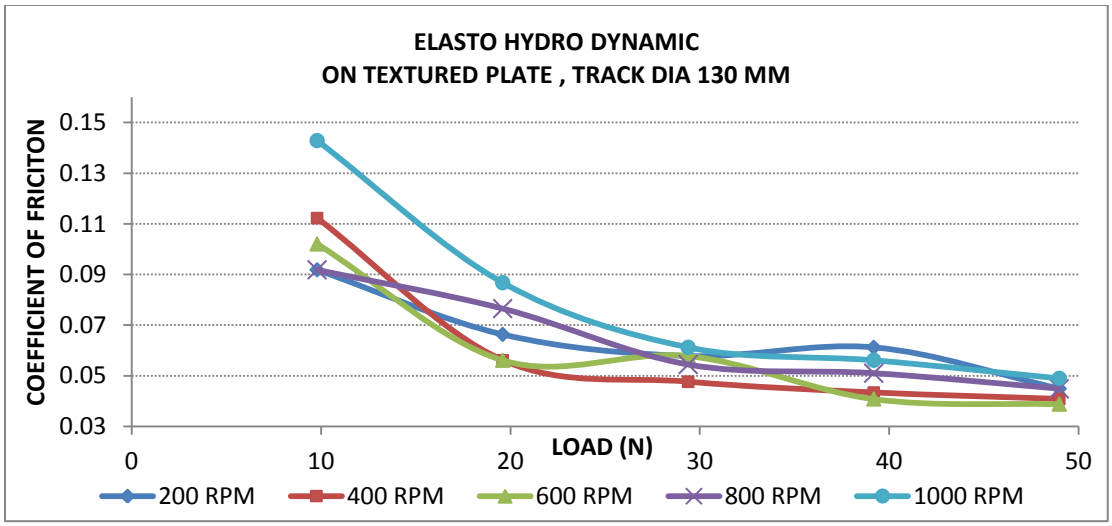

Figure 43

Figure 43 shows the graph between co-efficient of friction vs. load at various speed on textured plate at 130 mm track diameter. The co-efficient of friction is decresing as incresing the load for a same speed . further increasing the speed the curve is again decresing in nature with incresing the load. At 200 rpm, the coefficient of friction is 0.09 and 0.05 for 9.8N and 49N load respectively and at 1000 rpm the coefficient of friction value is 0.14 and 0.06 for 9.8N and 49N load respectively. On comparing with palin palte the value of coefficient of friction is less significantly.

4.2.2(E) Coefficient of Friction vs. Speed for Plain Plate at Track Dia 110 mm:-

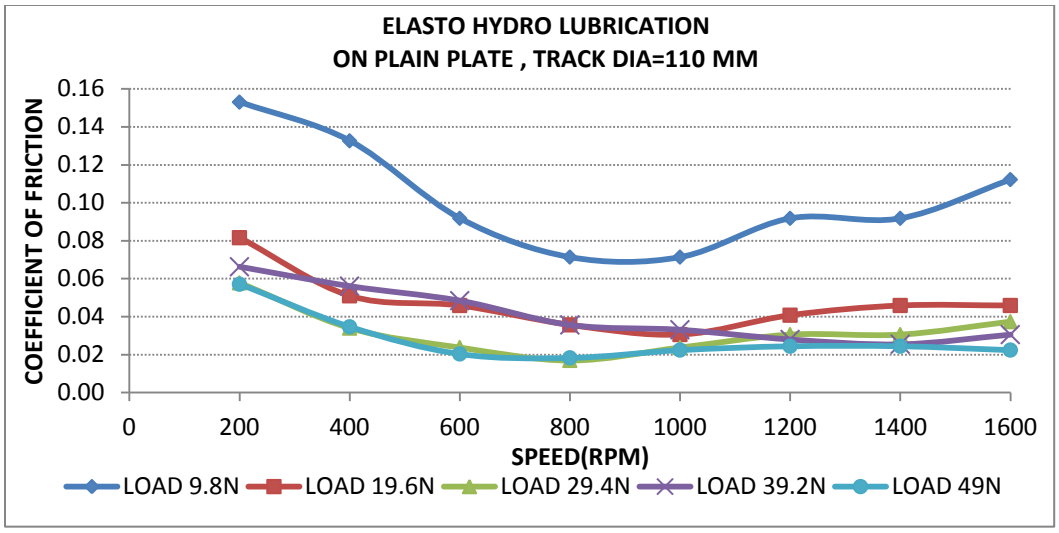

Figure 44

Figure 44 shows the variation of coefficient of friction vs. speed at different loading conditions for elastohydrodynamic lubrication at track dia 110 mm on plain plate. As the load is increasing the coefficient of friction is decreasing for varying speed. And after reaching a minimum point it started again increasing. The maximum value for coefficient of friction is 0.15 at the low load (9.8N), 200 rpm and the minimum value for coefficient of friction is 0.02 for 29.4 N, 800 rpm.

4.2.2(F) Coefficient of Friction vs. Speed for Textured Plate at Track Dia 110 mm:-

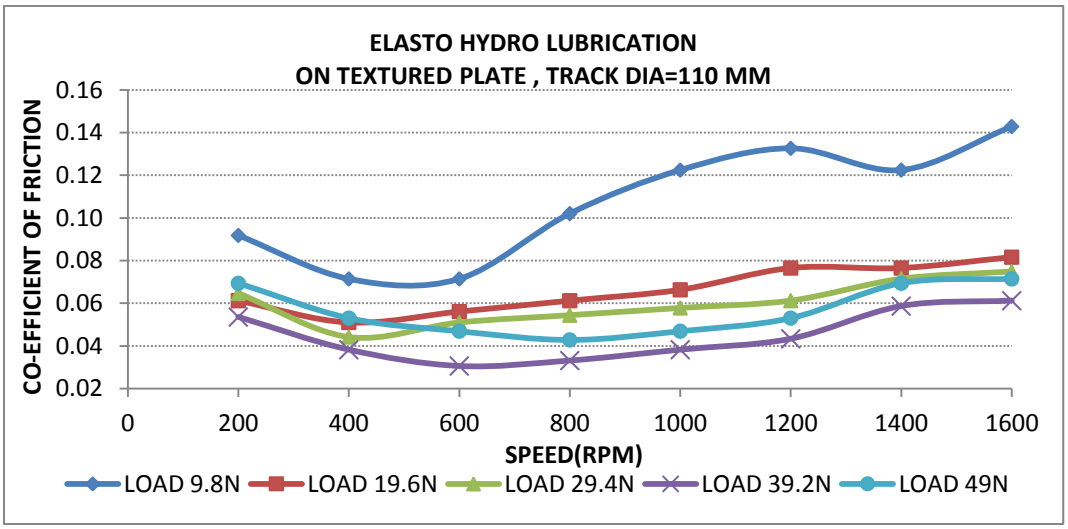

Figure 45

Figure 45 shows the variation of coefficient of friction vs. speed at different loading conditions for elasto hydrodynamic lubrication at track dia 110 mm on textured plate. On comparing this graph with plain plate the coefficient of friction value is increasing with increases the load as well as the speed. Due to the debris this behaviour is coming. The maximum value for coefficient of friction is 0.14 at the load (9.8N), 1600 rpm and the minimum value for coefficient of friction is 0.03 for 39.2 N, 600 rpm. The coefficient of friction is decreasing with increasing the load

4.2.2(G) Coefficient of Friction vs. Speed for Plain Plate at Track Dia 50 mm:-

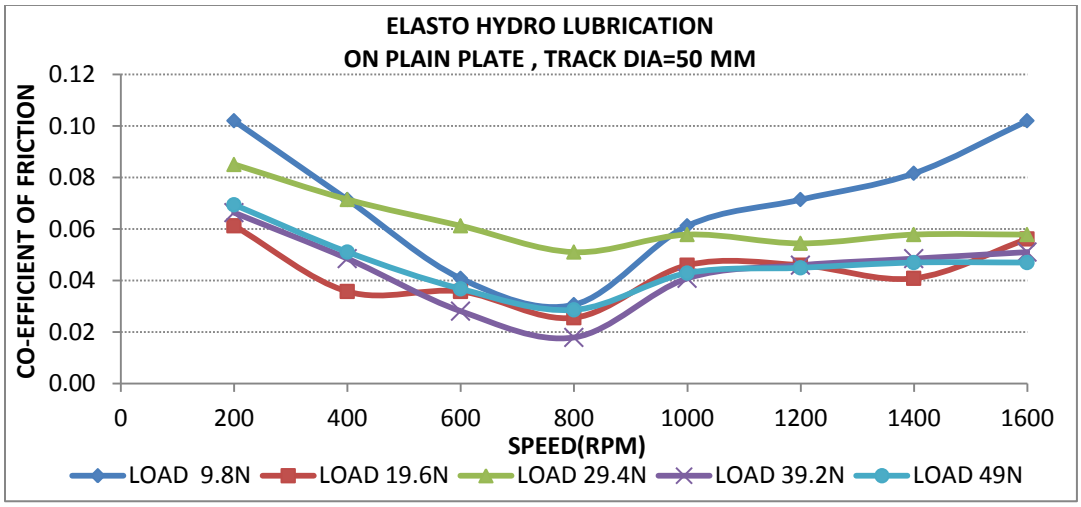

Figure 46

Figure 46 shows the variation of coefficient of friction vs. speed at different loading conditions for elasto hydrodynamic lubrication at track dia 50 mm on plain plate. As the load is increasing the coefficient of friction is decreasing for varying speed. And after reaching a minimum point it started again increasing. The maximum value for coefficient of friction is 0.10 at the low load (9.8N), 1600 rpm and the minimum value for coefficient of friction is 0.02 for 39.2 N, 800 rpm.

4.2.2(H) Coefficient of Friction vs. Speed for Textured Plate at Track Dia 50 mm:-

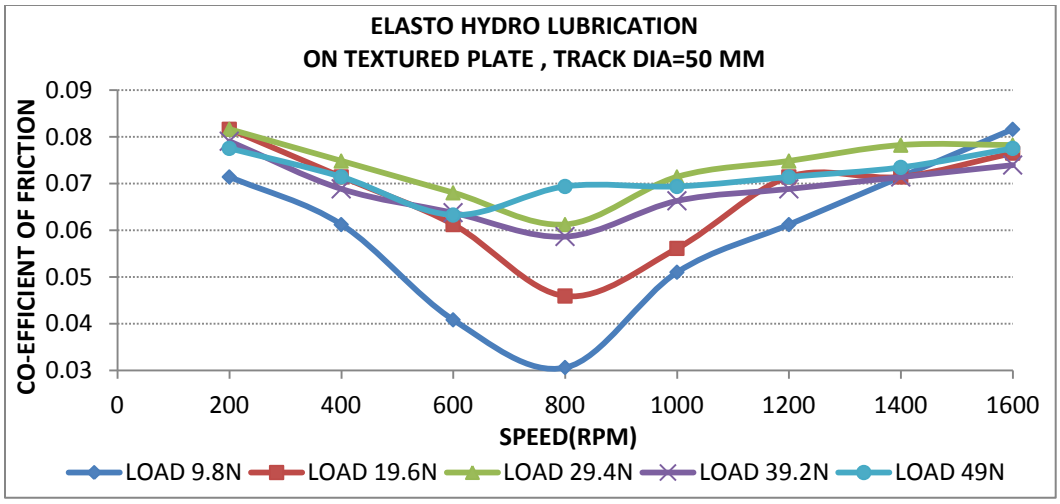

Figure 47

Figure 47 shows the variation of coefficient of friction vs. speed at different loading conditions for elasto hydrodynamic lubrication at track dia 50 mm on textured plate. On comparing this graph with plain plate the coefficient of friction value is increasing with increases the load as well as the speed. Due to the debris this behaviour is coming. The maximum value for coefficient of friction is 0.08 at the load (9.8N), 1600 rpm and the minimum value for coefficient of friction is 0.03 for 9.8 N, 800 rpm.

4.2.3 HYDRODYNAMIC LUBRICATION:- The comparison of co-efficient of friction vs. speed at various loads for plain plate and textured plate for different track dia is as following.

4.2.3(A) Coefficient of Friction vs. Speed for Plain Plate at Track Dia 130 mm:-

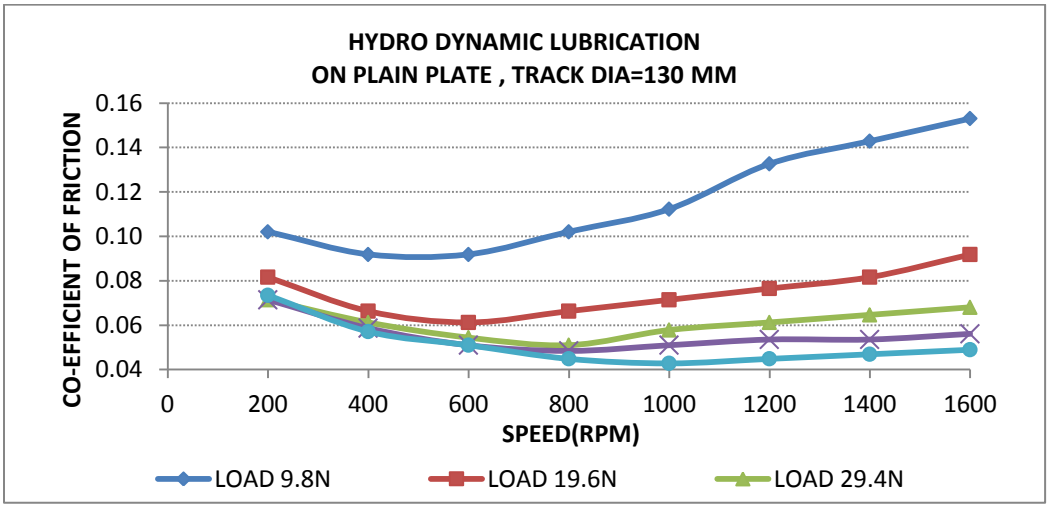

Figure 48

Figure 48 shows the variation of coefficient of friction vs. speed at different loading conditions for hydrodynamic lubrication at track dia 130 mm on plain plate. As the load is increasing the coefficient of friction is decreasing and further varying speed the coefficient of friction is again increasing. The again increasing behaviour in curve is due to the less debris particles at the higher speed. The maximum value for coefficient of friction is 0.15 at the low load (9.8N), 1600 rpm and the minimum value for coefficient of friction is 0.04 for 49 N, 800 rpm. The coefficient of friction is decreasing with increasing the load.

4.2.3(B) Coefficient of Friction vs. Speed for Textured Plate at Track Dia 130 mm:-

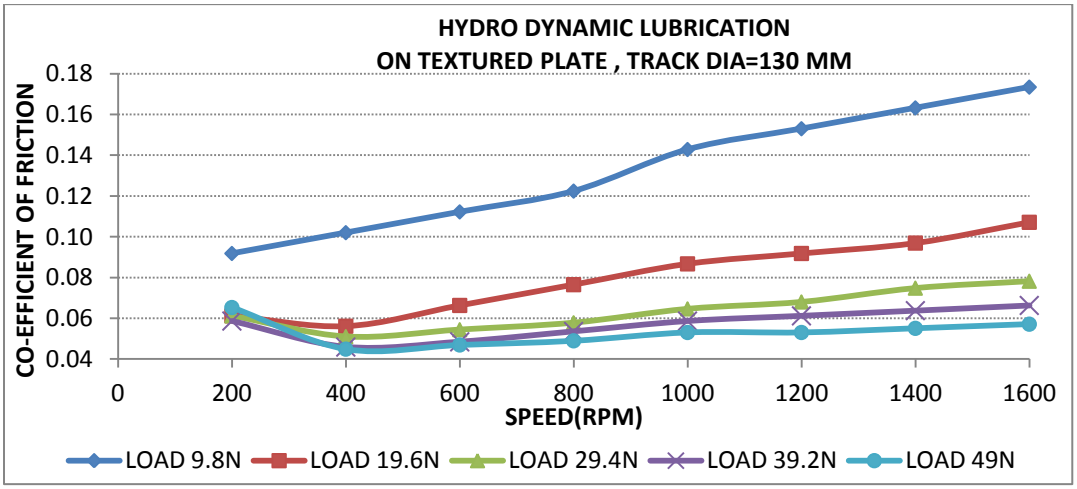

Figure 49

Figure 49 shows the co-efficient of friction with respect to speed at various increasing loading condition for hydrodynamic lubrication on textured plate for track dia 130mm. The trend is as same as the curve of plain plate. But the maximum and minimum value is slightly more as compare to plain plate. As incresing the load (19.6N,29.4N,39.2N,49N) the co-efficient of friction is decresing and on comparing with co-efficient of friction for plain plate, the value are slighty more.At 49N the maximum value of co-efficient of friction is 0.05 and minimum value is 0.04.

4.2.3(C) Coefficient of Friction vs. Load for Plain Plate at Track Dia 130 mm:-

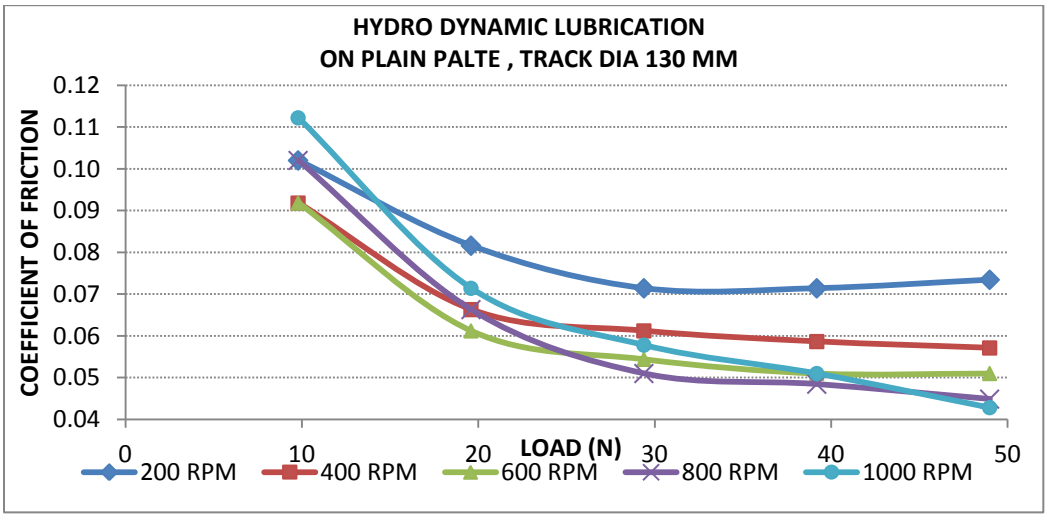

Figure 60

Figure 50 shows the graph between co-efficient of friction vs. load at various speed on plain plate at 130 mm track diameter for hydrodynamic regime of lubrication. The co-efficient of friction is decresing as incresing the load for a same speed .Further increasing the speed the curve is again decresing in nature with incresing the load. At 200 rpm and the coefficient of friction is 0.10 for 9.8N load and 0.07 for 49 N load and at 1000 rpm, the coefficient of friction value is 0.11 and 0.04 for 9.8N load and 49N load respectively.

4.2.3(D) Coefficient of Friction vs. Load for Textured Plate at Track Dia 130 mm:-

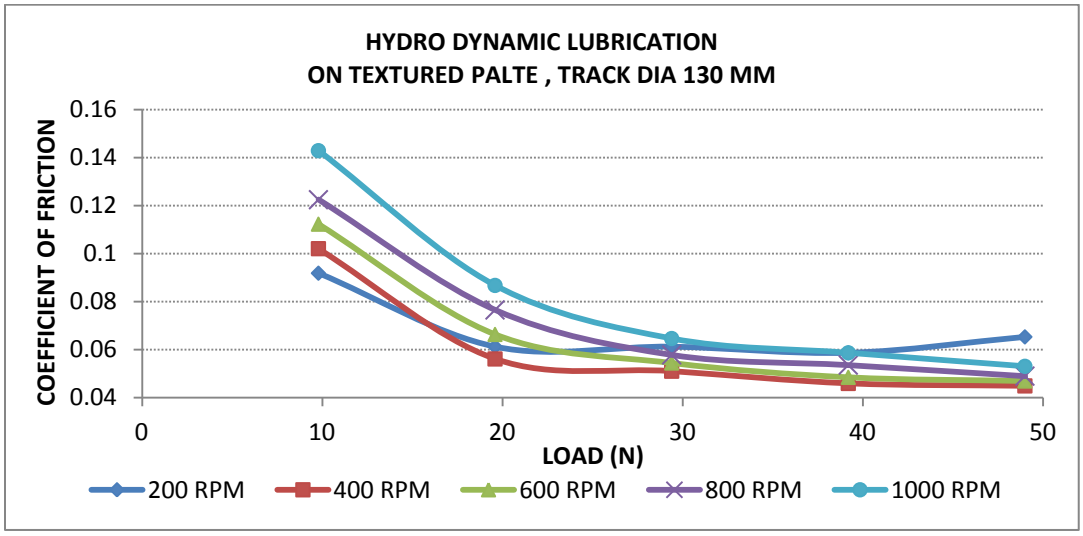

Figure 51

Figure 51 shows the graph between co-efficient of friction vs. load at various speed on textured plate at 130 mm track diameter. The co-efficient of friction is decresing as incresing the load for a same speed . further increasing the speed the curve is again decresing in nature with incresing the load. At 200 rpm, the coefficient of friction is 0.09 and 0.04 for 9.8N and 49N load respectively and at 1000 rpm the coefficient of friction value is 0.14 and 0.05 for 9.8N and 49N load respectively. On comparing with palin palte the value of coefficient of friction is more.

4.2.3(E) Coefficient of Friction vs. Speed for Plain Plate at Track Dia 110 mm:-

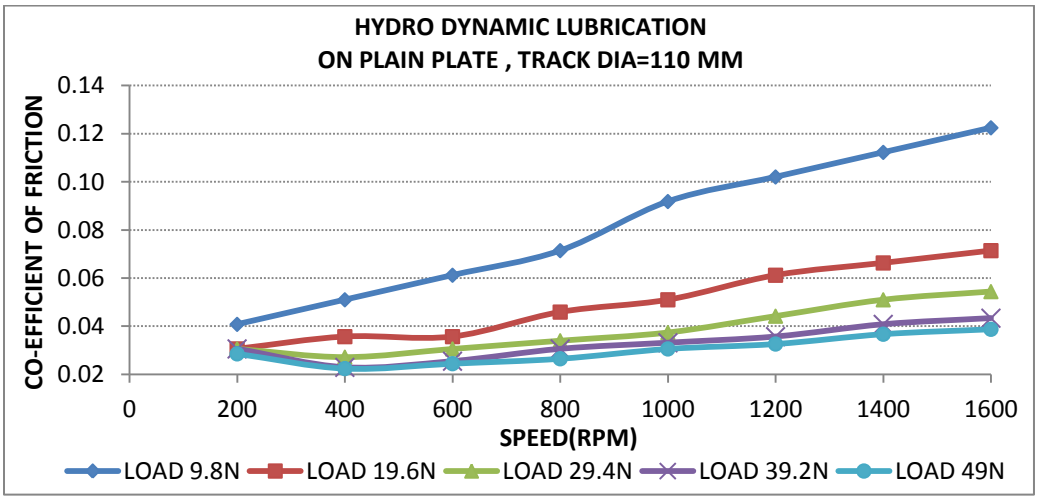

Figure 52

Figure 52 shows the variation of coefficient of friction vs. speed at different loading conditions for hydrodynamic lubrication at track dia 110 mm on plain plate. As the load is increasing the coefficient of friction is decreasing and further varying speed the coefficient of friction is again increasing. The again increasing behaviour in curve is due to the less debris particles at the higher speed. The maximum value for coefficient of friction is 0.123 at the low load (9.8N), 1600 rpm and the minimum value for coefficient of friction is 0.022 for 49 N, 400 rpm. The coefficient of friction is decreasing with increasing the load.

4.2.3(F) Coefficient of Friction vs. Speed for Textured Plate at Track Dia 110 mm:-

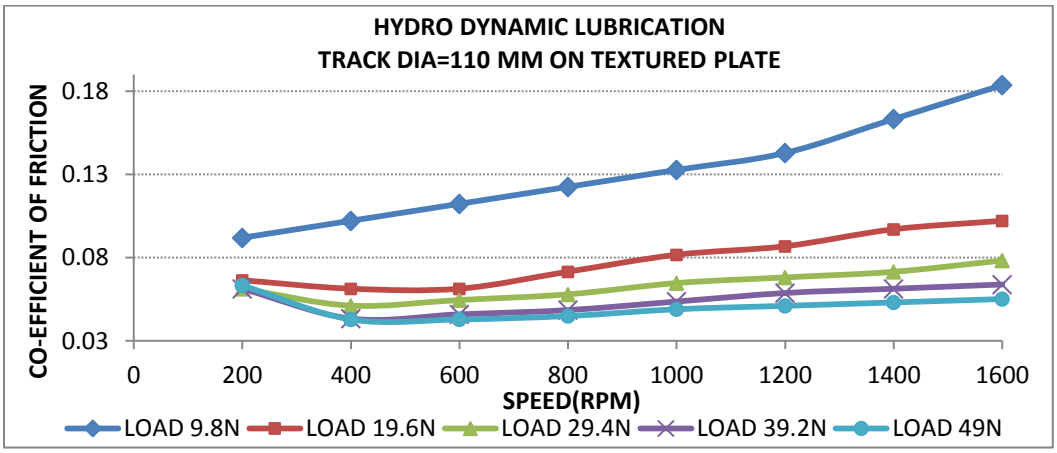

Figure 53

Figure 53 shows the co-efficient of friction with respect to speed at various increasing loading condition for hydrodynamic lubrication on textured plate for track dia 110mm. The trend is as same as the curve of plain plate. As incresing the speed the co-efficient of friction is decresing. On comparing with co-efficient of friction for plain plate, the value are slighty more.At 39.2N the maximum value of co-efficient of friction is 0.18 and minimum value is 0.08.

4.2.3(G) Coefficient of Friction vs. Speed for Plain Plate at Track Dia 50 mm:-

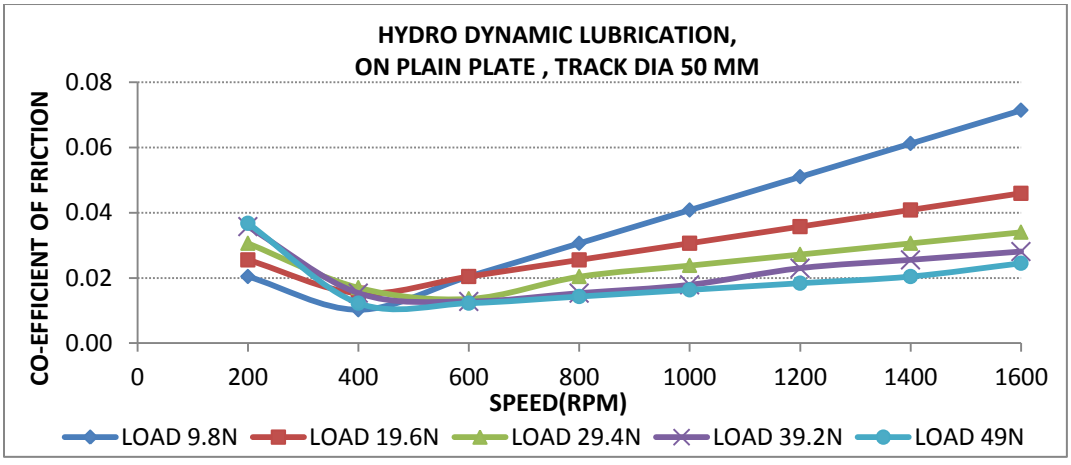

Figure 54

Figure 54 shows the variation of coefficient of friction vs. speed at different loading conditions for hydrodynamic lubrication at track dia 50 mm on plain plate. As the load is increasing the coefficient of friction is decreasing and further varying speed the coefficient of friction is again increasing. The again increasing behaviour in curve is due to the less debris particles at the higher speed. The maximum value for coefficient of friction is 0.07 at the low load (9.8N), 1600 rpm and the minimum value for coefficient of friction is 0.01 for 9.8 N, 400 rpm. The coefficient of friction is decreasing with increasing the load.

4.2.3(H) Coefficient of Friction vs. Speed for Textured Plate at Track Dia 50 mm:-

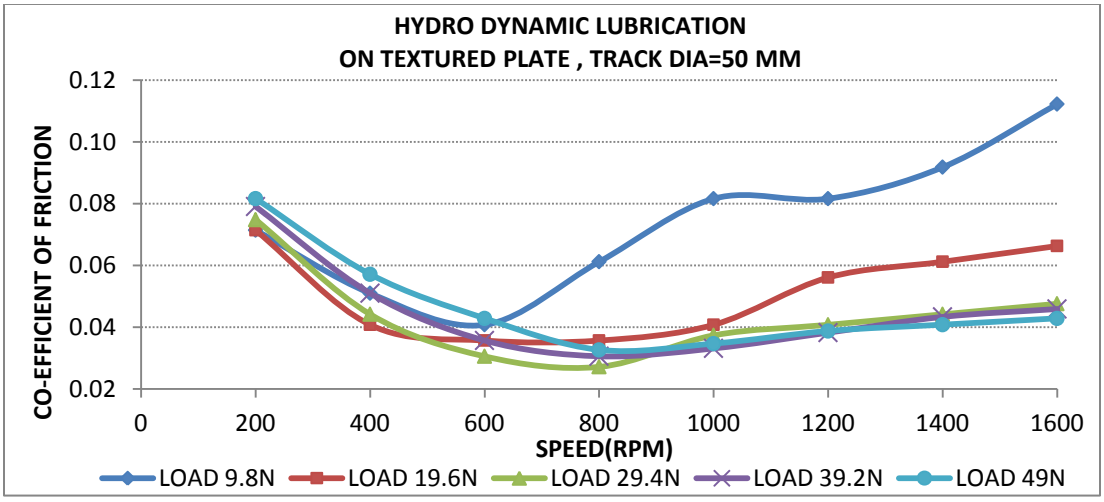

Figure 55

Figure 55 shows the co-efficient of friction with respect to speed at various increasing loading condition for hydrodynamic lubrication on textured plate for track dia 110mm. The trend is as same as the curve of plain plate. But the maximum and minimum value is slightly more as compare to plain plate. As incresing the load (19.6N,29.4N,39.2N,49N) the co-efficient of friction is decresing and on comparing with co-efficient of friction for plain plate, the value are slighty more.At 9.8N the maximum value of co-efficient of friction is 0.11 and minimum value is 0.04.

OSA³ MICROLAB ON-SITE OIL ANALYZER

Company: NEWOIL	**City:**	**Lakshya Enterprises**	**Phone:**
Address:	**State:**	**B-595, Pandav Nagar**	
Phone:	**Zip Code**	**Opp. Naraina Depot**	**Fax:**
Email:	**Fax:**	**New Delhi** **India**	**110008**

Vehicle Make:	GENERAL			**VIN#:**	NEWOIL
Vehicle Model:	GENERAL	**Engine Size:**	2.5	**Test Date:**	07/09/2012
Sump Capacity:	0 Quarts			**Equipment:**	Diesel Engine

Date Taken:	WEAR METALS (in Parts per Million):																				Viscosity Mode: Measured							V40 94.9 - 142.9 V100 12.5 - 16.3		
	Iron	Chromium	Lead	Copper	Tin	Aluminum	Nickel	Moly:	Titanium	Manganese	Vanadium	Silicon	Boron	Magnesium	Calcium	Barium	Phosphorus	Zinc	Sodium	Potassium	Water	Oxidation	Soot	Glycol		TBN	Nitration	V40	V100	VIndex
07/09/2012	14	<2	4	15	<2	4	0	<2	0	5	6	6	1	39	1923	0	919	1222	<2	5	0.1	<2	<0.1	-		9.3	<2	139	15.4	114
Sample ID: 44	N	N	N	N	N	N	N	N	N	N	N	N	N	N	N	N	N	N	N	N	N	N	N	ND		N	N	N	N	N
Oil Brand: SERVO	Diagnostic Code Not Available.																													
Oil Type: MULTIGRADE																														
Oil Weight: 20W40																														
Miles on Unit: 0																														
Miles on Oil: 0																														

Date Taken:	WEAR METALS (in Parts per Million):																				Viscosity Mode: Measured							V40 94.9 - 142.9 V100 12.5 - 16.3		
	Iron	Chromium	Lead	Copper	Tin	Aluminum	Nickel	Moly:	Titanium	Manganese	Vanadium	Silicon	Boron	Magnesium	Calcium	Barium	Phosphorus	Zinc	Sodium	Potassium	Water	Oxidation	Soot	Glycol		TBN	Nitration	V40	V100	VIndex
07/04/2012	5	6	4	6	<2	<2	0	<2	0	1	2	<2	0	9	1126	0	103	162	38	13	<0.1	<2	<0.1	-		8.1	2.4	146	18.2	140
Sample ID: 38	N	N	N	N	N	N	N	N	N	N	N	N	N	N	N	N	N	N	N	N	N	N	N	ND		N	N	A	A	N
Oil Brand: SERVO	PHYSICAL DATA SUGGESTS THAT OIL IS EITHER NEW OR LIGHTLY USED. ALL ENGINE WEAR RATES NORMAL. POSSIBLE MINOR FUEL DILUTION OCCURRING. LOW LEVELS OF DIESEL FUEL CAN BE DIFFICULT TO IDENTIFY IN DIESEL OIL SINCE THEY ARE REFINED FROM SIMILAR OIL STOCKS. VISCOSITY HIGHER THAN TYPICAL FOR THE GIVEN OIL TYPE. VISCOSITY LOWER THAN TYPICAL FOR THE GIVEN OIL TYPE. CHECK FUEL SYSTEM. DRAIN OIL AND CHANGE FILTER IF NOT ALREADY DONE. RESAMPLE AT 1/2 NORMAL INTERVAL TO CONFIRM.																													
Oil Type: MULTIGRADE																														
Oil Weight: 20W40																														
Miles on Unit: 0																														
Miles on Oil: 0																														

ASSUMING NORMAL OIL CONSUMPTION AND BASED ON PROVIDED INFORMATION, WEAR METAL EVALUATION VARIES PER MAKE, MODEL, TOTAL MILES/HOURS AND THE MILES/HOURS THE OIL HAS BEEN IN SERVICE.

A=ABNORMAL S=SEVERE NA=NON APPLICABLE ND=NOT DETECTED D=DETECTED N=NORMAL X=NOT TESTED

Chapter 5

Conclusions

5.1 Brass pin on M.S Plate –

The experiment has been carried on textured plate and plain plate for different sliding speeds (200, 400, 600, 800, 1000 rpm), different loads (9.8N, 19.6N, 29.4N, 39.2N, 49N) and different track diameter (130mm, 110mm, 50mm) for dry regime of lubrication at room temperature. At dry regime of lubrication the coefficient of friction decreases as load increases for both the plates i.e. the value of coefficient of friction is less in case of textured plate. At 9.8N load and 50 mm track diameter the maximum value of coefficient of friction is 0.17 on plain plate and on textured plate is 0.14 for 200 rpm speed. For high speed such as 1000 rpm the maximum value of coefficient of friction is 0.12 on plain plate and on textured plate is 0.09.

It has been observed that in elastohydrodynamic regime of lubrication the coefficient of friction increases as load decreases for both the plates and the value of coefficient of friction is more on textured plate as comparing with plain plate at room temperature. At 9.8N and 130 mm track diameter the maximum value of coefficient of friction is 0.11 on plain plate and on textured plate is 0.14 for 1000 rpm speed.

On comparing coefficient of friction for textured plate and plain plate for different sliding speeds (200, 400, 600, 800, 1000 rpm), different loads (9.8N, 19.6N, 29.4N, 39.2N, 49N) and different track diameter (130mm, 110mm, 50mm) for hydrodynamic regime of lubrication at room temperature, the coefficient of friction increases as load decreases for both the plates. The coefficient of friction is less in case of textured plate. At high speed 1600 rpm, 49 N load the maximum value of coefficient of friction is 0.05 on plain plate and on textured plate it is 0.04.For 9.8 N load and 1600 rpm speed the maximum vale of coefficient of friction is 0.18 on plain plate and on textured plate is 0.09.

5.2 Mild Steel pin on Mild Steel Plate –

The experiment has been carried on textured plate and plain plate for different sliding speeds (200, 400, 600, 800, 1000 rpm), different loads (9.8N, 19.6N, 29.4N, 39.2N, 49N) and different track diameter (130mm, 110mm, 50mm) for dry regime of lubrication at room temperature. The coefficient of friction increases as load decreases for both the plates. The value for coefficient of friction is less in case of textured plate. At 130 mm track diameter and speed 1400 rpm the maximum value of coefficient of friction is 0.41 on plain plate and on textured plate is 0.36 for 49N load. For same track and same rpm speed the maximum value of coefficient of friction is 0.42 on plain plate and on textured plate is 0.36 for 9.8N load.

It has been observed that in elastohydrodynamic regime of lubrication the coefficient of friction increases as load decreases for both the plates and the value for coefficient of friction is low on textured plate as comparing with plain plate at room temperature. At 1600 rpm speed and 50 mm track diameter the maximum value of coefficient of friction is 0.1 for 9.8N load on plain plate and on textured plate is 0.08. For 49N load the coefficient of friction is 0.06 on plain palte and 0.05 on textured plate for same rpm speed and same track diameter.

. On comparing coefficient of friction for textured plate and plain plate for different sliding speeds (200, 400, 600, 800, 1000 rpm), different loads (9.8N, 19.6N, 29.4N, 39.2N, 49N) and different track diameter (130mm, 110mm, 50mm) for hydrodynamic regime of lubrication at room temperature, The coefficient of friction increases as load decreases for both the plates. The value of coefficient of friction is more in case of textured plate as comparing with plain plate. At high speed 1600 rpm, and track diameter 130 mm the maximum value of coefficient of friction is 0.05 on plain plate and on textured plate is 0.06 at 49N load. For same speed rpm and same track diameter the maximum vale of coefficient of friction is 0.15 on plain plate and on textured plate is 0.17 at 9.8N load.

Chapter 6

FUTURE SCOPE OF WORK

The investigation may be done on different shapes and sizes of the micro dimpled textures on different pins and plate material. Different quality of lubricating oil may also taken for the experiment. The study may extands for the various depth of the deep holes on textured plate. Further the experiment may be carried out for different speed that is reciprocating nature or having different curves to the path of pin with respect to the plate for different acceleration and velocities. The results may be applied for different application s on our daily life uses i.e. I.C Engine , compressors, power screws etc.

REFRENCES

[1] E. S. Yoon, H. Kong, O. K. Kwon, J. E. Oh, Evaluation of frictional characteristics for a pin-on-disk apparatus with different dynamic parameters, in 1997.

[2] S. H. Teoh, R. Thampuran, W. K. H. Seah, Coefficient of friction under dry and lubricated conditions of a fracture and wear resistance P/M titanium-graphite composite for biomedical applications in October 1997.

[3] M. K. Stanford, V. K. Jain, Friction and wear characteristics of hard coatings, in 2001.C. Met, L. Vandenbulcke, M.C. Sainte Catherine, Friction and wear characteristics of various prosthetic materials slidind against smooth diamond-coated titanium alloy, in 2003.

[4] Pradeep, L. Menezes, Kishore, S. V. Kailas, Influence of surface texture on coefficient of friction and transfer layer formation during sliding of pure magnesium pin on 080 M 40(EN8) steel plate (2006).

[5] S. Guicciardi, D. Sciti, C. Melandri, G. Pezzotti, Dry sliding wear behavior of nano-sized SiC pins against SiC and Si3N4 discs in July 2006.

[6] T. Larsen, T. L. Andersen, B. Thorning, A. Horsewell, M. E. Vigild, Comparison of friction and wear for an epoxy resin reinforced by a glass or a carbon/aramid hybrid weave in November 2006.

[7] K. Hirasata, K. Hayashi, Y. Inamoto, Friction and wear of several kinds of cast irons under severe sliding conditions, in May 2007.

[8] K. Elangovan, V. Balasubramanian, Inflences of tool pin profile and welding speed on the formation of friction stir processing zone in AA2219 aluminium alloy in July 2007.

[9] M. Yamane, T. A. Stolarski, S. Tobe, Influence of counter material on friction and wear performance of PTFE-metal binary coating ,in September 2007.

[10] P. Marklund, R. Larsson, Wet clutch Friction obtained from simplified pin on disc test (2008).

[11] N. Sundaram, T.N. Farris, The generalized advancing conformal contact problem with friction, pin loads and remote loading-case of rigid pin ,in December 2009.

[12] T. S. Kan, O. Bican, Dry sliding friction and wear properties of Al-25Zn-3Cu-3Si alloy, in January 2010.

[13] K. Gong, Z. Zhou, P.W. Shum, H. Luo, Z. Tian, C. Li , Tribological evaluation on Ni3Al based alloy and its composites under unlubricated wear condition ,in November 2010.

[14] J. Corrochano, J. C. Walker, M. Lieblich, J. Ibanez, W. M. Rainforth, Dry sliding wear behavior of powder metallurgy Al-Mg-Si alloy-MoSi2 composites and the relationshipwith the microstructure, in February 2011.

[15] A. Senatore, V. D Agostino, R. D. Giuda, V. Petrone, Experimental investigation and neural network prediction of bracks and clutch material frictional behavior considering the sliding acceleration influence , in May 2011.

[16] A. T. Perez, G. G. Atance Fatjo, M. Hadfield, S. Austen, A model of friction on pin on disc configuration with imposed pin rotation(2011).

[17] M. Jahangiri, M. Hashempour, H. Razavizadeh, H. R. Rezaie, A new method to investigate the sliding wear behavior of materials based on energy dissipation:W-25 wt%Cu composite, in August 2011.

[18] S. P. Mishra, A. A. Polycarpou, Tribological studies of unpolished laser surface textures under starved lubrication condition, in August 2011

[19] Wear and Lubrication, Glossary of terms and definition in the field of Friction,(Tribology) Research Group on Wear of Engineering Materials, OECD, Paris, 1969.

[20] K. Kato, Wear in relation to friction - a review, Wear 241 (2000) 162–169.

[21] J. Takeda, M. Niinomi, T. Akahori, Gunawarman, Effect of microstructure on fretting fatigue and sliding wear of highly workable titanium alloy (Ti–4.5Al–3V2Mo–2Fe), Toyohashi, Japan 19 December 2003.

[22] R. P. Nair, D. Griffin, N. X. Randall, The use of the pin-on-disk Tribology test method to study three unique industrial applications, Wear 267 (2009) 823–827.

[23] D. K. Dwivedi, T. S. Arjun, P. Thakur, H. Vaidya, K. Singh, Sliding wear and friction behavior of Al–18% Si–0.5% Mg alloy, Journal of Materials Processing Technology 152 (2004) 323–328.

[24] J. Takeda, M. Niinomi, T. Akahori, Gunawarman, Effect of microstructure on fretting fatigue and sliding wear of highly workable titanium alloy (Ti–4.5Al–3V2Mo–2Fe), Toyohashi, Japan 19 December 2003.

[25] S. Tao, Z. Yin, X. Zhou, C. Ding, Sliding wear characteristic of Al_{2O3} and Cr_{2O3} coatings against copper alloy under severe conditions, Tribology international 43 (2010), 69-75.

[26] G .W. Stachowaik, A .W. batchelor, Engineering Tribology, 172-179.

[26] C. M. Taylor, Engine Tribology, Elsevier publications, 145-151.

[27] M .J. Nede, The Tribology Handbook, 2nd Edition, 109-125.

APPENDIX-1

Calculation for square micro dimpled on plate-

a=1mm

We know that,

$2\pi R = aN$

Where, R is the PCR

A is the arc travel between dimple centres

N is the no. of dimples.

Now, $2\pi R = a_1 N_1$

and, $2\pi R = a_2 N_2$

$\Rightarrow N_2 = (a_1/a_2)\, N_1$

Here, $a_1 = 2mm$ & $a_1 = 1mm$

$\Rightarrow N_2 = 2N_1$

S No.	R (in mm)	Angle From previous line	Angle form vertical	N_1	N for a= 1mm
1	10	0	0	35	70
2	11	3.47	3.47		
3	12	3.18	6.65		
4	13	2.94	9.59	44	88
5	14	2.73	12.32		
6	15	2.55	14.87		
7	16	2.39	17.26	53	106
8	17	2.25	19.51		
9	18	2.12	21.63		
10	19	2.01	23.64	63	126
11	20	1.91	25.55		
12	21	1.82	27.32		
13	22	1.74	29.06	72	144
14	23	1.66	30.72		
15	24	1.59	32.31		
16	25	1.53	33.84	82	164
17	26	1.47	35.31		
18	27	1.42	36.73		
19	28	1.36	38.09	91	182
20	29	1.32	39.41		

21	30	1.27	40.68		
22	31	1.23	41.91	100	200
23	32	1.19	43.1		
24	33	1.16	44.27		
25	34	1.12	45.39	110	220
26	35	1.09	46.48		
27	36	1.06	47.54		
28	37	1.03	48.57	119	238
29	38	1.01	49.58		
30	39	0.98	50.56		
31	40	0.96	51.52	129	258
32	41	0.93	52.45		
33	42	0.91	53.36		
34	43	0.89	54.25	138	276
35	44	0.87	55.12		
36	45	0.85	55.97		
37	46	0.83	56.8	148	296
38	47	0.81	57.61		
39	48	0.80	58.41		
40	49	0.78	59.19	157	314
41	50	0.76	59.95		
42	51	0.75	60.7		
43	52	0.73	61.43	166	332
44	53	0.72	62.15		
45	54	0.71	62.86		
46	55	0.69	63.55	176	352
47	56	0.68	64.23		
48	57	0.67	64.9		
49	58	0.66	65.56	185	370
50	59	0.65	66.21		
51	60	0.64	66.85		
52	61	0.63	67.48	195	390
53	62	0.62	68.1		
54	63	0.61	68.71		
55	64	0.60	69.31	204	408
56	65	0.59	69.90		
57	66	0.58	70.48		
58	67	0.57	71.05	214	428
59	68	0.56	71.66		
60	69	0.55	72.21		